AFCRL - 63-539

ADVANCED ANTENNA TECHNIQUES

Leo W. Procopio
Thomas K. Kashihara
Stephen Czorpita
Kenneth Abend
Terrence A. Lenahan

Philco Scientific Laboratory
Blue Bell, Pa.

Contract No. AF 19(628)-2403

Project No. 4600

Program Element 62405304

Scientific Report No. 1

October 1963

Prepared
for

AIR FORCE CAMBRIDGE RESEARCH LABORATORIES
OFFICE OF AEROSPACE RESEARCH
UNITED STATES AIR FORCE
BEDFORD, MASSACHUSETTS

NOTICES

"Requests for additional copies by Agencies of the Department of Defense, their contractors, and other Government agencies should be directed to the:

DEFENSE DOCUMENTATION CENTER (DDC)
CAMERON STATION
ALEXANDRIA, VIRGINIA

Department of Defense contractors must be established for DDC services or have their 'need-to-know' certified by the cognizant military agency of their project or contract."

All other persons and organizations should apply to the:

U. S. DEPARTMENT OF COMMERCE
OFFICE OF TECHNICAL SERVICES
WASHINGTON 25, D. C.

PATENT: When Government drawings, specifications, or other data are used for any purpose other than in connection with a definitely related Government procurement operating, the United States Government thereby incurs no responsibility nor any obligation whatsoever and the fact that the Government may have formulated, furnished, or in any way supplied the said drawings, specifications or other data is not to be regarded by implication or otherwise as in any manner licensing the holder or any other person or corporation, or conveying any rights or permission to manufacture, use, or sell any patented invention that may in any way be related thereto.

FOREWORD

This scientific report summarizes partial results of an investigation into advanced antenna techniques. The work was performed by the Philco Scientific Laboratory for the Air Force Cambridge Research Laboratories under Contract No. AF 19(628)-2403, Project No. 4600, Program Element 62405304, and covers effort performed during the period 1 December 1962 to 30 September 1963.

Major research effort during the study was performed by Thomas K. Kashihara (Secs. II, IV), Stephen Czorpita (Sec V), Kenneth Abend (Sec. III), and Terrence A. Lenahan (Sec. VI). General supervision of the study was under Leo W. Procopio.

ABSTRACT

A generalized theory of resolution for linear array antennas is presented. The theory indicates that angular resolution is determined by the width of the autocorrelation of the field pattern and not by the width of the pattern itself. Hence a well defined main beam is not a prerequisite for achieving angular resolution; even noiselike beams can be characterized by an autocorrelation function of narrow width. It is shown that this basic principle leads to the concept of angular dispersion and compression, a phenomenon for angular beam patterns akin to dispersion and compression of radar pulses. A new procedure for synthesizing antennas for given resolution properties is also presented. The theory is applied to antennas with time-invariant and time-varying illumination functions, and is used to reexamine classical theories of superdirectivity. Antennas which intimately link resolution properties in range and angle are also analyzed; arrays in which each radiator operates at a different frequency are shown to be an example of this class. In addition to an exposition of angular resolutions theory, preliminary concepts for achieving angular dispersion and compression, and superdirectivity are also presented.

TABLE OF CONTENTS

TABLE OF CONTENTS (cont)

TABLE OF CONTENTS (cont)

TABLE OF CONTENTS (cont)

TABLE OF CONTENTS (cont)

LIST OF ILLUSTRATIONS

LIST OF ILLUSTRATIONS (cont)

LIST OF ILLUSTRATIONS (cont)

SECTION I

INTRODUCTION

A study program has been conducted to determine the properties of signals and radiating systems which affect and limit the attainment of angular resolution. Emphasis in the program has been placed on the development of new antenna concepts which achieve resolution through unconventional signal processes; time-varying and time invariant aperture illumination functions have been considered, and linear rather than non-linear signal processes have been stressed. This report contains a description of some preliminary results obtained in the program thus far, including a summary of ambiguity theory as applied to angular resolution, and analysis of several new antenna techniques.

A significant result of the theoretical investigation indicates that the resolution of a radiating aperture is determined by the autocorrelation of the field pattern and not by the field pattern itself. This primary result, demonstrated in general for linear arrays, implies a number of corollary theorems. For example, it states that resolution can be obtained with a noiselike field pattern i. e., a pattern with no well defined main beam. It also implies that phase tolerances at the radiators of an array are not important, a fact which opens the way for drastic simplifications in the design of large array antennas. Since these properties may be of great practical interest to the antenna designer, a preliminary examination of resolution principles as viewed in terms of new antenna concepts has been undertaken.

With the advent of a new theory of resolution for linear array antennas, the general theory of pattern synthesis has been reexamined. Particular emphasis has been placed on a reexamination of the classical theories of superdirectivity with the hope that new synthesis procedures might be used to alleviate some of the severe problems heretofore associated with superdirective antennas. Only preliminary results of this study are presented in this report; further research is being conducted and will be documented later.

The report contains an exposition of resolution theory for both time invariant and time varying illumination functions. In the latter case the coupled nature of range resolution and angular resolution becomes evident and the ambiguity theory must be extended to account for this. Hence, in addition to developments concerning dispersed beam antennas and the means for extracting resolution from them, analysis of antennas in which range

resolution and angular resolution is intimately connected has also been performed. These antennas are apertures in which the individual radiators transmit or receive different portions of the signal spectrum ("multiple frequency arrays"); in the limit where each radiator transmits the same signal spectrum this antenna type assumes the properties of the more conventional antennas, in which, for small bandwidth, the range and angular resolutions are separable.

The work has been subdivided into five main categories, each representing a particular aspect of the antenna theory which has been developed. The sections involved include (1) resolution theory for time invariant illuminations, (2) resolutions theory for time varying illuminations, (3) theory of superdirective antennas, (4) techniques for achieving angular dispersion and compression, and (5) multiple frequency arrays. Finally, a section summarizing the major conclusions of the study has been added. Recommendations for further research have been discussed from time to time in the various sections. More detailed recommendations for further research will be described in future reports.

SECTION II

THE THEORY OF RESOLUTION OF LINEAR ARRAY ANTENNAS TIME INVARIANT ILLUMINATION FUNCTIONS

I. Introduction

This section reports on the development of a theory of angular resolution for antenna systems. The intent of this study is to define clearly the basic limitations of angular resolution in terms of antenna and signal parameters and to develop techniques whereby optimum illumination functions can be synthesized to obtain a prescribed angular resolution.

Angular resolution refers to the capability of separating, or distinguishing, two or more sources differing in their angular positions. A basic problem is to establish some reasonable criterion to measure this capability of separation and to indicate the ultimate limits of resolution in terms of the illumination function and the signal structure. Such an analysis could properly proceed from the formulation of ambiguity functions similar to those used by Woodward,[1] Elspas,[2] and expanded in scope by Urkowitz et al.[3] Woodward was able to show the ultimate limitations of the signal in resolving targets in range and/or range-rate.

An analogous formulation is sought for angular resolution. This section is limited to the consideration of angular resolution of antenna systems with time invariant illumination functions and with linear processing of signals.

II. Measure of Difference

In order to resolve two or more sources, some difference must exist in the signals received from them. It is reasonable to expect that the larger the difference between the signals, the more easily can the sources be

1. P. M. Woodward, Probability and Information Theory, with Applications to Radar, Pergamon Press, London, 1953.

2. B. Elspas, "A Radar System Based on Statistical Estimation and Resolution Considerations," Stanford Electronics Labs, Stanford Univ., Calif., Tech Rept. No. 361-1, August 1, 1955.

3. H. Urkowitz, C. A. Hauer, J. F. Koval, "Generalized Resolution in Radar Systems," Proc. IRE, Vol 50, October 1962, pp 2093-2105.

resolved. Hence, a measure of signal difference is required to determine the resolution capabilities of the array. The measure used successfully by Woodward was the integrated squared difference of two signals. This measure, which provided both a physically reasonable and mathematically tractable criterion, also serves as the basis for determining angular resolution.

Consider the case where two identical sources, differing only in their angular coordinates, are to be resolved with a linear array. The geometry of the situation is illustrated in Figure 1. Let x be a point on the array and let the angular orientation of the array be given by the coordinates θ, ϕ. Assume the two sources to be situated at R_o, θ_o, ϕ_o, and R_o, $\theta_o + \Delta\theta_o$, $\phi_o + \Delta\phi_o$, respectively. Consider now the various possible measures of difference, all based on the integrated squared difference criterion, defined by the equations below.

$$\epsilon^2 = \iint |S_1 - S_2|^2 dx dt \tag{1}$$

$$\epsilon^2 = \int |S_1 - S_2|^2 dt \tag{2}$$

$$\epsilon^2 = \iiint |S_1 - S_2|^2 \sin\theta d\theta d\phi dt \tag{3}$$

where $s_1 dx$ and $s_2 dx$ are the signals received from the sources by an incremental length of the array and S_1 and S_2 are the signals received by the entire array. Considering only the dependence of the signal structures on the array factor and using the far-field approximation, the signals are proportional to*

---

* The factor, ω, has been added in the signal expressions because arbitrary bandwidth signals will be discussed in this and later sections. It properly belongs in the diffraction and radiation equations (see, for example S. Silver, Microwave Antenna Theory and Design, McGraw-Hill, 1949, p 97 and p 167) but can be neglected, or assumed to be constant, for narrowband signals.

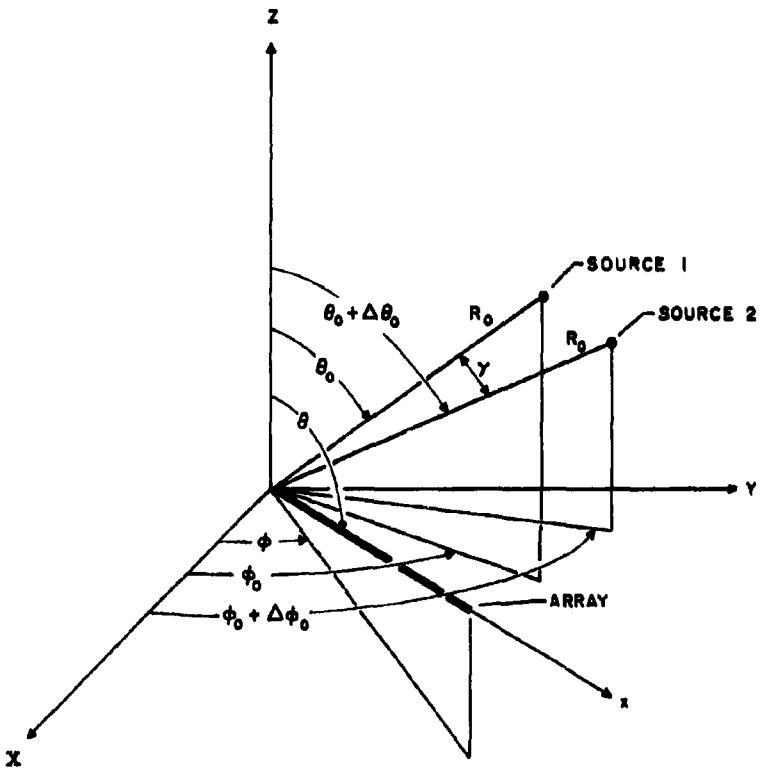

Figure 1 Array-Source Geometry for Linear Array Resolution

$$s_1 dx = \int_{-\infty}^{\infty} \omega I(x) A(\omega-\omega_0) e^{i\omega\left[t - \frac{R_0}{c} + \frac{x}{c}\cos\gamma_1\right]} d\omega dx \tag{4}$$

$$s_2 dx = \int_{-\infty}^{\infty} \omega I(x) A(\omega-\omega_0) e^{i\omega\left[t - \frac{R_0}{c} + \frac{x}{c}\cos\gamma_2\right]} d\omega dx \tag{5}$$

$$S_1 = \int_{-a}^{a} s_1 dx \tag{6}$$

$$S_2 = \int_{-a}^{a} s_2 dx \tag{7}$$

where I(x) is the illumination function, c is the velocity of propagation, A(ω) is the modulation spectrum of the signal, ω_0 is the center frequency, a is the half-length of the array, and

$$\cos\gamma_1 = \cos\theta\cos\theta_0 + \sin\theta\sin\theta_0\cos(\phi-\phi_0) \tag{8}$$

$$\cos\gamma_2 = \cos\theta\cos(\theta_0+\Delta\theta_0) + \sin\theta\sin(\theta_0+\Delta\theta_0)\cos(\phi-\phi_0-\Delta\phi_0) \tag{9}$$

The first criterion, Equation 1, used by Urkowitz et al[4] provided considerable insight into resolution properties of radar systems. It suffers from the weakness, however, that the phase function across the aperture of the antenna is assumed, by definition, not to affect the resolution properties of the array. This can be seen by substituting Equations 4 and 5 into Equation 1. If the signals $s_1 dx$ and $s_2 dx$ are assumed to arise from an illumination function $I(x) = |I(x)|\, e^{i\psi(x)}$, note that the phase term $\psi(x)$ will be eliminated from consideration; hence, subsequent theory is powerless to indicate a dependence of angular resolution on the aperture phase function. This deficiency may be important, especially in the description of superdirective apertures in which the rapidly varying phase function is believed to be a necessity for the attainment of abnormal angular resolution.

The criterion expressed by Equation 2 accounts for the aperture phase function, but leads to difficulties in mathematical tractability and, in addition,

4. Op cit.

leads to a description of attainable resolution in terms of the absolute angular coordinates of the aperture. Since the antenna can be rotated, this latter deficiency is objectionable because it does not provide an inherent measure of the antenna capability. The last criterion expressed by Equation 3 has been designed to overcome all of these objections. It accounts for the possible influence of the aperture phase function and provides a fundamental parameter describing the aperture capability which is independent of the absolute coordinates. This measure is used in the following discussion, where its utility is demonstrated.

The integrated squared difference criterion to be used was defined as

$$\epsilon^2 = \iiint |S_1 - S_2|^2 \sin\theta \, d\theta \, d\theta \, d\phi \, dt$$

where $S_1(t)$ and $S_2(t)$ are the signals received by the array, of length 2a, from the two sources. For good resolution, ϵ^2 should be large for all $\Delta\theta_o$, $\Delta\phi_o$ not equal to zero. The measure can be expanded as

$$\epsilon^2 = \iiint |S_1|^2 \sin\theta \, d\theta \, d\theta \, d\phi \, dt + \iiint |S_2|^2 \sin\theta \, d\theta \, d\theta \, d\phi \, dt - 2 \mathrm{Re} \iiint S_1 S_2^* \sin\theta \, d\theta \, d\theta \, d\phi \, dt \qquad (10)$$

where the real part of the third integral is to be evaluated and the asterisk denotes the complex conjugate. It can be shown that the first two integrals of Equation 10 are equal and independent of source angular coordinates; both integrals are proportional to the energies of the received signals.

The function which determines the resolution characteristics of the array is associated with the expression

$$\Phi = \mathrm{Re} \iiint S_1 S_2^* \sin\theta \, d\theta \, d\theta \, d\phi \, dt \qquad (11)$$

The function Φ is called the angular ambiguity function. For good resolution properties, Φ is to be minimized for all $\Delta\theta_o$, $\Delta\phi_o$ not equal to zero.

III. The Angular Ambiguity Function

A. One-Dimensional Formulation

Consider the restricted case where the sources to be resolved and the linear array are constrained to lie in a fixed plane. Without loss of any more generality, this plane can be chosen as the $\theta = \pi/2$ plane.

The ambiguity function, with $\theta_0 = \pi/2$ and $\Delta\theta_0 = 0$, can be written as

$$\Phi = \rho_e \iiint \delta(\theta - \tfrac{\pi}{2}) S_1 S_2^* \sin\theta \, d\theta \, d\phi \, dt \tag{12}$$

where $\delta(\theta)$ is the delta function. Substitution of Equations 6 and 7 into Equation 12, and performing the integration with respect to θ yields

$$\Phi = \rho_e \iiiint\!\!\iint I(x_1) I^*(x_2) \omega_1 \omega_2 A(\omega_1 - \omega_0) A^*(\omega_2 - \omega_0) e^{i\omega_1\left[t - \frac{R_0}{c} + \frac{x_1}{c}\cos(\phi - \phi_0)\right]} e^{-i\omega_2\left[t - \frac{R_0}{c} + \frac{x_2}{c}\cos(\phi - \phi_0 - \Delta\phi_0)\right]} dx_1 dx_2 d\omega_1 d\omega_2 d\phi \, dt \tag{13}$$

Collecting terms in t and performing the integration

$$\int_{-\infty}^{\infty} e^{i(\omega_1 - \omega_2)t} dt = 2\pi \delta(\omega_1 - \omega_2) \tag{14}$$

Hence, Φ has a value only for $\omega_1 = \omega_2$ and can be written as

$$\Phi = 2\pi \rho_e \iiint\!\!\iint I(x_1) I^*(x_2) |\omega A(\omega - \omega_0)|^2 e^{i\frac{\omega}{c} x_1 \cos(\phi - \phi_0)} e^{-i\frac{\omega}{c} x_2 \cos(\phi - \phi_0 - \Delta\phi_0)} dx_1 dx_2 d\omega \, d\phi \tag{15}$$

Performing the integration with respect to ϕ yields

$$\int_{-\pi}^{\pi} e^{i\frac{\omega}{c}[x_1\cos(\phi-\phi_0)-x_2\cos(\phi-\phi_0-\Delta\phi_0)]}\,d\phi = 2\pi J_0\left\{\frac{\omega}{c}\left[x_1^2+x_2^2-2x_1x_2\cos(\Delta\phi_0)\right]^{1/2}\right\} \tag{16}$$

where J_0 is the Bessel function of the first kind of order zero. Application of the addition theorem provides[5]

$$J_0\left\{\frac{\omega}{c}\left[x_1^2+x_2^2-2x_1x_2\cos(\Delta\phi_0)\right]^{1/2}\right\} = \sum_{p=0}^{\infty}\epsilon_p J_p\left(\frac{\omega x_1}{c}\right)J_p\left(\frac{\omega x_2}{c}\right)\cos(p\Delta\phi_0) \tag{17}$$

where ϵ_p is the Neumann number ($\epsilon_p = 1$ for $p = 0$, $\epsilon_p = 2$ for $p > 0$). The ambiguity function can now be written as

$$\Phi = (2\pi)^2\rho_t\sum_p \epsilon_p\cos(p\Delta\phi_0)\iiint I(x_1)I^*(x_2)|\omega A(\omega-\omega_0)|^2 J_p\left(\frac{\omega x_1}{c}\right)J_p\left(\frac{\omega x_2}{c}\right)dx_1\,dx_2\,d\omega \tag{18}$$

$$= (2\pi)^2\sum_p \epsilon_p\cos(p\Delta\phi_0)\int\left|\int I(x)\,\omega A(\omega-\omega_0)J_p\left(\frac{\omega x}{c}\right)dx\right|^2 d\omega \tag{19}$$

Note that, for a given signal spectrum and illumination function, the integrals of Equation 19 are a function of p. Define the coefficient

$$A_p = (2\pi)^2\int\left|\int I(x)\,\omega A(\omega-\omega_0)J_p\left(\frac{\omega x}{c}\right)dx\right|^2 d\omega \tag{20}$$

so that

$$\Phi = \sum_p \epsilon_p A_p\cos(p\Delta\phi_0) \tag{21}$$

which will be recognized as a Fourier series expansion.

5. A. Andrews, G. B. Mathews, and T. M. MacRobert, Bessel Functions, Macmillan & Co., 1931, p. 73.

Note that the Fourier series expansion indicates the manner in which the spatial harmonics, $p\,\Delta\phi_o$, are related to the signal spectrum and illumination function. The series also provides the necessary condition that a realizable ambiguity function be an even function (as one would expect from the physics of the situation) and that the coefficients be positive. In addition, the synthesis of an illumination function, as well as a possible trade-off between signal spectrum and the illumination function to provide a prescribed ambiguity function, is indicated in the expansion.

B. CW Transmission with Discrete Radiators

The role of the illumination function in determining the characteristics of the ambiguity function is more readily seen by considering CW transmission from the sources, and a linear array consisting of discrete radiators.

For the CW case, the definition of the measure of difference must be slightly modified as

$$\epsilon^2 = \frac{\omega_0}{2\pi} \int_{-\frac{\pi}{\omega_0}}^{\frac{\pi}{\omega_0}} \int_0^{2\pi} |S_1 - S_2|^2 \, d\phi \, dt \tag{22}$$

For discrete radiators, the received signals are proportional to

$$S_1 = \sum_{n=1}^{N} I_n e^{i\omega_0 \left[t - \frac{R_0}{c} + \frac{x_n}{c} \cos(\phi - \phi_0)\right]} \tag{23}$$

$$S_2 = \sum_{n=1}^{N} I_n e^{i\omega_0 \left[t - \frac{R_0}{c} + \frac{x_n}{c} \cos(\phi - \phi_0 - \Delta\phi_0)\right]} \tag{24}$$

where

I_n = relative complex illumination of the n-th radiator

x_n = position of the n-th radiator

N = total number of radiators

The ambiguity function is, then,

$$\Phi = \frac{\omega_0}{2\pi} k \sum_n \sum_m I_n I_m^* \iint e^{i\frac{\omega_0}{c}\left[x_n \cos(\phi-\phi_0) - x_m \cos(\phi-\phi_0-\Delta\phi_0)\right]} d\phi dt$$

$$= k \sum_n \sum_m I_n I_m^* \int e^{i\frac{\omega_0}{c}\left[x_n \cos(\phi-\phi_0) - x_m \cos(\phi-\phi_0-\Delta\phi_0)\right]} d\phi \qquad (25)$$

But

$$\sum_n I_n e^{i\frac{\omega_0}{c} x_n \cos\phi} \qquad (26)$$

as a function of ϕ, simply describes the principal field pattern of the array. Thus, if G is the pattern function, then

$$\Phi = k \int G(\phi-\phi_0) G^*(\phi-\phi_0-\Delta\phi_0) d\phi \qquad (27)$$

It is seen that the ambiguity function is the complex autocorrelation function of the pattern.* If the array is allowed to scan (ϕ is varied) so that the signals from the sources vary as the pattern functions, then a matched filter is prescribed to obtain the maximum resolution where the filter is matched to the antenna pattern.**

Integration of Equation 25 yields

$$\Phi = 2\pi k \sum_n \sum_m I_n I_m^* J_0\left\{\frac{\omega_0}{c}\left[x_n^2 + x_m^2 - 2x_n x_m \cos(\Delta\phi_0)\right]^{1/2}\right\} \qquad (28)$$

---

* This is a general result which also holds for the continuous illumination function.

** Some implications of Equation 27 are discussed by H. Urkowitz et al, op cit.

Application of the addition theorem for the Bessel function reduces the ambiguity function to

$$\Phi = \sum_{p=0}^{\infty} \epsilon_p A_p \cos(p\alpha\phi_0) \tag{29}$$

$$A_p = 2\pi \left| \sum_n I_n J_p\left(\frac{\omega_0}{c} x_n\right) \right|^2 \tag{30}$$

*

The above Fourier series can be used to synthesize a current distribution. For example, given a desired ambiguity function, its Fourier coefficients can be determined. In general, an infinite set of coefficients is obtained. However, with N radiators, there exists, at most, 3N - 2 factors to be determined corresponding to N - 1 amplitudes, N - 1 phases, and N positions of the radiators. A technique which can be applied is to find the current distribution that provides the best fit, in the least square sense, to M(M > 3N - 2) of the Fourier coefficients. Another technique would be to determine the current distribution which exactly satisfies any given set of 3N - 2 Fourier coefficients. If some of the positions, phases, or amplitudes are initially fixed, obviously the number of factors to be determined is correspondingly reduced.

Further insight into the ambiguity function can be obtained by expanding Equation 28 as follows

$$\Phi = 2\pi \mathrm{Re}\left\{ \sum_n |I_n|^2 J_0\left[\frac{2\omega_0}{c} x_n \sin\left(\frac{\Delta\phi_0}{2}\right)\right] \right. \tag{31}$$

$$\left. + \sum_n \sum_m (1-\delta_{nm}) I_n I_m^* J_0\left[\frac{\omega_0}{c}(x_n^2 + x_m^2 - 2x_n x_m \cos\Delta\phi_0)^{1/2}\right] \right\}$$

or

$$\Phi = 2\pi \mathrm{Re}\left\{ \sum_n |I_n|^2 J_0\left[\frac{2\omega_0}{c} x_n \sin\left(\frac{\Delta\phi_0}{2}\right)\right] \right. \tag{32}$$

$$\left. + \sum_n \sum_m (1-\delta_{nm}) |I_n I_m| \cos(\psi_n - \psi_m) J_0\left[\frac{\omega_0}{c}(x_n^2 + x_m^2 - 2x_n x_m \cos\Delta\phi_0)^{1/2}\right] \right\}$$

---

* For the continuous illumination function, $A_p = 2\pi \left| \omega_0 \int I(x)\, J_p(\omega_0 x/c)\, dx \right|^2$.

where δ_{nm} is the Kronecker delta ($\delta_{nm} = 1$ for $n = m$, $\delta_{nm} = 0$ for $n \neq m$), and ψ_n and ψ_m are the phase angles of the illumination coefficients I_n and I_m respectively. Note that the first summation in Equation 32 represents the sum of the ambiguity functions for the individual radiators taken independently. Also, the importance of the phases of the radiating elements in forming an ambiguity function is clearly indicated by the terms in the second (double) summation. It is evidenced that considerable control of the ambiguity function is lost with the conventional uniform phase illumination.

C. Two-Dimensional Formulation

Consider the general problem of two-dimensional scanning with arbitrary source positions. The geometry of the problem is shown in Figure 1. A one-dimensional linear array is assumed.

The general ambiguity function, given by Equation 11 is now applicable.

$$\Phi = R_e \iiint S_1 S_2^* \sin\theta \, d\theta \, d\phi \, dt \tag{11}$$

$$S_1 = \iint I(x)\, \omega A(\omega-\omega_0)\, e^{i\omega\left[t - \frac{R_0}{c} + \frac{x}{c}\cos\gamma_1\right]} dx\, d\omega \tag{6}$$

$$S_2 = \iint I(x)\, \omega A(\omega-\omega_0)\, e^{i\omega\left[t - \frac{R_0}{c} + \frac{x}{c}\cos\gamma_2\right]} dx\, d\omega \tag{7}$$

where

$$\cos\gamma_1 = \cos\theta\cos\theta_0 + \sin\theta\sin\theta_0\cos(\phi-\phi_0) \tag{8}$$

$$\cos\gamma_2 = \cos\theta\cos(\theta_0+\Delta\theta_0) + \sin\theta\sin(\theta_0+\Delta\theta_0)\cos(\phi-\phi_0-\Delta\phi_0) \tag{9}$$

Substituting Equations 6 and 7 into Equation 11, collecting terms in t, and performing the integration with respect to time yields

$$\int_{-\infty}^{\infty} e^{i(\omega_1-\omega_2)t}\, dt = 2\pi\delta(\omega_1-\omega_2) \tag{33}$$

Hence, Φ can be expressed as

$$\Phi = 2\pi \iiiint I(x_1)\, I^*(x_2)\, |W A(w-w_0)|^2 e^{i\frac{w}{c}[x_1\cos\gamma_1 - x_2\cos\gamma_2]} \sin\theta\, d\theta\, d\phi\, dx_1\, dx_2\, dw \qquad (34)$$

Now the integral

$$\iint e^{i\frac{w}{c}[x_1\cos\gamma_1 - x_2\cos\gamma_2]} \sin\theta\, d\theta\, d\phi \qquad (35)$$

can be evaluated using the expansion [6]

$$e^{i\frac{w}{c}x_1\cos\gamma_1} = \sum_{n=0}^{\infty} (2n+1)(i)^n j_n\left(\frac{wx}{c}\right) P_n(\cos\gamma_1) \qquad (36)$$

where j_n is the spherical Bessel function, together with the addition theorem for the Legendre polynomial[7]

$$P_n(\cos\gamma_1) = \sum_{m=0}^{n} \epsilon_m \frac{(n-m)!}{(n+m)!} P_n^m(\cos\theta) P_n^m(\cos\theta_0) \cos[m(\phi-\phi_0)] \qquad (37)$$

and the orthogonality relations

$$\int_0^{\pi} P_q^s(\cos\theta) P_r^s(\cos\theta) \sin\theta\, d\theta = \begin{cases} \frac{2}{2q+1} \frac{(q+s)!}{(q-s)!}, & \text{for } q=r \\ 0, & \text{for } q\neq r \end{cases} \qquad (38)$$

$$\int_0^{2\pi} \cos[q(\phi-\phi_0)] \cos[r(\phi-\phi_0-\Delta\phi_0)]\, d\phi = \begin{cases} \frac{2\pi}{\epsilon_q} \cos(q\Delta\phi_0), & \text{for } q=r \\ 0, & \text{for } q\neq r \end{cases} \qquad (39)$$

---

6. J. A. Stratton, Electromagnetic Theory, McGraw-Hill, p. 409.

7. Ibid, p. 408.

Equation 35 reduces to

$$\iint e^{i\frac{w}{c}[x_1\cos\gamma_1 - x_2\cos\gamma_2]}\sin\theta\,d\theta\,d\phi = 4\pi\sum_n (2n+1)\,j_n\left(\frac{wx_1}{c}\right)j_n\left(\frac{wx_2}{c}\right)P_n(\cos\gamma) \tag{40}$$

where γ, given by

$$\gamma = \arccos\left[\cos\theta_0\cos(\theta_0+\Delta\theta_0) + \sin\theta_0\sin(\theta_0+\Delta\theta_0)\cos(\Delta\phi_0)\right] \tag{41}$$

is the angular separation between the sources (see Figure 1). Substituting Equation 40 into Equation 34, the ambiguity function can be expressed as

$$\Phi = 8\pi^2 k_p \sum_n (2n+1)P_n(\cos\gamma)\iiint I(x_1)I^*(x_2)|wA(w-w_0)|^2 j_n\left(\frac{wx_1}{c}\right)j_n\left(\frac{wx_2}{c}\right)dx_1dx_2\,dw \tag{42}$$

$$= 8\pi^2\sum_n (2n+1)P_n(\cos\gamma)\int\left|\int I(x)wA(w-w_0)j_n\left(\frac{wx}{c}\right)dx\right|^2 dw \tag{43}$$

or

$$\Phi = \sum_n A_n P_n(\cos\gamma) \tag{44}$$

$$A_n = 8\pi^2(2n+1)\int\left|\int I(x)wA(w-w_0)j_n\left(\frac{wx}{c}\right)dx\right|^2 dw \tag{45}$$

Equation 44 expresses the ambiguity function as the sum of zonal harmonics in terms of the angular separation of the sources. Viewed in this manner, the ambiguity function expresses the fact that a linear one-dimensional array is capable of providing only one-dimensional angular resolution.

D. Transmit-Receive

The ambiguity function for a combined transmitting-receiving system is considered here. It is assumed, as in Subsection IIA, that the targets are in the scanning plane of the array. The geometry of the

situation is shown in Figure 2. Assuming far-field conditions, the received signals reflected from the targets are proportional to

$$S_1 = \iiint I_1(x_1) I_2(x_2) \omega^2 A(\omega-\omega_0) e^{i\omega\left[t - \frac{2R_0}{c} + \frac{x_1+x_2}{c}\cos(\phi-\phi_0)\right]} dx_1 dx_2 d\omega \tag{46}$$

$$S_2 = \iiint I_1(x_1) I_2(x_2) \omega^2 A(\omega-\omega_0) e^{i\omega\left[t - \frac{2R_0}{c} + \frac{x_1+x_2}{c}\cos(\phi-\phi_0-\Delta\phi_0)\right]} dx_1 dx_2 d\omega \tag{47}$$

where I_1 and I_2 are the illumination functions of the transmitting and receiving arrays, respectively. Substituting the above expressions into Equation 12 for the one-dimensional analysis and performing the integration with respect to time yields

$$\Phi = 2\pi \operatorname{Re}\iiiint I_1(x_1) I_2(x_2) I_1^*(y_1) I_2^*(y_2) |\omega^2 A(\omega-\omega_0)|^2 e^{i\frac{\omega}{c}\left[(x_1+x_2)\cos(\phi-\phi_0)\right]} e^{-i\frac{\omega}{c}\left[(y_1+y_2)\cos(\phi-\phi_0-\Delta\phi_0)\right]} dx_1 dx_2 dy_1 dy_2 d\phi d\omega \tag{48}$$

Integration with respect to ϕ provides

$$\int_0^{2\pi} e^{i\frac{\omega}{c}\left[(x_1+x_2)\cos(\phi-\phi_0) - (y_1+y_2)\cos(\phi-\phi_0-\Delta\phi_0)\right]} d\phi = 2\pi \sum_{p=0}^{\infty} \epsilon_p J_p\left[\frac{\omega}{c}(x_1+x_2)\right] J_p\left[\frac{\omega}{c}(y_1+y_2)\right] \cos(p\Delta\phi_0) \tag{49}$$

Substituting Equation 49 into 48, the ambiguity function can be written as

$$\Phi = (2\pi)^2 \sum_p \epsilon_p \cos(p\Delta\phi_0) \int \left| \int \omega^2 A(\omega-\omega_0) I_1(x_1) I_2(x_2) J_p\left[\frac{\omega}{c}(x_1+x_2)\right] dx_1 dx_2 \right|^2 d\omega \tag{50}$$

Using the addition theorem for J_p,[8] the ambiguity function can be expressed as

$$\Phi = (2\pi)^2 \sum_p \epsilon_p \cos(p\Delta\phi_0) \int \left| \omega^2 A(\omega-\omega_0) \sum_{q=-\infty}^{\infty} \int I_1(x) J_q\left(\frac{\omega x}{c}\right) dx \int I_2(x) J_{p-q}\left(\frac{\omega x}{c}\right) dx \right|^2 d\omega \tag{51}$$

---

8. A. Gray, G. B. Mathews, and T. M. MacRobert, op. cit. p. 36.

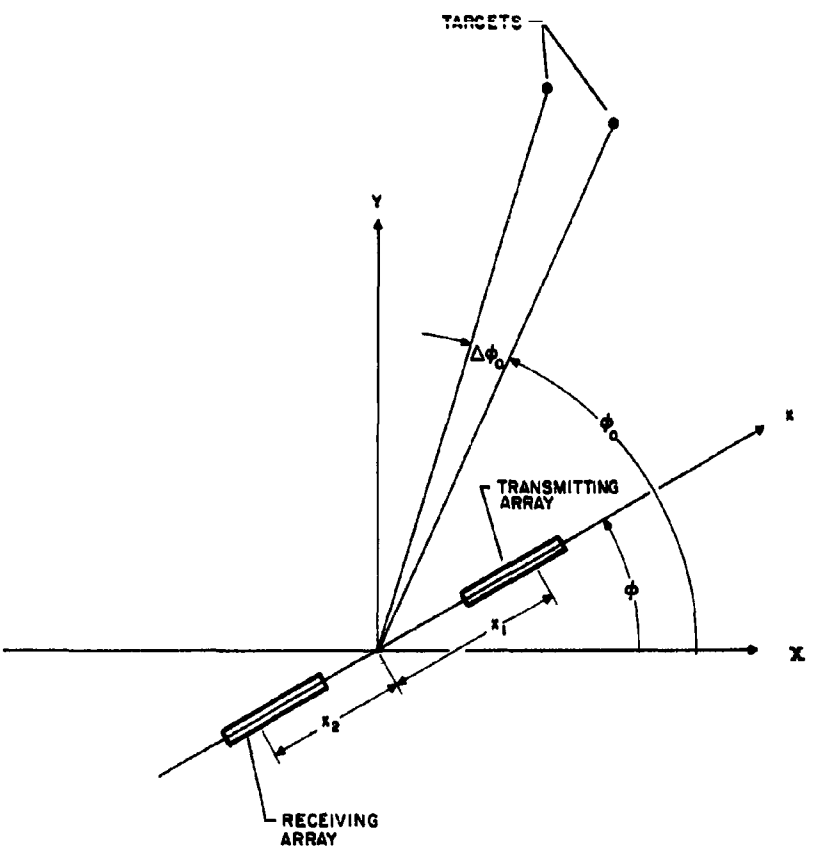

Figure 2 Transmit-Receive Geometry

or

$$\Phi = \sum_{p} \epsilon_p A_p \cos(p\Delta\phi_0) \tag{52}$$

$$A_p = (2\pi)^2 \int \left| \omega^2 A(\omega-\omega_0) \sum_{q} \int I_1(x) J_q\left(\tfrac{\omega x}{c}\right) dx \int I_2(x) J_{p-q}\left(\tfrac{\omega x}{c}\right) dx \right|^2 d\omega \tag{53}$$

Note that in the case of an isotropic transmitter (or receiver) where $I_1(x) = \delta(x)$, Equation 51 reduces to the one-way ambiguity function as given by Equation 19.

In the case of CW transmission, the ambiguity function can be written as the correlation of the product of the receiving and transmitting patterns

$$\Phi = R_e \int G_1(\phi-\phi_0) G_2(\phi-\phi_0) G_1^*(\phi-\phi_0-\Delta\phi_0) G_2^*(\phi-\phi_0-\Delta\phi_0)\, d\phi \tag{54}$$

where G_1 and G_2 are the transmitting and receiving patterns and

$$G_1 = \omega_0 \int I_1(x) e^{i\frac{\omega_0}{c} x\cos\phi}\, dx \tag{55}$$

$$G_2 = \omega_0 \int I_2(x) e^{i\frac{\omega_0}{c} x\cos\phi}\, dx \tag{56}$$

IV. Antenna Pattern and Ambiguity Functions

In this subsection, and in the subsequent technical subsections, the discussion will be limited to the one-dimensional analysis of the array pattern and ambiguity function for CW transmission as formulated in Subsections IIA and B. The purpose is to present the main points of the material as clearly as possible since there is generally greater familiarity with cylindrical harmonics than with spherical harmonics. The development for the two-dimensional analysis, corresponding to the formulation in Subsection IIC, however, is quite similar and footnote descriptions will be given to point out the differences.

The ambiguity function for CW transmission is given by

$$\Phi = R_e \int G(\phi-\phi_0) G^*(\phi-\phi_0-\Delta\phi_0)\, d\phi \tag{27}$$

where $G(\phi)$ is the field pattern of the array. Now $G(\phi - \phi_0)$ is a periodic function and is representable in a Fourier series* as

$$G(\phi-\phi_0) = \omega_0 \int I(x) e^{i\beta_0 x \cos(\phi-\phi_0)}\, dx \tag{57}$$

$$= \sum_{p=0}^{\infty} (i)^p \epsilon_p \cos[p(\phi-\phi_0)] \int \omega_0 I(x) J_p(\beta_0 x)\, dx \tag{58}$$

$$= \sum_{p} \epsilon_p a_p \cos[p(\phi-\phi_0)] \tag{59}$$

where

$$\beta_0 = \frac{\omega_0}{c} \tag{60}$$

$$a_p = (i)^p \omega_0 \int I(x) J_p(\beta_0 x)\, dx \tag{61}$$

Substitution of Equation 59 into Equation 27 yields

$$\Phi = 2\pi \sum_{p} \epsilon_p |a_p|^2 \cos(p\Delta\phi_0) \tag{62}$$

Thus, the Fourier coefficients of the ambiguity function are the squared magnitudes of the coefficients of the corresponding space harmonic of the pattern. It is clearly indicated in the development that only the magnitudes, and not the phases, of the harmonic content of the pattern are of importance

* In the two-dimensional analysis, the zonal harmonic expansion

$$G = \omega_0 \int I(x) e^{i\beta_0 x \cos\gamma}\, dx$$

$$= \sum_{n=0}^{\infty} (2n+1)(i)^n P_n(\cos\gamma) \int \omega_0 I(x) j_n(\beta_0 x)\, dx$$

is used to decompose pattern.

in determining the resolution capability of the array. Hence a highly directive beam pattern is not a necessary condition to achieve high resolution

V. Synthesis of Patterns and Ambiguity Functions

A. Fourier Expansion

The discussion thus far has been concerned with the analysis of the ambiguity function and the array pattern in terms of the illumination function of the array and the spectrum of the signal. The subsection, still restricted to CW operation, will describe some aspects of the synthesis problem.

The discussion will be directed toward the determination of illumination functions to synthesis a realizable ambiguity function or array pattern. As shown in the previous section, the expansion coefficients for the ambiguity function and the pattern are simply related; that is, if

$$\Phi = \sum_{p=0}^{\infty} \epsilon_p A_p \cos(p\Delta\phi_0)$$

and

$$G = \sum_{p=0}^{\infty} \epsilon_p Q_p \cos(p\phi) \tag{63}$$

then

$$A_p = 2\pi |a_p|^2 \tag{64}$$

The synthesis problem is considered by determining the set of illumination functions which independently control the expansion coefficients.

Now

$$A_p = 2\pi w_0^2 \left| \int_{-a}^{a} L(x) J_p(\beta_0 x) dx \right|^2 \tag{65}$$

or

$$A_p = 2\pi\omega_o^2 \left| \int_{-\infty}^{\infty} I'(x) J_p(\beta_o x)\, dx \right|^2 \tag{66}$$

where

$$I'(x) = \begin{cases} I(x), & |x| \le a \\ 0, & |x| > a \end{cases} \tag{67}$$

Let $I'(x)$ be Fourier transformable with the transform $F(z)$

$$I'(x) = \frac{1}{2\pi} \int_{-\infty}^{\infty} F(z) e^{-ixz}\, dz \tag{68}$$

The transform of the Bessel function is given by[9]

$$\frac{1}{2\pi} \int_{-\infty}^{\infty} J_p(\beta_o x) e^{-ixz}\, dx = \begin{cases} \dfrac{(-i)^p}{\pi\beta_o} \dfrac{T_p\left(\frac{z}{\beta_o}\right)}{\left[1-\left(\frac{z}{\beta_o}\right)^2\right]^{1/2}}, & \text{for } \left|\frac{z}{\beta_o}\right| < 1 \\ 0, & \text{for } \left|\frac{z}{\beta_o}\right| > 1 \end{cases} \tag{69}$$

where T_p is the Tschebyscheff polynomial of the first kind. Substituting Equations 68 and 69 into Equation 66 yields

$$A_p = \frac{2\omega_o^2}{\pi} \left| \int_{-1}^{1} \frac{F(z) T_p\left(\frac{z}{\beta_o}\right)}{\left[1-\left(\frac{z}{\beta_o}\right)^2\right]^{1/2}} d\left(\frac{z}{\beta_o}\right) \right|^2 \tag{70}$$

Now, if

$$F(z) = \sum_{m=0}^{M} b_m T_m\left(\frac{z}{\beta_o}\right) \tag{71}$$

---

9. H. Bateman, Tables of Integral Transforms, Vol. I, McGraw-Hill, 1954, pp 43 and 99.

at least within the interval $(z/\beta_0) < 1$, then, by the orthogonality relation of the Tschebyscheff polynomial[10]

$$A_p = \frac{2\pi\omega_0^2 |b_p|^2}{\epsilon_p^2} \quad , \quad p = 0, 1, 2, \cdots, M \tag{72}$$

Hence, all A_p's can be independently controlled and all A_p's can be generated by letting the maximum index, M, tend to infinity.*

The question, now, is the nature of the illumination defined by Equations 68 and 71. $T_m(z/\beta_0)$ is obviously a polynomial in z of order of m. The Fourier transform of these polynomials consists of delta functions and derivatives of delta functions.[11] Hence, if the transform of the illumination function is identically equal to the sum of Tschebyscheff polynomials, the illumination function itself will consist of the sum of delta functions, doublets, triplets, etc., all located at x = 0. Note that the side condition, given by Equation 67 is satisfied in this case.

Another viewpoint on the required character of the illumination function is obtained if it is recalled that independent control of the A_p's implies independent control of the coefficients of the Fourier series expansion of the pattern (see Equation 64). Hence, the required illumination

---

10. W. Magnus and F. Oberhettinger, Special Functions of Mathematical Physics, Chelsea Publishing Co., 1948, p. 80.

* In the two-dimensional analysis, the coefficients of the ambiguity function expansion is given by

$$A_n = 4\pi\omega_0^2(2n+1)\left|\int_{-a}^{a} I(x) j_n(\beta_0 x)\, dx\right|^2$$

for CW transmission. By applying Parsevals' relation,

$$A_n = \pi\omega_0^2(2n+1)\left|\int_{-1}^{1} F(z) P_n\left(\frac{z}{\beta_0}\right) d\left(\frac{z}{\beta_0}\right)\right|^2$$

where the Legendre polynomial is the transform at the spherical Bessel function (see H. Bateman, op. cit., pp. 122, 123). Independent control of the A_n's is obtain when

$$F(z) = \sum_{m=0}^{M} b_m P_m\left(\frac{z}{\beta_0}\right)$$

11. A. Papoulis, The Fourier Integral and Its Applications, McGraw-Hill 1962, p. 41.

function to generate independent A_p's (a_p's) is that function which produces cosinusoidal patterns. That this function is given by the transform of the Tschebyscheff polynomial is easily verified by substituting the illumination function

$$I'(x) = \frac{1}{2\pi}\int_{-\infty}^{\infty} T_m\left(\frac{z}{\beta_0}\right) e^{-ixz}\, dz$$

into

$$G = \omega_0 \int_{-\infty}^{\infty} I'(x)\, e^{i\beta_0 x\cos\phi}\, dx$$

and recognizing that

$$T_m(\cos\phi) = \cos(m\phi) \tag{73}$$

B. An Approximation Using Hermite Polynomials

In the previous section, it was shown that the illumination function required to obtain independent control of the coefficients of the Fourier series of the ambiguity function and the pattern was given by

$$I'(x) = \frac{1}{2\pi}\sum_m b_m \int T_m\left(\frac{z}{\beta_0}\right) e^{-ixz}\, dz$$

But

$$T_m\left(\frac{z}{\beta_0}\right) = C_m\left(\frac{z}{\beta_0}\right)^m + C_{m-2}\left(\frac{z}{\beta_0}\right)^{m-2} + \cdots \tag{74}$$

so that

$$I'(x) = \beta_0 \sum_m b_m \left[C_m (i)^m \frac{d^m \delta(\beta_0 x)}{d(\beta_0 x)^m} + C_{m-2}(i)^{m-2} \frac{d\delta^{m-2}(\beta_0 x)}{d(\beta_0 x)^{m-2}} + \cdots \right] \tag{75}$$

This illumination function, consisting of singular functions, is not of great physical interest. Consequently, the effects of approximating the delta function by a continuous function is investigated. In particular, the approximation to the delta function given by

$$f(k, \beta_o x) = \frac{k}{\sqrt{2\pi}} e^{-\frac{1}{2}(k\beta_o x)^2} \tag{76}$$

where

$$\lim_{k \to \infty} f(k, \beta_o x) = \delta(\beta_o x) \tag{77}$$

is considered. The value of the constant, k, in Equation 76 is yet to be determined. Now the m-th derivative of $f(k, \beta_o x)$ can be expressed as

$$f^{(m)} = \frac{d^m f}{d(\beta_o x)^m} = \frac{(-1)^m k^{m+1}}{\sqrt{2\pi}} e^{-\frac{1}{2}(k\beta_o x)^2} He_m(k\beta_o x) \tag{78}$$

where He_m is the Hermite polynomial.[12]

Using the above approximation, the illumination function is

$$I(x) = \beta_o \sum_m b_m \left[C_m (-i)^m \frac{k^{m+1}}{\sqrt{2\pi}} e^{-\frac{1}{2}(k\beta_o x)^2} He_m(k\beta_o x) + \cdots \right] \tag{79}$$

Consider, for the moment, the pattern due to an illumination function consisting of only the m-th derivative of $f(k, \beta_o x)$.

$$G_m = \frac{w_o C_m (-i)^m k^{m+1}}{\sqrt{2\pi}} \int_{-\beta_o a}^{\beta_o a} e^{-\frac{1}{2}(k\beta_o x)^2} He_m(k\beta_o x) e^{i\beta_o x \cos\phi} d(\beta_o x) \tag{80}$$

where the constant b_m is suppressed. The finite limits of integration can be replaced by infinite limits if it is shown that for any $\beta_o a > 0$ and any m,

$$\lim_{k \to \infty} \left[k^{m+1} \int_{\beta_o a}^{\infty} e^{-\frac{1}{2}(k\beta_o x)^2} He_m(k\beta_o x) e^{i\beta_o x \cos\phi} d(\beta_o x) \right] = 0 \tag{81}$$

---

12. W. Magnus and F. Oberhettinger, op. cit., p. 80.

or

$$\lim_{k\to\infty}\left[\int_{\beta_0 a}^{\infty} f^{(m)} e^{i\beta_0 x\cos\phi}\, d(\beta_0 x)\right] = 0 \tag{82}$$

To demonstrate, integrate Equation 82 by parts so that

$$\int_{\beta_0 a}^{\infty} f^{(m)} e^{i\beta_0 x\cos\phi}\, d(\beta_0 x) = f^{(m-1)} e^{i\beta_0 x\cos\phi}\Big|_{\beta_0 a}^{\infty} - (i\cos\phi)\int_{\beta_0 a}^{\infty} f^{(m-1)} e^{i\beta_0 x\cos\phi}\, d(\beta_0 x) \tag{83}$$

Referring to Equation 78, it is seen that

$$\lim_{k\to\infty}\left[f^{(m-1)} e^{i\beta_0 x\cos\phi}\Big|_{\beta_0 a}^{\infty}\right] = 0 \tag{84}$$

since the term is identically equal to zero at the upper limit of integration and vanishes exponentially under the limiting processing for all m and $\beta_0 a > 0$. Continued integration of Equation 83, with application of Equation 84, leaves only the term proportional to

$$C = \int_{\beta_0 a}^{\infty} f\, e^{i\beta_0 x\cos\phi}\, d(\beta_0 x) = \frac{K}{\sqrt{2\pi}}\int_{\beta_0 a}^{\infty} e^{-\frac{1}{2}(k\beta_0 x)^2}\, e^{i\beta_0 x\cos\phi}\, d(\beta_0 x) \tag{85}$$

to be considered. But

$$|C| \le \frac{K}{\sqrt{2\pi}}\int_{\beta_0 a}^{\infty}\left|e^{-\frac{1}{2}(k\beta_0 x)^2}\, e^{i\beta_0 x\cos\phi}\right| d(\beta_0 x) = \frac{K}{\sqrt{2\pi}}\int_{\beta_0 a}^{\infty} e^{-\frac{1}{2}(k\beta_0 x)^2}\, d(\beta_0 x) \tag{86}$$

$$|C| \le \frac{K}{\sqrt{2\pi}}\int_{\beta_0 a}^{\infty} e^{-\frac{1}{2}k^2\beta_0^2 x}\, d(\beta_0 x) = \sqrt{\frac{2}{\pi}}\,\frac{e^{-\frac{1}{2}(k\beta_0 a)^2}}{K\beta_0 a}$$

so that

$$\lim_{k\to\infty}\left[|C|\right] = 0 \tag{87}$$

Hence, the pattern given by Equation 80 can be written as

$$G_m = \frac{w_0 c_m (-i)^m k^{M+1}}{\sqrt{2\pi}} \int_{-\infty}^{\infty} e^{-\frac{1}{2}(k\beta_0 x)^2} He_m(k\beta_0 x) e^{i\beta_0 x \cos\phi} d(\beta_0 x) \tag{88}$$

with arbitrarily small error for k sufficiently large. Integration of Equation 88 yields [13]

$$G_m = w_0 c_m e^{-\frac{1}{2}\left(\frac{\cos\phi}{k}\right)^2} \cos^M\phi \tag{89}$$

and, since k is large,

$$G_m = w_0 c_m \cos^m\phi \tag{90}$$

Returning to the complete illumination function, it is obvious that the function given by Equation 79 gives rise to the pattern

$$G = w_0 \sum_m b_m \left[c_m \cos^m\phi + c_{m-2} \cos^{m-2}\phi + \cdots \right] \tag{91}$$

But, from Equations 74 and 73 this is equal to:

$$G = w_0 \sum_m b_m T_m(\cos\phi) = w_0 \sum_m b_m \cos(m\phi) \tag{92}$$

The Gaussian-weighted Hermite functions, thus, provide continuous functions over a finite aperture to approximately generate (independently) the Fourier components of the beam pattern and the ambiguity function.

13. F. Oberhettinger, Tabellen zur Fourier Transformation, Springer-Verlag, 1957, pp. 45 and 156.

C. Some Interesting Patterns

It was shown in the previous section that, if

$$I(x) = \frac{\beta_0 (-i)^m K^{m+1}}{\omega_0 \sqrt{2\pi}} e^{-\frac{1}{2}(K\beta_0 x)^2} He_m(K\beta_0 x) \tag{93}$$

then the resulting pattern is

$$G_m = \cos^m \phi$$

Note that G_m is a highly directive pattern with a front and back lobes of equal magnitude. Further note that the pattern is not a function of array length or operating frequency. In fact, in the derivation of the pattern, it was shown that the above pattern could be obtained with any array of length greater than zero. It has been further shown that the consinusoidal patterns needed to independently control the coefficients of the Fourier expansions of the pattern and the ambiguity function can be obtained with an array of arbitrary length. Thus the possibility of obtaining super-directivity and/or superresolution is present with illumination functions consisting of Gaussian-weighted Hermite functions.

If the illumination function of Equation 93 is modified by a linear phase shift

$$I(x) = \frac{\beta_0 (-i)^m K^{m+1}}{\omega_0 \sqrt{2\pi}} e^{-\frac{1}{2}(K\beta_0 x)^2} He_m(K\beta_0 x) e^{i\xi\beta_0 x} \tag{94}$$

then

$$G_1 = (\xi + \cos\phi)^m \tag{95}$$

Note that for $\xi = 1$ (or - 1), an endfire pattern is obtained with no backlobe.

If a broadside pattern[14] of the type

$$G = \sin^{2n}\phi \tag{96}$$

is desired, then the relation

$$\sin^{2n}\phi = (1-\cos^2\phi)^n = \sum_{m=0}^{n} (-1)^m \binom{n}{m} \cos^{2m}\phi \tag{97}$$

is utilized, from which it is seen that the illumination function is given by

$$I(x) = \frac{\beta_0 K}{\omega_0\sqrt{2\pi}} \sum_{m=0}^{n} \binom{n}{m} K^{2m} e^{-\frac{1}{2}(K\beta_0 x)^2} H_{e_{2m}}(K\beta_0 x) \tag{98}$$

The factor $\left|\begin{matrix} n \\ m \end{matrix}\right|$ is the binomial coefficient.

VI. Summary

The kernal of a general theory on the resolution capability of linear arrays has been developed. One of the major points of the paper is that the resolution capability is characterized by the complex autocorrelation function of the array pattern and is limited only by the magnitudes, and not the phases, of the spatial harmonic content of the array pattern.

Several expansions of the ambiguity function are given which provide new viewpoints on the relations between resolution, array pattern, signal spectrum and the illumination function. Further, these expansions provide expressions through which array illumination functions can be synthesized. The particular case of determining the illumination function which independently controls the expansion coefficients of the ambiguity function and the pattern has been analyzed in some detail. It is shown one set of continuous functions consists of Gaussian-weighted Hermite polynomials.

Most of the detailed analysis is restricted to the case of CW transmission. The interesting problem of examining the structure of signal modulation functions to control the ambiguity function has not been undertaken.

14. The following pattern and illumination function is developed by C. J. Bouwkamp and N. G. DeBruijn, "The Problem of Optimum Antenna Current Distribution," Philips Res. Repts., Vol. 1, No. 2, Jan. 1946, pp. 135-158.

SECTION III

THE THEORY OF RESOLUTION OF LINEAR ARRAY ANTENNAS
TIME VARYING ILLUMINATION FUNCTIONS

I. Introduction

The resolution properties of an antenna are related to the manner in which it can make signals received from different points of space different. The measure of this difference will be taken as the squared difference of the signals integrated over all space and time. Simultaneous resolution in range, as well as in angle, will be considered; this will lead to the range-angle ambiguity function.

The function f(x, t), giving the signal at each point on the transmitting aperture for all time, is the most general description of a linear transmitting array, and can result in any desired time varying pattern. The nature of the following treatment (in which the transmit-receive case is also discussed) is general enough to include superdirectivity and aperture "transmit time" problems. With a time varying illumination function, the time structure of the returns from different angles can be made to be as different as possible. Shanks [1] describes a special case without provision for range resolution, in which the returns from different angles are at different frequencies.

II. Transmitting Array

A. The Pattern

Denote the signal originating at a point x on a linear array by f(x, t), or equivalently by F(x, ω)

$$\begin{cases} f(x,t) = a(x,t)e^{i\omega_0 t} = \int A(x,\omega)e^{i(\omega+\omega_0)t}\,d\omega = \int A(x,\omega-\omega_0)e^{i\omega t}\,d\omega & (1) \\ F(x,\omega) = \frac{1}{2\pi}\int f(x,t)e^{-i\omega t}\,dt = A(x,\omega-\omega_0) & (2) \end{cases}$$

---

1. H. E. Shanks, "A New Technique for Electronic Scanning," IRE Trans. Antennas and Propagation, Vol. AP-9, pp. 162-166, March, 1961.

where $F(x, \omega)$ and $A(x, \omega)$ are the Fourier transforms of $f(x, t)$ and $a(x, t)$, respectively. In this notation, $a(x, t)$ is the complex time variable illumination function and can be considered as an illumination function at any instant t, or as a modulation function at any point x. For the special case of a time invariant illumination function, $a(x, t) = I(x)\, a(t)$ where $a(t)$ is the modulation function of the signal.

The signal at a point R_o, ϕ in two-dimensional space, with ϕ measured counterclockwise from the array axis, can be expressed as

$$S(t) = \iint \omega A(x, \omega - \omega_o)\, e^{i\omega\left(t - \frac{R_o}{c} + \frac{x}{c}\cos\phi\right)}\, dx\, d\omega \tag{3}$$

$$S(\omega) = \omega \int A(x, \omega - \omega_o)\, e^{-i\frac{\omega}{c}(R_o - x\cos\phi)}\, dx \tag{4}$$

where only the signal dependence on the form factor of the array is considered. Equation 3 can be rewritten as

$$S(t) = \iint (\omega + \omega_o) A(x, \omega)\, e^{i(\omega+\omega_o)\left(t - \frac{R_o}{c} + \frac{x}{c}\cos\phi\right)}\, dx\, d\omega \tag{5}$$

$$= \int \left[\omega_o a\left(x, t - \frac{R_o}{c} + \frac{x}{c}\cos\phi\right) - i\frac{\partial}{\partial t} a\left(x, t - \frac{R_o}{c} + \frac{x}{c}\cos\phi\right)\right] e^{i\omega_o\left(t - \frac{R_o}{c} + \frac{x}{c}\cos\phi\right)}\, dx \tag{6}$$

Now define the generalized beam pattern by the pair

$$g(\phi, t) = \int \left[\omega_o a\left(x, t + \frac{x}{c}\cos\phi\right) - i\frac{\partial}{\partial t} a\left(x, t + \frac{x}{c}\cos\phi\right)\right] e^{i\omega_o\left(t + \frac{x}{c}\cos\phi\right)}\, dx \tag{7}$$

$$= \iint \omega A(x, \omega - \omega_o)\, e^{i\omega t}\, e^{i\frac{\omega x}{c}\cos\phi}\, dx\, d\omega \tag{8}$$

$$G(\phi, \omega) = \int \omega A(x, \omega - \omega_o)\, e^{i\frac{\omega x}{c}\cos\phi}\, dx \tag{9}$$

so that, with $\tau = \dfrac{R_o}{c}$, Equations 3, and 4 become

$$\begin{cases} s(t) = g(\phi, t-\tau) & (10) \\ S(\omega) = G(\phi, \omega) e^{-i\omega\tau} & (11) \end{cases}$$

Equations 7 and 8 have been defined so that they reduce to the standard expressions for the beam pattern, multiplied by $\exp(i\omega_0 t)$, in the particular case of transmission of an CW sinusoid at frequency ω_0.

B. The Ambiguity Function

Consider the signals at the points (R_0, ϕ) and $(R_0 + \Delta R, \phi - \Delta\phi)$ and define a measure of their difference as

$$\epsilon^2 = \iint |s_1 - s_2|^2 \, d\phi \, dt \quad (12)$$

$$= \iint |s_1|^2 d\phi dt + \iint |s_2|^2 d\phi dt - 2 \mathrm{Re} \iint s_1 s_2^* \, d\phi \, dt \quad (13)$$

For good resolution, ϵ^2 should be large for all ΔR, $\Delta\phi$ not equal to zero. Neglecting the amplitude dependence of the signal on ΔR (for small $\frac{\Delta R}{R_0}$, it is negligible), the first two integrals are equal and independent of ΔR and $\Delta\phi$ The function of interest is

$$\Phi(\Delta\phi, \Delta\tau) = \mathrm{Re} \iint s_1 s_2^* \, d\phi \, dt \quad (14)$$

which should be small for all $\Delta\phi$, ΔR not equal to zero. Substituting Equation 10, with $\Delta\tau = \frac{\Delta R}{c}$, yields

$$\Phi = \mathrm{Re} \iint g(\phi, t-\tau) g^*(\phi - \Delta\phi, t - \tau - \Delta\tau) \, d\phi \, dt \quad (15)$$

Applying Parseval's formula

$$\int_{-\infty}^{\infty} g_1(t) g_2^*(t) \, dt = 2\pi \int_{-\infty}^{\infty} G_1(\omega) G_2^*(\omega) \, d\omega \quad (16)$$

to Equation 15, there results

$$\Phi = 2\pi R_e \iint G(\phi,\omega) G^*(\phi-\Delta\phi,\omega) e^{i\omega\Delta\tau} \, d\phi \, d\omega \tag{17}$$

It should be pointed out that the analysis, thus far, applies to finite energy signals where

$$\int_{-\infty}^{\infty} |f(t)|^2 dt < \infty \tag{18}$$

For finite power signals, which include periodic signals and where

$$\langle |f(t)|^2 \rangle = \lim_{T\to\infty} \frac{1}{2T} \int_{-T}^{T} |f(t)|^2 dt < \infty \tag{19}$$

the time integrations should be replaced by time averages and spectral densities should be employed rather then Fourier transforms.[2] For example, Equation 15 should be replaced by

$$\Phi = R_e \left\langle \int_0^{2\pi} g(\phi,t-\tau) g^*(\phi-\Delta\phi, t-\tau-\Delta\tau) d\phi \right\rangle \tag{20}$$

Note that by putting $\Delta\tau = 0$, the angular ambiguity function is the time average of the autocorrelation function of the beam pattern and not the correlation function of the time-averaged beam pattern.

C. Synthesis of the Ambiguity Function

Consider the class of finite energy signals. By substituting Equation 9 into Equation 17, the ambiguity function can be expanded as

$$\Phi = 2\pi R_e \iiiint \omega^2 A(x_1, \omega-\omega_0) A^*(x_2, \omega-\omega_0) e^{i\frac{\omega}{c}[x_1\cos\phi - x_2\cos(\phi-\Delta\phi)]} e^{i\omega\Delta\tau} \, dx_1 \, dx_2 \, d\phi \, d\omega \tag{21}$$

2. A Papoulis, The Fourier Integral and its Applications, McGraw-Hill, New York, 1962, Chapter 12.

Performing the integration with respect to ϕ yields

$$\int_0^{2\pi} e^{i\frac{\omega}{c}[x_1\cos\phi - x_2\cos(\phi-\Delta\phi)]}\,d\phi = 2\pi J_0\left\{\frac{\omega}{c}\left[x_1^2+x_2^2-2x_1x_2\cos(\Delta\phi)\right]^{1/2}\right\} \tag{22}$$

where J_0 is the Bessel function of the first kind of order zero. Application of the addition theorem yields

$$J_0\left\{\frac{\omega}{c}\left[x_1^2+x_2^2-2x_1x_2\cos(\Delta\phi)\right]^{1/2}\right\} = \sum_{p=0}^{\infty}\epsilon_p J_p\left(\frac{\omega x_1}{c}\right)J_p\left(\frac{\omega x_2}{c}\right)\cos(p\Delta\phi) \tag{23}$$

where ϵ_p is the Neumann number ($\epsilon_p = 1$ for $p = 0$, $\epsilon_p = 2$ for $p > 0$). The ambiguity function can now be expressed as a Fourier series in $\Delta\phi$

$$\Phi = \mathrm{Re}\sum_{p=0}^{\infty}\epsilon_p\left[\int A_p(\omega)\,e^{i\omega\Delta\tau}\,d\omega\right]\cos(p\Delta\phi) \tag{24}$$

$$= \sum_{p}\epsilon_p\int A_p(\omega)\cos(\omega\Delta\tau)\,d\omega\,\cos(p\Delta\phi) \tag{25}$$

$$A_p(\omega) = (2\pi)^2\left|\omega\int A(x,\omega-\omega_0)J_p\left(\frac{\omega x}{c}\right)dx\right|^2 \tag{26}$$

For good range resolution, $A_p(\omega)$ should be wideband in ω; for good angular resolution, $A_p(\omega)$ should be "wideband" in p. To synthesize a desired ambiguity function, $A(x,\omega)$ must be chosen such that

$$\left|2\pi\omega\int A(x,\omega-\omega_0)J_p\left(\frac{\omega x}{c}\right)dx\right|^2 = \frac{1}{2\pi}\int_{-\infty}^{\infty}\int_0^{2\pi}\Phi\cos(p\Delta\phi)\cos(\omega\Delta\tau)\,d(\Delta\phi)\,d(\Delta\tau) \tag{27}$$

where the right-hand side of Equation 27 is a double Fourier cosine transform of the ambiguity function.

Note that if the pattern given by Equation 9 is expanded in a Fourier series as

$$G(\psi,\omega) = \int \omega A(x,\omega-\omega_0)\left[\sum_p \epsilon_p (i)^p J_p\left(\frac{\omega x}{c}\right)\cos(p\phi)\right] dx \tag{28}$$

$$= \sum_p \epsilon_p (i)^p \left[\int \omega A(x,\omega-\omega_0) J_p\left(\frac{\omega x}{c}\right) dx\right] \cos(p\phi) \tag{29}$$

$$= \sum_p \epsilon_p a_p(\omega)\cos(p\phi) \tag{30}$$

where

$$a_p(\omega) = (i)^p \int \omega A(x,\omega-\omega_0) J_p\left(\frac{\omega x}{c}\right) dx \tag{31}$$

then it is seen that

$$A_p(\omega) = (2\pi)^2 |a_p(\omega)|^2 \tag{32}$$

III. Transmit-Receive Operation

A. Ambiguity Function

Let the time variable illumination functions of the transmitting and receiving arrays be given by $f_1(x,t)$ and $f_2(y,t)$, respectively, with Fourier transforms given by $F_1(x,\omega)$ and $F_2(y,\omega)$. The signal reflected off at a target at R_0,ϕ and incident at a point y on the time variable receiving array is of the form

$$S(\omega) = \int \omega F_1(x,\omega) e^{-i\frac{\omega}{c}[2R_0-(x+y)\cos\phi]} dx \tag{33}$$

The illumination function of the receiving array is

$$\begin{cases} f_2(y, t - \frac{2R_0}{c}) & (34) \\ F_2(y, \omega) e^{-i\frac{\omega}{c}(2R_0)} & (35) \end{cases}$$

so that the received signal is of the form

$$S(\omega) = \iint \omega^2 F_1(x,\omega) F_2(y,\omega) e^{-i\frac{\omega}{c}[4R_0 - (x+y)\cos\phi]} dx dy \quad (36)$$

As in the previous section, define the generalized transmitting pattern, $G_1(\phi, \omega)$, and receiving pattern, $G_2(\phi, \omega)$, as

$$G_1(\phi,\omega) = \int \omega F_1(x,\omega) e^{i\frac{\omega}{c}x\cos\phi} dx \quad (37)$$

$$G_2(\phi,\omega) = \int \omega F_2(y,\omega) e^{i\frac{\omega}{c}y\cos\phi} dy \quad (38)$$

and a two-way pattern as

$$G(\phi,\omega) = G_1(\phi,\omega) G_2(\phi,\omega) \quad (39)$$

With $\tau_0 = \dfrac{4 R_0}{c}$, the received signal can be expressed as

$$S(\omega) = G(\phi,\omega) e^{-i\omega\tau_0} \quad (40)$$

Note that, if $G_2(\phi,\omega) = G_1^*(\phi,\omega) e^{i\omega\frac{\tau_0}{2}}$, the receiver is matched in range to the transmitted signal and the output signal,

$$S(\omega) = |G(\phi,\omega)|^2 e^{-i\omega\frac{\tau_0}{2}} \tag{41}$$

$$s(t) = \int |G(\phi,\omega)|^2 e^{i\omega(t-\frac{\tau_0}{2})} d\omega \tag{42}$$

is a collapsed pulse, obtained without any further processing, occurring at $t = \frac{\tau_0}{2} = \frac{2R_0}{c}$.

The form of the received signal in the transmit-receive operation as expressed by Equation 40, is the same as that for the transmit case, as expressed by Equation 11. Using the same difference measure of signals as in the previous analysis, the combined range-angle ambiguity function for the transmit-receive operation can be written as

$$\Phi = 2\pi R_t \iint G(\phi,\omega) G^*(\phi-\Delta\phi,\omega) e^{i\omega\Delta\tau_0} d\phi d\omega \tag{43}$$

$$= 2\pi R_t \iint G(\phi+\Delta\phi,\omega) G^*(\phi,\omega) e^{i\omega\Delta\tau_0} d\phi d\omega \tag{44}$$

where, again, $\Delta R_0 = \frac{c\Delta\tau_0}{4}$ is the range separation of the targets.

B. Implementation

For illustrative pruposes, a direct method of synthesizing the ambiguity function of Equation 44 will be described.

Assume that the output of the receiving antenna is fed into a bank of filters, the p-th filter having an impulse response $h_p(t)$ and frequency response $H_p(\omega)$. The received signal, from a target at R, ϕ, is given by Equation 40 as

$$S(\omega) = G(\phi,\omega) e^{-i\omega\tau} \tag{45}$$

The filter output, $S_p(\omega)$, is

$$S_p(\omega) = G(\phi, \omega) H_p(\omega) e^{-i\omega\tau} \tag{46}$$

Now assume that the filter is matched to the signal structure from a return at the angle ϕ_r, i.e., assume

$$H_p(\omega) = G^*(\phi_r, \omega)$$

Then

$$S_p(\omega) = G(\phi, \omega) G^*(\phi_r, \omega) e^{-i\omega\tau} \tag{47}$$

Let

$$\phi = \phi_r + \Delta\phi_r \tag{48}$$

so that

$$\begin{cases} S_p(\omega) = G(\phi_r + \Delta\phi_r, \omega) G^*(\phi_r, \omega) e^{-i\omega\tau} & (49) \\ s_p(t) = \int G(\phi_r + \Delta\phi_r, \omega) G^*(\phi_r, \omega) e^{i\omega(t-\tau)} d\omega & (50) \end{cases}$$

The filter output should be highly peaked at $\Delta\phi_r = 0$ and $t = \tau$, and small for all other values. It is seen that the real parts of the outputs at the filters (which could be obtained through coherent detection) is an angle dependent ambiguity function, each filter being matched to a different angle. In order to facilitate the decision making process of determining the presence of a target, or to resolve several targets, it would be desirable to have $s_p(t)$ relatively independent of p. Note that the sum of the filter outputs, if the filters are matched at discrete points throughout all ϕ, approximate the ambiguity function of Equation 44.

If the real part of the output of a single filter is used and the antenna is rotated, then the output integrated over all angles is

$$\mathrm{Re}\int S_p(t)\,d\phi = \mathrm{Re}\iint G(\phi+\Delta\phi,\omega)G^*(\phi,\omega)e^{j\omega(t-\tau)}\,d\omega\,d\phi \qquad (51)$$

which is the ambiguity function of Equation 44.

SECTION IV

THE THEORY OF SUPERDIRECTIVE ARRAYS

I. Introduction

Previous approaches to superdirectivity have been primarily concerned with the direct synthesis of narrow beam patterns. This approach has been applied even in situations where angular resolution, and not directivity per se, was of particular interest. There is no denying that there exists a strong relation between angular resolution and pattern directivity but the relationship is not fundamental.[1,2] In this paper some classical approaches to superdirectivity will be discussed first. This will then be followed by a description of some recent progress in the theory of superdirectivity and superresolution made through analyses based on the angular ambiguity function.

Apparently, the first suggestion of superdirectivity was by Oseen[3] in 1922. The subject lay more or less dormant until 1943. In that year, Schelkunoff[4] published a paper on the theory of linear arrays in which he discussed the synthesis of superdirective arrays. This paper received a wide audience and is sometimes credited with having introduced the concept of superdirectivity. In 1946, a paper of fundamental importance appeared by Bouwkamp and deBruijn;[5] these authors rigorously proved that there is no limit to the gain obtainable with a linear array. Since then, the literature on the subject has grown impressively: methods of achieving superdirectivity through

1. H. Urkowitz, C. Hauer, J. Koval "Generalized Resolution in Radar Systems," Proc. IRE, Vol. 50, Oct. 1962, pp. 2093-2105.

2. See paper on "The Theory of Resolution of Linear Array Antennas, Time Invariant Illumincation Functions."

3. C. W. Oseen, "Die Einsteinsche Nadelstichstrahlung und die Maxwellschen Gleichungen," Annalen der Physik, Vol. 69, 1922, p. 202.

4. S. A. Schelkunoff, "A Mathematical Theory of Linear Arrays," Bell System Tech Jour. Vol. 22, Jan 1943, p. 80

5. C. W. Bouwkamp and N. G. deBruijn, "The Problem of Optimum Antenna Current Distribution," Philips Res. Repts., Vol. 1, Jan. 1946, p. 135.

various linear and nonlinear techniques with possible applications in radar, communications, acoustics, sonar, and radio astronomy have been discussed. A bibliography, compiled previously by Bloch et al,[6,7] is included.

Despite the obvious theoretical advantages to be gained with superdirective arrays in a wide variety of applications, the experimental work in the field has been meager. For reasons to be enumerated later, large superdirective arrays have been deemed to be impractical. Consequently, the experimental efforts which have been performed have all had the limited objective of obtaining a modest improvement in directivity. Spitz[8] reports on an effort to obtain superdirectivity using a five element array, 0.75 wavelengths long, and an eleven element array, 1.67 wavelengths long at 9 Gc. The arrays consisted of stacks of open-ended waveguides with the narrow dimensions reduced. Using the five element array, he reports obtaining a 3 db beamwidth of 18 degrees with sidelobes down 25 db. Ferrite isolators were used in the feed lines to reduce mutual coupling effect. Although the losses in the isolators and attenuators (for amplitude adjustment) could not be exactly accounted for, an approximate measurement of the gain of the five element array showed it to be slightly greater than the gain of a uniformly illuminated horn of the same dimensions.

There also appears to be some interest arising in the possible use of superdirective arrays at the VLF frequencies. In VLF applications some of the detrimental properties characteristic of superdirective techniques may be tolerable. A similar situation may prevail in sonar applications

II. Classical Properties

One of the more concise statements of the problems associated with superdirective arrays is given by Taylor.[9] An indication of the problems which Taylor discusses can be obtained from some typical illumination functions

6. A. Bloch, R. G. Medhurst, S. D. Pool, "A New Approach to the Design at Superdirective Aerial Arrays," Proc. IEE, Vol. 100, Part III, 1953 p. 303.

7. A. Bloch, R. G. Medhurst, S. D. Pool, "Superdirectivity," Proc. IRE, Vol. 48, June 1960, p. 1164.

8. E. Spitz, "Supergain and Volumetric Antennas," AFCRL-TD-59-194, 15 June 1959, Final Rept. AF 61(052)-102.

9. T. T. Taylor, "A Discussion of the Maximum Directivity of an Antenna," Proc. IRE, Vol. 36, Sept 1948, p. 1135.

computed by Yaru[10] and Woodward and Lawson.[11]

Briefly, the classical superdirective aperture is formed by exciting an array of elements in which the interelement spacing is less than a half wavelength. As the degree of superdirectivity is increased, the dynamic range of currents which excite the radiating element increases and it is found that adjacent elements are 180 degrees out of phase. These characteristics give rise to the following problems:

1. Excessive mutual coupling - Large mutual coupling effects are due to the close spacings of the radiators. The mutual coupling effect can prevent the realization of the required illumination function.

2. Large error sensitivity - The peak value of the beam is a small fraction of the field produced by any one radiator; hence, small amplitude and phase errors can have large effects on beam formation.

3. High ohmic losses - Large copper losses are due to the large currents, required at the radiating elements.

4. Low antenna bandwidth - Since reactive fields are generated in the vicinity of the aperture, the antenna impedance must be matched with high Q circuits; use of these circuits reduces usable bandwidth.

5. Dynamic range of currents - Large variations in the relative values of the current at the radiators are required to achieve superdirective beams; hence, practical problems exist in attempting to design practical feed networks.

III. Historical Approaches

A variety of analytical techniques exist to determine illumination functions for superdirective arrays. A small sampling of these techniques, as they have been derived in the past, will be described very briefly.

---

10. N. Yaru, "A Note on Super-Gain Antenna Arrays," Proc. IRE, Vol. 39, Sept. 1951, p. 1081

11. P. M. Woodward and J. D. Lawson, "The Theoretical Precision with which an Arbitary Radiation Pattern may be Obtained from a Source of Finite Size, J. of IEE, Vol. 95, Part III, 1948, p. 363.

A. Schelkunoff[12]

By a simple transformation of variables,

$$e^{i\left(\frac{2\pi}{\lambda} d \cos\phi - \alpha\right)} = z \qquad (1)$$

where

λ = wavelength

d = interelement spacing

ϕ = angle measured from array axis

α = progressive phase delay

Schelkunoff was able to show that the form factor of a linear array of n elements, with commensurable element separation, can be expressed as a polynomial in z, of degree n - 1. The variable z lies on the unity circle in the complex plane, and the range of z, corresponding to its range of values for $|\cos\phi| \leq 1$, is determined by d/λ and α. In this representation, nulls of the pattern correspond to the zeros of the polynomial, and these values of z (as with all values of z giving rise to fields in the range $|\cos\phi| \leq 1$) lie on the unit circle in the range of z.

The zeros of the polynomial corresponding to a uniform array are equispaced on the unit curcle since they correspond to the n^{th} roots of unity. It was reasoned that zeros occuring outside the range of z could not effectively contribute to the formation of the real pattern. With this descriptive logic Sehelkunoff was able to demonstrate that considerable improvement in the directivity could be obtained by equispacing all zeros of the array polynomial within the range of z. This procedure presumably allowed greater control of formation of the real patterns.

B. Dolph-Riblet[13, 14]

If Schelkunoff's technique of equispacing the nulls is applied to the broadside pattern, it is found that superdirective patterns are not obtained as

12. op. cit.

13. C. L. Dolph, "Current Distribution for Broadside Arrays which Optimizes the Relationship between Beam Width and Side-Lobe Level," Proc. IRE, Vol. 34, June 1946, p. 335.

14. C. L. Dolph and H. J. Riblet, "A Current Distribution for Broadside Arrays which Optimizes the Relationship between Beam Width and Side-Lobe Level," Proc. IRE, Vol. 35, May 1947, p. 489.

the element spacing is decreased. However, broadside superdirective patterns can be synthesized by using the properties of the Tschebyscheff polynominal. Dolph showed the method whereby an "optimum" pattern could be synthesized by equating the array factor of n equispaced elements to the Tschebyscheff polynomial of degree n - 1. The pattern was given by

$$G = T_{n-1}(x) = \begin{cases} \cos\left[(n-1)\cos^{-1}x\right] & , |x| < 1 \\ \cosh\left[(n-1)\cosh^{-1}x\right] & , |x| > 1 \end{cases} \tag{2}$$

$$x = x_0 \cos\left(\frac{\pi d}{\lambda}\cos\phi\right) \tag{3}$$

$T_{n-1}(x_0)$ = peak-to-sidelobe level

Dolph's original technique was valid only for cases when $d \geq \lambda/2$. However, Riblet extended the technique and showed, by a simple shift and scale change of the variable x, that superdirective Tschebyscheff patterns could be obtained if the number of radiating elements was odd.

C. Bouwkamp and de Bruijn [15]

LaPaz and Miller [16] attempted to solve the problem of determining the "optimum" current distribution on a vertical antenna of given length which would provide the maximum possible field strength on the horizon for a given input power. In re-examining this problem, Bouwkamp and de Bruijn corrected the paper of LaPaz and Miller, and showed that there was no exact solution to this problem, and that the field strength could be made arbitrarily large. In their development, Bouwkamp and de Bruijn proved the following theorem:

15. op. cit.

16. L. LaPaz and G. Miller, "Optimum Current Distributions on Vertical Antennas," Proc IRE, Vol. 31, May 1943, p. 214.

Suppose "a" is a given positive number and G(t) is a given function, continuous or the interval ($-1 \leq t \leq 1$). Then, given any ϵ function g(x) in the interval ($-a \leq x \leq a$) such that uniformly in t:

$$\left| G(t) - \int_{-a}^{a} g(x) e^{ixt} dx \right| < \epsilon \qquad (4)$$

Hence, they reasoned, there exists an illumination function, g(x), distributed over an array of arbitrary length which will produce a pattern approximating any desired pattern, G(t) with arbitrarily small error. As an example, Bouwkamp and de Bruijn used the Gaussian weighted Hermite functions to produce superdirective broadside patterns of the type $\sin^{2n} \phi$. Riblet,[17] again, extended the formulation to two dimensional apertures.

D. Woodward and Lawson[18]

In this technique the authors employed the concept of the angular spectrum[19] as a basis for their theory of superdirectivity. In essence, they attempted to provide physical significance to the fields associated with the integral of Equation (4) for $|t| > 1$; these fields, called evanescent waves, travel parallel to the plane of the aperture and decay exponentially in the direction of the array normal. No outward flow of power is associated with the evanescent waves. As a consequence of this extended wave concept, they developed a Fourier transform pair relation between the aperture field and the pattern (as a function of t, $|t| < \infty$); the radiation pattern was determined within the interval $|t| \leq 1$. Now using the facts that "radiation patterns and their corresponding aperture-distributions may be added linearly, and secondly, that it is possible to define an unlimited number of linearly independent radiation-patterns and associated field-distributions over a given finite aperture," their synthesis procedure was as follows: Let G(t) be the desired pattern and specify G(t) at N points, t_r where $|t_r| \leq 1$. Then

17. H. J. Riblet, "Note on the Maximum Directivity of an Antenna," Proc. IRE, Vol. 36, May 1948, p 620

18. op. cit.

19. M. Born and E. Wolf, Principles of Optics, Pergamon Press, 1959, p. 558.

$$G(t) \approx \sum_{s=0}^{N} A_s G_s(t) \tag{5}$$

where $G_s(t)$ are N of the linearly independent patterns. The constants, A_s, were determined from the set of equations:

$$G(t_r) = \sum_s A_s G_s(t_r) \quad , \quad r = 1, 2, \cdots, N \tag{6}$$

In their example,

$$G_s(t) = \frac{\sin\left[\pi W\left(t - \frac{s}{W}\right)\right]}{\pi W\left(t - \frac{s}{W}\right)} \tag{7}$$

which is the pattern obtained from an aperture of width $W\lambda$ with constant amplitude illumination and a linear phase shift across the aperture of $2\pi s$ radians. By means of their synthesis equation (5) they were able to derive superdirective aperture illuminations.

E. Berman and Clay[20]

These authors considered receiving arrays subjected to nonlinear signal processing. In particular, the array response to a single point-source was examined for various multiplicative and time-averaging schemes. It was shown that highly directive receiving patterns could be obtained. For example, the time-averaged product of the output from a two-element array is of the form $\cos(\beta d \cos\theta)$. Now a signal in the form of a polynomial in $\cos(\beta d \cos\theta)$,

$$\sum_{p=0}^{N} B_p \left[\cos(\beta d \cos\theta)\right]^p \tag{8}$$

can be obtained through multiplications, amplifications, and additions. This signal representation has the same form as the array factor of a linear additive array of $2N+1$ equispaced elements. Hence, a highly directive beam could be synthesized from a simple two-element array. Now the array factor, instead of being written as in Equation (8), is usually represented as the trigonometric sum.

---

20. A. Berman and C. S. Clay, "Theory of Time-Averaged Products Arrays," J. Acoust. Soc. Amer., Vol. 29, July 1957, p. 805.

$$\sum_{n=0}^{N} C_n \cos(n\beta d \cos\theta) \tag{9}$$

Drane [21] in his investigation of nonlinear superdirective techniques has developed the relation between the coefficients C_n and B_p.

IV. Ambiguity Analysis Approach

An analytical formulation of the angular resolution capability of linear arrays was developed through an ambiguity function.[1, 2] It is shown through the ambiguity formulation that, if the array pattern is decomposed in a Fourier series, only the magnitudes of the Fourier components are of importance in determining resolution capability.[22] Thus, a highly directive beam with a particular Fourier decomposition is but one pattern function in a set, all members of the set having identical resolution capability; the set consists of functions with the same component magnitudes. In the subsections to follow, some superdirective beams will be derived and their characteristics discussed. Subsequently, some conjectures on superdirective and superresolving beams which circumvent the classical problems previously outlined will be discussed.

A. Review of Hermite Approximation

It can be shown that the illumination function given by

$$I(x) = \frac{1}{2\pi} \sum_{m=0}^{M} \int_{-\infty}^{\infty} T_m\left(\frac{z}{\beta_0}\right) e^{-ixz}\, dz \tag{10}$$

$$= \frac{1}{2\pi} \sum_{m} \int \left[C_m \left(\frac{z}{\beta_0}\right)^m + C_{m-2} \left(\frac{z}{\beta_0}\right)^{m-2} + \cdots \right] e^{-ixz}\, dz$$

$$= \beta_0 \sum_{m} \left[C_m (i)^m \frac{d^m \delta(\beta_0 x)}{d(\beta_0 x)^m} + C_{m-2} (i)^{m-2} \frac{d^{m-2} \delta(\beta_0 x)}{d(\beta_0 x)^{m-2}} + \cdots \right]$$

---

21. C. J. Drane, "Phase Modulated Antennas," AFCRC-TR-59-138, April 1959.

22. See paper on "A Theory of Resolution of Linear Array Antennas, Time Invariant Illumincation Functions."

$$\beta_o = \frac{\omega}{c} \tag{11}$$

where T_m is the Tschebyscheff polynomial, gives rise to the pattern

$$G_T = \cos(m\phi) \tag{12}$$

The angle ϕ is measured counterclockwise from the array axis. Furthermore, the illumination function

$$I(x) = \beta_o (i)^m \frac{d^m \delta(\beta_o x)}{d(\beta_o x)^m} \tag{13}$$

gives rise to the pattern

$$G_T = \cos^m \phi \tag{14}$$

These illumination functions, consisting of singular functions, could theoretically produce superdirective beams; they are, however, not of great physical interest. For this latter reason substitution of the Gaussian weighted Hermite functions

$$f(k, \beta_o x) = \frac{K}{\sqrt{2\pi}} e^{-\frac{1}{2}(k\beta_o x)^2} \tag{15}$$

$$\frac{d^m f}{d(\beta_o x)^m} = \frac{(-1)^m K^{m+1}}{\sqrt{2\pi}} e^{-\frac{1}{2}(k\beta_o x)^2} He_m(k\beta_o x) \tag{16}$$

for the singular functions of Equation (13) was investigated The pattern resulting from an illumination function given by Equation (16) is

$$G_T = \frac{(-i)^m K^{m+1}}{\sqrt{2\pi}} \int_{-\beta_o a}^{\beta_o a} e^{-\frac{1}{2}(k\beta_o x)^2} He_m(k\beta_o x) e^{i\beta_o x \cos\phi} d(\beta_o x) \tag{17}$$

It can be shown that, for any m and any $\beta_o a > 0$, the finite limits of integration can be replaced with infinite limits with arbitrarily small error for k sufficiently large. Under these circumstances, Equation (17) becomes

$$G_T = \cos^m \phi \qquad \text{(Endfire beam-forward and backward lobes)} \tag{17a}$$

The following pattern-illumination function pairs were also previously derived. *

$$\begin{cases} I(x) = \dfrac{\beta_0 (-i)^m k^{m+1}}{\sqrt{2\pi}} e^{-\frac{1}{2}(k\beta_0 x)^2} He_m(k\beta_0 x)\, e^{i\beta_0 x} \\ G = (1+\cos\phi)^m \qquad \text{(Endfire beam-forward lobe only)} \end{cases} \tag{18}$$

$$\begin{cases} I(x) = \dfrac{\beta_0 K}{\sqrt{2\pi}} \sum_{n=0}^{m} \binom{m}{n} K^{2n} e^{-\frac{1}{2}(k\beta_0 x)^2} He_{2n}(k\beta_0 x) \\ G = \sin^{2m}\phi \qquad \text{(Broadside beam)} \end{cases} \tag{19}$$

B. Frequency Characteristics

The response of superdirective apertures with respect to varying input frequency will be examined in this section. Patterns of the form expressed by Equations 17, 18, and 19 will be considered; peak gain, beamwidth and sidelobe characteristics, and coupled range-angle resolution properties will be investigated.

1. Varying Input Frequency

Consider the case where the illumination function of the array is

$$I(x) = \beta_0 (-i)^m \frac{k^{m+1}}{\sqrt{2\pi}} e^{-\frac{1}{2}(k\beta_0 x)^2} He_m(k\beta_0 x) \tag{20}$$

and the signal transmitted by the source in the far field is of the form

$$s(t) = e^{i\omega t} \tag{21}$$

---

* The pair given by Equation (19) was derived by Bouwkamp and de Bruijn, op. cit. Equation (18) is found in reference 2.

The received signal is

$$S = e^{i\omega(t-\frac{R_o}{c})} \int_{-a}^{a} \omega I(x) e^{i\frac{\omega x}{c}\cos\phi}\, dx \tag{22}$$

$$= (-i)^m \frac{K^{m+1}}{\sqrt{2\pi}} e^{i\omega(t-\frac{R_o}{c})} \int_{-\beta_o a}^{\beta_o a} \omega\, e^{-\frac{1}{2}(K\beta_o x)^2} H_{e_m}(K\beta_o x) e^{i\beta_o x(\frac{\omega}{\omega_o}\cos\phi)}\, d(\beta_o x) \tag{23}$$

where $(R_o\ \phi)$ are the coordinates of the source (see Figure 1). It can be shown that, for any ω, m, and $\beta_o a > 0$, there exist values of k sufficiently large such that the finite limits of integration in Equation (33) can be replaced by infinite limits with arbitrarily small error. Performing the integration with infinite limits yields:

$$S = e^{i\omega(t-\frac{R_o}{c})} \left[\omega(\tfrac{\omega}{\omega_o}\cos\phi)^m\right] e^{-\frac{1}{2}(\frac{\omega}{K\omega_o}\cos\phi)^2} \tag{24}$$

For large k, *

$$S = e^{i\omega(t-\frac{R_o}{c})}\, \omega(\tfrac{\omega}{\omega_o})^m \cos^m\phi \tag{25}$$

Note that the endfire pattern is independent of ω, but that the response varies as ω^{m+1}. The function is shown in Figure 2a.

As indicated by Equation (18), an endfire pattern with no backlobe was obtained, at $\omega = \omega_o$, when a linear phase taper given by $\exp(i\,\beta_o x)$ was inserted in the illumination function. At an arbitrary frequency ω, the signal is of the form

$$S = e^{i\omega(t-\frac{R_o}{c})}\, \omega(1+\tfrac{\omega}{\omega_o}\cos\phi)^m \tag{26}$$

This pattern as a function of frequency is shown in Figure 2b.

Now examine pattern characteristics when the illumination function consists of more then one Hermite polynomial. Let

---

* In the following discussions, it will be assumed that k is sufficiently large for the approximations to hold.

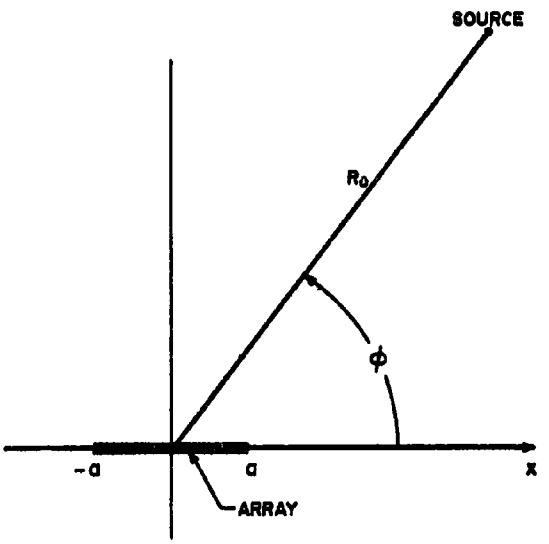

Figure 1 Array Geometry

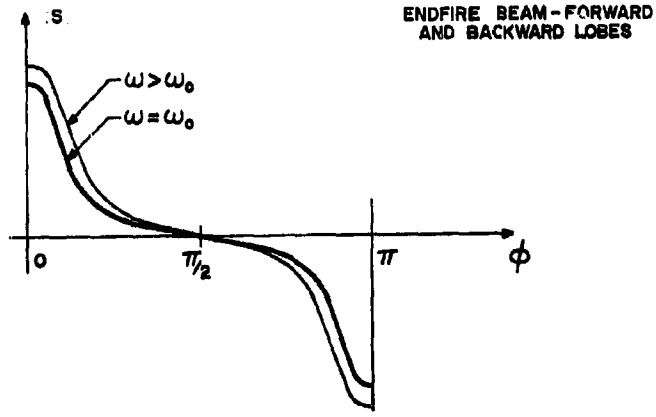

(a) NO LINEAR PHASE TAPER IN APERTURE

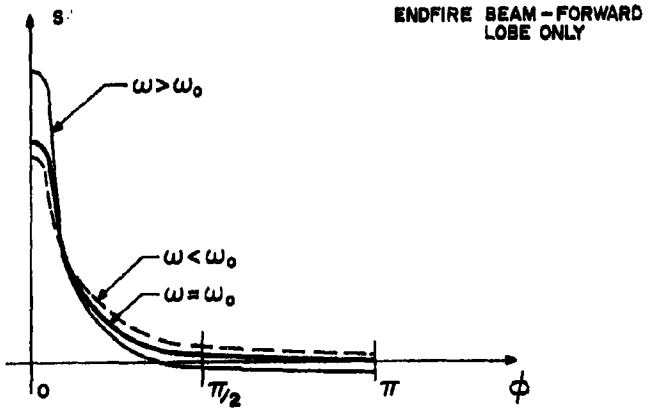

(b) LINEAR PHASE TAPER IN APERTURE

Figure 2 Aperture Response As A Function of Frequency
(Aperture Illumination = Single Hermite Polynomial)

$$I(x) = \beta_0 \sum_{n=0}^{N} C_n (-i)^n \frac{K^{n+1}}{\sqrt{2\pi}} e^{-\frac{1}{2}(K\beta_0 x)^2} He_n(K\beta_0 x) \tag{27}$$

The received signal in this case is:

$$S = e^{i\omega(t-\frac{R_0}{c})} \left[\omega \sum_n C_n \left(\frac{\omega}{\omega_0} \cos\phi \right)^n \right] \tag{28}$$

The signal is expressed as a polynomial in the variable ($\omega/\omega_0 \cos\phi$). If the coefficients C_n are expressed in the form:

$$C_n = C_n^0 r^n \tag{29}$$

where r is an arbitrary constant and the C_n^0's correspond to the coefficients of the m-th degree Tschebyscheff polynomial, then

$$S = e^{i\omega(t-\frac{R_0}{c})} \omega T_m \left(\frac{r\omega}{\omega_0} \cos\phi \right) \tag{30}$$

But Equation (30) is the expression for a Tschebyscheff-type pattern when $r\omega/\omega_0 > 1$. For $r\omega/\omega_0 > 1$, an endfire pattern results with equal front and back lobes and a peak-to-sidelobe ratio of $T_m(r\omega/\omega_0)$. The pattern is sketched in Figure 3a.

If the phase shift expressed by

$$e^{i\beta_0 x(1-\frac{1}{r})} \tag{31}$$

is added to the illumination function of Equation (27), the Tschebyscheff pattern

$$T_m \left[r\left(1 - \frac{1}{r} + \frac{\omega}{\omega_0} \cos\phi\right) \right] \tag{32}$$

is obtained with no backlobe at $\omega = \omega_0$. The pattern is shown in Figure 3b.

If the illumination function of the array is given by Equation (19), then the received signal at an arbitrary frequency ω is

$$S = e^{i\omega(t-\frac{R_0}{c})} \omega \left[1 - \left(\frac{\omega}{\omega_0} \cos\phi \right)^2 \right]^m \tag{33}$$

and a broadside pattern is formed. Unlike the endfire patterns, (produced without the added linear phase taper in the illumination function) the broadside pattern

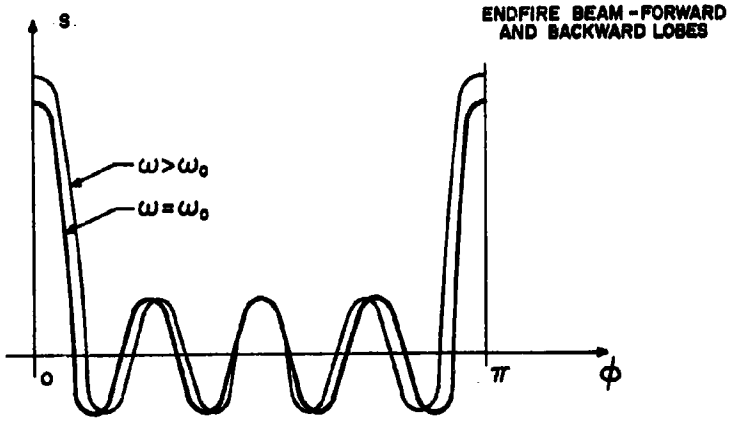

(a) NO PHASE TAPER IN APERTURE

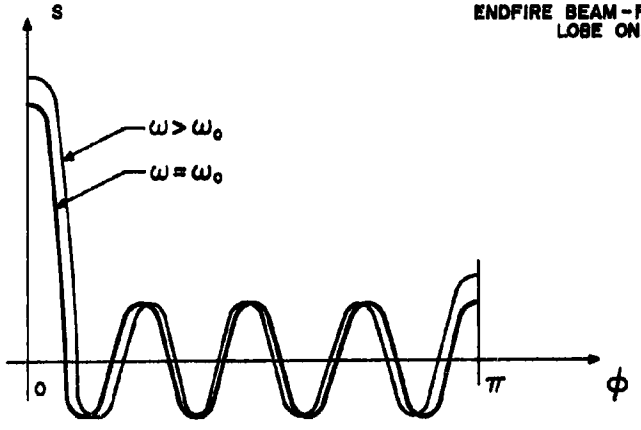

(b) LINEAR PHASE TAPER IN APERTURE

Figure 3 Aperture Response As A Function of Frequency
(Aperture Illumination = Sum of Hermite Polynomials)

is a function of ω. However, for small relative deviations ($\omega/\omega_0 \approx 1$), the basic pattern is preserved. Figure 4a shows the form of the pattern.

If a broadside Tschebyscheff pattern of the type

$$G = T_m(r\sin^2\phi - 1) \tag{34}$$
$$= C_m^0(r\sin^2\phi - 1)^m + C_{m-2}^0(r\sin^2\phi - 1)^{m-2} + \cdots$$

is desired, the relation

$$(r\sin^2\phi - 1)^m = \left[(r-1) - r\cos^2\phi\right]^m \tag{35}$$
$$= \sum_{n=0}^{m} (-1)^n \binom{m}{n} (r-1)^{m-n} r^n \cos^{2n}\phi$$

is used to derive the illumination function

$$I(x) = C_m^0 \frac{\beta_0 K}{\sqrt{2\pi}} \sum_{n=0}^{m} \binom{m}{n} K^{2n} (r-1)^{m-n} r^n e^{-\frac{1}{2}(K\beta_0 x)^2} He_{2n}(K\beta_0 x) \tag{36}$$
$$+ C_{m-2}^0 \frac{\beta_0 K}{\sqrt{2\pi}} \sum_{n=0}^{m-2} \binom{m-2}{n} K^{2n} (r-1)^{m-2-n} r^n e^{-\frac{1}{2}(K\beta_0 x)^2} He_{2n}(K\beta_0 x)$$
$$+ \cdots$$

At the frequency ω

$$G = C_m^0 \sum_{n=0}^{m} (r-1)^{m-n} (-r)^n \left(\frac{\omega}{\omega_0}\cos\phi\right)^{2n} + \cdots \tag{37}$$
$$= T_m\left\{r\left(\frac{\omega}{\omega_0}\right)^2 \sin^2\phi - \left[1 - r + r\left(\frac{\omega}{\omega_0}\right)^2\right]\right\}$$
$$= T_m\left[r - 1 - r\left(\frac{\omega}{\omega_0}\right)^2 \cos^2\phi\right]$$

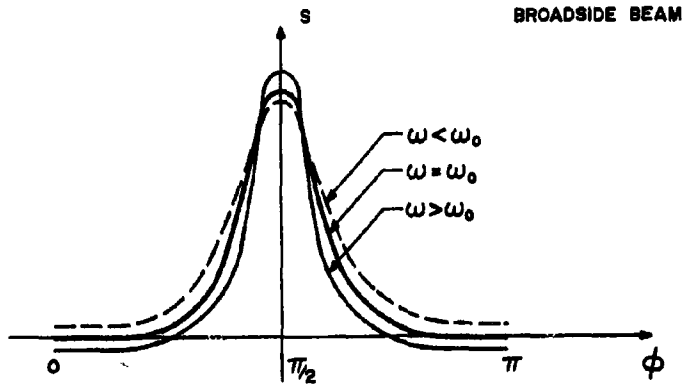

(a) PATTERN TYPE $\sim (1 - a^2 \cos^2 \phi)^m$

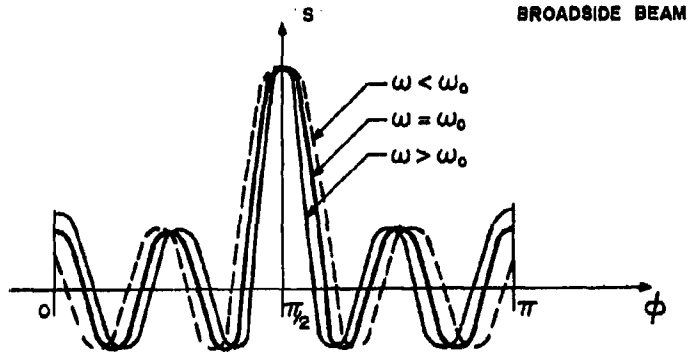

(b) PATTERN TYPE $\sim T_m(a^2 \sin^2 \phi - 1)$

Figure 4 Aperture Response As A Function of Frequency
(Aperture Illumination = Sum of Even Hermite Polynomials)

The broadside pattern is again a function of frequency. However, the peak value of the beam is not a function of frequency. For $\omega < \omega_o$, the beamwidth is broadened; for $\omega > \omega_o$, the beamwidth is narrowed but the sidelobes at $\phi = 0$ and π are increased. The patterns are shown in Figure 4b.

2. Finite Bandwidth Signals

The case where the signal in space has the time dependent form

$$s(t) = \int_{-\infty}^{\infty} A(\omega) e^{i(\omega+\omega_o)t} d\omega = \int_{-\infty}^{\infty} A(\omega-\omega_o) e^{i\omega t} d\omega \tag{38}$$

will be considered in this section. From the preceeding discussion, the following received signal-illumination function pairs are immediately derived:

$$\begin{cases} I(x) = \beta_o (-i)^m \frac{K^{m+1}}{\sqrt{2\pi}} e^{-\frac{1}{2}(K\beta_o x)^2} He_m(K\beta_o x) & (39) \\ S = \cos^m\phi \int \omega A(\omega-\omega_o)\left(\frac{\omega}{\omega_o}\right)^m e^{i\omega(t-\frac{\beta_o}{2})} d\omega & (40) \end{cases}$$

$$\begin{cases} I(x) = \beta_o (-i)^m \frac{K^{m+1}}{\sqrt{2\pi}} e^{-\frac{1}{2}(K\beta_o x)^2} He_m(K\beta_o x)\, e^{iK\beta_o x} & (41) \\ S = \int \omega A(\omega-\omega_o)\left(1+\frac{\omega}{\omega_o}\cos\phi\right)^m e^{i\omega(t-\frac{\beta_o}{2})} d\omega & (42) \end{cases}$$

$$\begin{cases} I(x) = \beta_o \sum_{n=0}^{m} C_n^o (-ir)^n \frac{K^{n+1}}{\sqrt{2\pi}} e^{-\frac{1}{2}(K\beta_o x)^2} He_n(K\beta_o x) & (43) \\ S = \int \omega A(\omega-\omega_o) T_m\left(\frac{\omega}{\omega_o}\cos\phi\right) e^{i\omega(t-\frac{\beta_o}{2})} d\omega & (44) \end{cases}$$

$$I(x) = \beta_0 \sum_{n=0}^{m} C_n^0 (-ir)^n \frac{K^{n+m}}{\sqrt{2\pi}} e^{-\frac{1}{2}(K\beta_0 x)^2} He_n(K\beta_0 x) e^{i\beta_0 x(1-\frac{1}{r})} \tag{45}$$

$$S = \int \omega A(\omega-\omega_0) T_m\left[r\left(1-\frac{1}{r}+\frac{\omega}{\omega_0}\cos\phi\right)\right] e^{i\omega(t-\frac{R_0}{c})} d\omega \tag{46}$$

$$I(x) = \beta_0 \frac{K}{\sqrt{2\pi}} \sum_{n=0}^{m} \binom{m}{n} e^{-\frac{1}{2}(K\beta_0 x)^2} He_{2n}(K\beta_0 x) \tag{47}$$

$$S = \int \omega A(\omega-\omega_0)\left[1-\left(\frac{\omega}{\omega_0}\cos\phi\right)^2\right]^m e^{i\omega(t-\frac{R_0}{c})} d\omega \tag{48}$$

$$I(x) = \sum_{n=0}^{m} C_n^0 \frac{\beta_0 K}{\sqrt{2\pi}} \left[\sum_{p=0}^{n} \binom{n}{p} K^{2p} (r-1)^{n-p} r^p e^{-\frac{1}{2}(K\beta_0 x)^2} He_{2p}(K\beta_0 x)\right] \tag{49}$$

$$S = \int \omega A(\omega-\omega_0) T_m\left[r-1-r\left(\frac{\omega}{\omega_0}\right)^2\cos^2\phi\right] e^{i\omega(t-\frac{R_0}{c})} d\omega \tag{50}$$

Note that the six transform pairs listed correspond, in order, to the narrow-band transform pairs illustrated successively in Figures 2(a) to 4(b). Exact effects of the finite bandwidth can be predicted once the signal modulation form has been chosen and the integrals in Equations, 40, 42, 44, 46, 48, and 50 have been solved.

3. Discussion

This subsection will discuss, qualitatively, the bandwidth limitations and capabilities of the superdirective arrays considered. In particular, the signals expressed by Equations (40) and (50) are of particular interest. Note that the angle dependent part of the signal described by Equation (40) does not vary with frequency. The array, in this case, simply acts like a filter

with transfer function proportional to ω^{m+1}. Thus, a filter with inverse characteristics over the frequency band of interest, would restore the modulation funtion, $A(\omega)$. However, the bandwidth over which equalization can be achieved with a practical filter would diminish with increasing index "m"

An interesting implication of Equation (40) is that, in theory, there is no fundamental trade-off between angular resolution and range resolution. A connection between range and angular resolution exists through the parameter "m", so that the trade-off appears to be one of practical, not of fundamental considerations, i.e., an equalizing filter following the aperture can adjust the range response without affecting the angular response.

Note that the pattern expressed by the Tschebyscheff polynomial in Equation (50) is independent of frequency at the peak of the beam ($\phi = \pi/2$). At $\phi = \pi/2$,

$$S = T_m(r-1)\int_{\omega} A(\omega-\omega_0)\, e^{i\omega(t-\frac{R_0}{c})}\, d\omega \qquad (51)$$

so that severe practical limitations do not exist on the bandwidth of the signal received at the peak of the beam. The pattern, however, is a function of frequency (see Figure 4b) and the appearance of high sidelobes at $\phi = 0$ and π can limit the bandwidth in some applications. These extraneous high sidelobes can be suppressed., however, by the proper choice of the element factor or by a modification of the illumination function. For example, let $\omega_0 + \Delta\omega = \omega_m$ be the maximum frequency of interest. The signal received with an illumintion function given by

$$I(x) = \sum_{n=0}^{m} C_n^0 \frac{\beta_0 K}{\sqrt{2\pi}} \left\{ \sum_{p=0}^{n} \binom{n}{p} (K^2 r)^p \left[r-1+r\left(\frac{2\Delta\omega}{\omega_0}\right) \right]^{n-p} e^{-\frac{1}{2}(K\beta_0 x)^2} He_{2p}(K\beta_0 x) \right\} \qquad (52)$$

would be

$$S = \int_{\omega} A(\omega-\omega_0) T_m \left\{ r-1+r\left[\left(1+\frac{\Delta\omega}{\omega_0}\right)^2 - 1 \right] - r\left(\frac{\omega}{\omega_0}\right)^2 \cos^2\phi \right\} d\omega \qquad (53)$$

Assuming that $(\Delta\omega/\omega_0)^2$ is negligible compared to $2\Delta\omega/\omega_0$,

$$S = \int_{\omega} A(\omega-\omega_0)\, T_m \left[r-1+r\left(\frac{2\Delta\omega}{\omega_0}\right) - r\left(\frac{\omega}{\omega_0}\right)^2 \cos^2\phi \right] d\omega \qquad (54)$$

The pattern function expressed by the Tschebyscheff polynomial in Equation (54) has a peak value independent of frequency; note that the sidelobe level for $\omega < \omega_0 + \Delta\omega$ is also independent of frequency if the maximum frequency ω_m is such as to limit the Tschebyscheff function to its constant sidelobe region. For narrow beams and a bandwidth of $2\Delta\omega$, the ratio of maximum to minimum beamwidths is approximately

$$\text{Beamwidth ratio} = \frac{2\Delta\omega}{\omega_0} \tag{55}$$

It is seen that the pattern degradation and signal distortion are small for small relative bandwidths with the superdirective illumination function of Equation (52).

It is obvious that the illumination function expressed by the Hermite function has the same characteristics as all known superdirective illumination functions, that of rapid amplitude changes and phase reversals. Hence, it might be inferred that the resulting pattern is highly sensitive to errors. Indeed, this may be the case. However, the Hermite function is only one of many continuous functions, with continuous derivatives, which approaches the delta function in the limit. Therefore, the conclusion is reached that it is not the "fine structure" of the function but the "gross" features which are of particular importance in superdirectivity. The illumination function expressed by Equation (39) consists of only one Hermite function. It gives rise to an endfire pattern, with equal front and back lobes, which is independent of frequency Furthermore, a linear phase shift still provides an endfire pattern but decreases either the front or the back lobe as implied by Equations (41) and (42). This can be shown as follows: If

$$I(x) = \beta_0 (-i)^m \frac{K^{m+1}}{\sqrt{2\pi}} e^{-\frac{1}{2}(k\beta_0 x)^2} He_m(k\beta_0 x) e^{i\xi\beta_0 x} \tag{56}$$

Then,

$$S = \int \omega A(\omega - \omega_0)\left(\xi + \frac{\omega}{\omega_0}\cos\phi\right)^m e^{i\omega\left(t - \frac{\rho_0}{c}\right)} d\omega \tag{57}$$

All broadside patterns can be expected to be sensitive to errors. This is not simply a reflection of the fact that the illumination function must consist of the sum of Hermite functions. The reason is that only the zeroth order Hermite function determines the peak value of the main beam; all higher order functions only serve to shape the main beam and sidelobe of the pattern.

C. Physical Interpretations

The scale factor "k" is used to force the major part of the Hermite function to lie within the interval $|x| \leq a$. In affecting the distribution of the illumination function, it appears as a multiplier of the free-space phase constant, β_0. The factor k, then, can be interpreted as being equal to $\sqrt{\epsilon_r \mu_r}$ where ϵ_r and μ_r are relative permittivity and permeability, respectively. In this interpretation, varying the parameter k, to adjust the distribution of the illumination function within a given interval, is simply an application of the principle of similitude.[23] Note also that requirement of large values of k to achieve superdirective action also implies alteration of the physical medium surrounding the antenna, i.e., it imples use of high dielectric materials in construction of the aperture.

V. Conjectures

A. Implementation Techniques

1. Modes in Confocal Cavities

The normal modes of an open cavity formed by two identical concave spherical reflectors has been analyzed for reflector separations equal to twice their radii of curvature. It has been shown that the mode patterns are approximately given by the orthogonal Hermite functions.[24] In the ideal case of a lossless cavity with infinitely large reflectors, the mode patterns are described exactly by these funtions.[25] The field distribution of the modes, in one dimension, at the focal plane is given by

$$\frac{E(x)}{E_0(n)} = e^{-\frac{1}{4}(\alpha x)^2} He_n(\alpha x) , \qquad \alpha = 2\sqrt{\frac{\beta}{b}} \tag{58}$$

where β is the propagation constant, b is the radius of curvature of the reflectors, and $E_0(n)$ is a function of the mode number, n. Assuming that the mode pattern is concentrated within the diameters of the reflectors, the beam pattern which

23. See, for example, J. A. Stratton, Electromagnetic Theory, McGraw-Hill, 1941 p. 488.

24. G. D. Boyd and J. P. Gordon, "Confocal Multimode Resonator for millimeter through Optical Wavelength Masors," Bell System Tech Journal, Vol. 40, March 1961, pp. 489-508.

25. G. D. Boyd and H. Kogelnik, "Generalized Confocal Resonator Theory," BSTJ, Vol. 41, July 1962, pp. 1347-1369.

results when the reflectors are partially transparent is approximately

$$G(\theta) = \int_{-\infty}^{\infty} e^{-\frac{1}{4}(\alpha x)^2} He_n(\alpha x)\, e^{i\beta x \cos\phi}\, dx \tag{59}$$

$$= \frac{2\sqrt{\pi}}{\alpha} (i)^n e^{-\frac{1}{4}\left(\frac{2\beta}{\alpha}\cos\phi\right)^2} He_n\left(\frac{2\beta}{\alpha}\cos\phi\right) \tag{60}$$

Hence, the beam pattern, as a function of cos θ, is essentially a replica of the mode pattern. Only the zeroth order mode provides a single main beam on the axis of the cavity system; all higher order functions provide multilobular beam patterns.

One can conceive of a dielectrically loaded microwave cavity which supports only (or primarily) the zeroth order mode. Now, as the dielectric constant is increased, the dimensions of the system can be reduced and, in effect, a superdirective array can be formed. If the mode pattern can be further tapered exponentially to provide a distribution given by:

$$E \propto e^{-\frac{1}{2}(\alpha x)^2} He_n(\alpha x) \tag{61}$$

then the beam pattern given by $\cos^n \phi$ will be obtained so that higher order modes could be used to advantage. Note that the beam pattern changes from a mulilobular pattern to a highly directive endfire pattern when the dielectric constant in the cavity and the amplitude taper of the mode pattern are increased.

2. Synthetic Superdirective Arrays

The usual beam pattern of an array of elements is formed by simultaneously exciting all elements. When this technique is applied to superdirective arrays, all of the problems previously outlined become evident. However, several undesirable properties of superdirective arrays can be circumvented by the synthetic aperture technique.

Only one radiating element is used. However, the position of the radiator is sequentially changed in time to coincide with the element positions of the usual superdirective array. The returns of successive transmissions (corresponding to different positions of the radiator) are coherently detected, amplitude tapered, phase shifted, and summed to form the superdirective beam. Amplitude tapering can be performed at video frequencies where large dynamic ranges are readily achievable. Note that the amplitude

of successive RF transmissions can be identical. Coherent summation can be performed in a reentrant delay line integrator or an optical integrator. Since only one radiator is used, the severe RF mutual coupling effects present in the usual superdirective techniques are avoided. Special provisions for impedance matching at RF need not be instrumented since large reactive fields are not created in the vicinity of the antenna; hence restrictions on antenna bandwidth need not be severe for the synthetic superdirective array. Sensitivity to errors are not reduced by this technique; the amplitude of the effective beam formed at video frequencies is still small compard to the amplitude of currents which are stored.

Note that the radiating element can be a relatively large parabola or conventional array; it's size is not restricted by interelement spacing. The receiver can have two channels, one for conventional processing of the signal received by the element, and the other for superdirective processing. Hence, the basic output of the element can be used even if the superdirective output is not useful under some circumstance.

The length of time required to form the superdirective beam is equal to the total time required to sequentially move the element over all positions. However, superdirective beams can be formed on a pulse-to-pulse basis if a number of separate frequencies are used to form separate beams; in this case, the number of discrete frequencies and discrete processing channels must be equal to the total number of radiator positions.

B. Synthesis Equations

It has been shown that the ambiguity function for a linear array of N discrete radiators is given by [26]

$$\Phi(\Delta\phi_o) = \sum_{p=0}^{\infty} \epsilon_p A_p \cos(p\Delta\phi_o) \tag{62}$$

$$A_p = 2\pi \left| \sum_{n=p}^{N-1} I_n J_p(\beta_o x_n) \right|^2 \tag{63}$$

26. See paper on "The Theory of Resolutions of Linear Array Antennas, Time Invariant Illumination Functions."

Furthermore, the beam pattern can be decomposed in a Fourier series as:

$$G(\phi) = \sum_{n=0}^{N-1} I_n e^{i\beta_0 x_n \cos\phi} \tag{64}$$

$$= \sum_{p=0}^{\infty} \epsilon_p a_p \cos(p\phi) \tag{65}$$

$$a_p = (i)^p \sum_{n=0}^{N-1} I_n J_p(\beta_0 x_n) \tag{66}$$

Therefore:

$$A_p = 2\pi |a_p|^2 \tag{67}$$

All previous synthesis techniques were directed toward the determination of an illumination function to provide a prescribed beam pattern. In the case of an array of discrete radiators, the usual practice is to assume commensurable element spacings. When this historical procedure is used to synthesize superdirective beams the computed current coefficient, I_n, invariably show large amplitude variations which alternate in phase by π radians. The spatial frequency spectrum of the resulting beam can be found from Equation (66).

If superresolution is the desired end result, it is quite possible that the large variations in the current coefficients can be avoided. In constrast with the requirements for directivity, Equation (67) indicates that resolution is dependent only on the magnitudes of the spatial frequencies. To illustrate this difference, assume that a superdirective pattern (generated by N elements whose positions are specified) has a spatial frequency spectum defined by the set of complex coefficients, a_{po} $p = 0, 1$ ----q, where a_{qo} is the highest component of significance. Now an array, with the same element positions, whose resolution capability is essentially the same as the superdirective array can be characterized by the set $a_{po}{}^{i\Psi p}$ where the phase Ψ_p is arbitrary. Using the least square difference measure of the patterns prescribed by Equation (65), note that:

$$\epsilon^2 = \int_{-\pi}^{\pi} \left| \sum_{p=0}^{q} \epsilon_p \left[a_{po} e^{i\psi_p} - a_p \right] \cos(p\phi) \right|^2 d\phi \tag{68}$$

Hence

$$\epsilon^2 = 2\pi \sum_p \epsilon_p \left| a_{p0} e^{i\psi_p} - a_p \right|^2 \tag{69}$$

and ϵ^2 must be minimized with respect to the complex current I_n. Substituting Equation (66) for a_p and performing the minimization derivative, the following set of equations must be satisfied. In matrix form,

$$\begin{bmatrix} \sum_p \epsilon_p J_p(\beta_0 x_0) a_{p0} e^{i\psi_p} (-i)^p \\ \vdots \\ \sum_p \epsilon_p J_p(\beta_0 x_{N-1}) a_{p0} e^{i\psi_p} (-i)^p \end{bmatrix} = \begin{bmatrix} \sum_p \epsilon_p J_p^2(\beta_0 x_0) & \cdots & \sum_p \epsilon_p J_p(\beta_0 x_0) J_p(\beta_0 x_{N-1}) \\ \sum \epsilon_p J_p(\beta_0 x_1) J_p(\beta_0 x_0) & \cdots & \vdots \\ \vdots & & \vdots \\ \sum \epsilon_p J_p(\beta_0 x_{N-1}) J_p(\beta_0 x_0) & \cdots & \sum \epsilon_p J_p^2(\beta_0 x_{N-1}) \end{bmatrix} \times \begin{bmatrix} I_0 \\ \vdots \\ I_{N-1} \end{bmatrix} \tag{70}$$

The symmetric transformation matrix consists of real elements. Hence, only one matrix need be inverted to determine the complex current coefficients. The original superdirective current distribution is approximated, of course, when ψ_p is independent of p; for all other cases, a current distribution is obtained whose pattern, though not necessarily superdirective, has resolution properties equal to the superdirective beam.

In the previous example, the elements were assumed to be equispaced. Obviously, this is an unnecessary restriction and, in fact, does not facilitate the computation of the current coefficients of Equation (70). In fact there is considerable interest in nonuniformity spaced arrays at the present time.

In summary, the number of parameters at one's disposal for synthesizing an ambiguity function are considerably greater than those available for pattern synthesis. Aside from the magnitudes and phases of the current coefficients and the positions of the radiators, the phases of the spatial frequencies can be arbitrarily varied. It is not unlikely that radical departures from conventional superdirective arrays will result from the ambiguity function approach. A possible sample will be a superdirective (or superresolving) array whose current coefficient are constant in magnitude or restricted to small variations in relative amplitude.

BIBLIOGRAPHY

1. Oseen, C. W. "Die Einsteinsche Nadelstichstrahlung und die Maxwellschen Gleichungen, Annalen der Physik, 1922, Vol. 69, p. 202.

2. Howell, W. T. "Electromagnetic Waves from a Point Source," Philosophical Magazine, 1936, Vol. 21, p. 384.

3. Hansen, W. W., and Woodyard, J. R. "A New Principle in Directional Antenna Design," Proceedings of the Institute of Radio Engineers, Vol. 26, p. 333.

4. Franz, K. "The Gain and the (Rudenberg) 'Absorption Surfaces' of Large Directive Arrays," Hochfrequenztechnik und Elektroakustik, 1939, Vol. 54, p. 198.

5. Franz, K. "The Improvement of the Transmission Efficiency by Directive Aerials," ibid., 1941, Vol. 57, p. 117.

6. Schelkunoff, S. A. "A Mathematical Theory of Linear Arrays," Bell System Technical Journal, 1943, Vol. 22, p. 80.

7. Franz, K. "Remarks on the Absorption Surfaces of Directive Aerials," Hochfrequenztechnik und Elektroakustik, 1943, Vol. 61, p. 51.

8. LaPaz, L., and Miller, G.A. "Optimum Current Distributions on Vertical Antennas," Proceedings of the Institute of Radio Engineers, 1943, Vol. 31, p. 214.

9. Bouwkamp, C. J. "Radiation Resistance of an Antenna with Arbitrary Current Distribution," Philips Research Reports, 1946, Vol. 1, p. 65.

10. Bouwkamp, C. J., and De Bruijn, N. G. "The Problem of Optimum Antenna Current Distribution," ibid., p 135

11. Dolph, C. L. "A Current Distribution for Broadside Arrays which Optimizes the Relationship between Beam Width and Side-lobe Level," Proceedings of the Institute of Radio Engineers, 1946, Vol. 34, p. 335.

12. Uzkov, A. I. "An Approach to the Problem of Optimum Directive Antennae Design," Comptes Rendus de l'Academie des Sciences de l'U.R.S.S., 1946, Vol. 53, p. 35.

13. Reid, D. G. "The Gain of an Idealized Yagi Array, Journal I. E. E., 1946, Vol. 93, Part IIIA, p. 564.

14. Riblet, H. J. Discussion, Reference 11 Proceedings of the Institute of Radio Engineers, 1947, Vol. 35, p. 489.

15. Gillett, G. D. "Analysis of Effect of Circulating Currents on the Radiation Efficiency of Broadcast Directive Antenna Designs" (summary only), ibid., 1948, Vol. 36, p. 372.

16. Riblet, H. J. "Note on the Maximum Directivity of an Antenna, ibid., p. 620.

17. Wilmotte, R. M. "Note on Practical Limitations in the Directivity of Antennas," Ibid., p. 878.

18. Bell, D. A. Discussion on Reference 16, ibid., p. 1134.

19. Taylor, T. T. Disucssion on Reference 16, ibid., p. 1135.

20. Woodward, P. M., and Lawson, J. D. "The Theoretical Precision with which an Arbitrary Radiation Pattern may be obtained from a Source of Finite Size," Journal I. E. E., 1948, Vol. 95, Part III, p. 363.

21. Chu, L. J. "Physical Limitations of Omni-Directional Antennas," Journal of Applied Physics, 1948, Vol. 19, p. 1163.

22. Bell, D. A. "Gain of Aerial Systems," Wireless Engineer, 1949, Vol. 26, p. 306.

23. Jordan, E. C. "Electromagnetic Waves and Radiating Systems," (Prentice-Hall, New York, 1950), p. 445.

24. Taylor, T. T., and Whinnery, J. R. "Applications of Potential Theory to the Design of Linear Arrays, Journal of Applied Physics, 1951, Vol. 22, p. 19.

25. Freedman, J. "Resolution in Radar Systems," Proceedings of the Institution of Radio Engineers, 1951, Vol. 39, p. 813.

26. Yaru, N. "A Note on Super-Gain Antennas Arrays," ibid., p. 1081.

27. "Supergain Antennas," QST, 1951, Vol. 35, p. 46.

28. Aigrain, P. "Les Antennes Super-Directives," L'Onde Electrique, 1952, Vol. 32, p. 51.

29. Goward, F. K. "An Improvement in End-Fire Arrays," Proc. IEE (London) Vol. 94, November, 1947, pp. 415-418.

30. Pritchard, R. L., and Rosenberg, M. D. "Optimum Directivity Patterns for Linear Arrays," J. Acoust. Soc. Amer., Vol. 20, July 1948 pp. 594-595.

31. Knudson, H. L. "Superforstaerkning hos Antenner," Elektrotek Tiddsskr., Vol. 64, June 5, 1951, pp. 213-221 (In Danish).

32. Sinclair, G., and Cairns, F. V. "Optimum Patterns for Arrays of Non-Isotropic Sources," IRE Trans. on Antennas and Propagation, Vol. AP-1, February 1952, pp. 50-59.

33. Dunbar, A. S. "On the Theory of Antenna Beam Shaping," J. Appl. Phys., Vol. 23, August 1952, pp. 847-853.

34. Bailin, L. L., and Ehrlich, M. J. "Factors Affecting the Performance of Linear Arrays," Proc. IRE, Vol. 41, February 1953, pp. 235-341.

35. DuHamel, R. H. "Optimum Patterns for Endfire Arrays," Proc. IRE, Vol. 41, May 1953, pp. 652-659.

36. Pistolkors, A. A. "Use of Mathieu Functions for Computing Field Distribution in an Antenna to Obtain a Given Directional Diagram," Dokl. Akad. Nauk SSSR, Vol. 89, No. 5, April 11, 1953, pp. 849-852, Natl. Sci. Foundation Transl. NSF-tr-113.

37. Bakhrakh, L. D. "A Solution of the Integral Equation for a Linear Antenna," Dokl. Akad. Nauk USSR, Vol. 92, No. 4, October 1, 1953, pp. 755-758. Natl. Sci. Foundation Transl. NSF-tr211, February 1954.

38. Pritchard, R. K. "Optimum Directivity Patterns for Linear Point Arrays," J. Acoust. Soc. Amer. Vol. 25, September 1953, pp. 879-891.

39. Pritchard, "Maximum Directivity Index of a Linear Point Array," J. Acoust. Soc. Amer., Vol. 26, November 1954, pp. 1034-1039.

40. Taylor, T. T. "Design of Line-Sources for Narrow Beamwidth and Low Side-Lobes," IRE Trans. on Antennas and Propagation, Vol. AP-3 January 1955, pp. 16-28.

41. Pritchard, R. L. "Discussion on Optimum Patterns for Endfire Arrays," IRE Trans. on Antennas and Propagation, Vol. Ap-3, January 1955, pp. 40-43.

42. Gilbert, E. N., and Morgan, S. P. "Optimum Design of Directive Antenna Arrays Subject to Random Variations," Bell Sys. Tech. J., Vol. 34, May 1955, pp. 637-663.

43. Kovacs, R., and Solymar, L. "Theory of Aperture Aerials Based on the Properties of Entire Functions of the Exponential Type," Acta Phys. Acad. Sci. Hung., Vol. 6, No. 2, 1956, pp. 161-184.

44. Uzsoky, M., and Solymar, L. "Theory of Super Directive Linear Arrays," Acta Phys. Acad. Sci. Hung., Vol. 6, No. 2, 1956, pp. 185-205.

45. di Francia, G. T. "Directivity Super-Gain and Information," IRE Trans. on Antennas and Propagation, Vol. AP-4, July 1956, pp. 473-479.

46. Bloch, A. "N-Terminal Networks: Some Theorems With Applications to the Directive Properties of Aerial Arrays," Wireless Engr., Vol. 33, December 1956, pp. 295-300.

47. Pokrovskii, V. L. "On the Theory of Optimal Linear Antennas," Radio Engrg. and Electronics, Vol. 2, No. 12, 1957, p. 123.

48. Tucker, D. G. "Signal/Noise Performance of Super-Directive Arrays," Acustica, Vol. 8, No. 2, 1958, pp. 112-116.

49. Solymar, L. "A Reactance Theorem for Antennas," Proc. IRE, Vol. 46, April 1958, p. 779.

50. Solymar, "Maximum Gain of a Line Source Antenna if the Distribution Function is a finite Fourier Series," IRE Trans. on Antennas and Propagation, Vol. Ap-6, July 1958, pp. 215-219.

51. Harrington, R. F. "On the Gain and Beamwidth of Directional Antennas," IRE Trans. on Antennas and Propagation, Vol. AP-6, July 1958, pp. 219-225.

52. Broussard, G. "Contribution a l'etude Theorique Rayonnement," in "Comme. Pres. au Congres International Circuits et Antennes Hyperfrequences," Vol. 1, 1957, pp. 58-62, suppl. to L'Onde Elec. August 1958.

53. Barber, N. F. "Design of Optimum Arrays for Direction-Finding," Elec. and Radio Engr., Vol. 36, June 1959, pp. 222-232.

54. Lawson, J.D. "Electromagnetic Wave Problems," Elec. and Radio Engr., Vol. 36, September 1959, pp. 332-338.

55. Kyle, R.F. "Super-Gain Aerial Beam," Elec and Radio Engr., Vol. 36 September 1959, pp. 338-340.

56. Franz, K. "Die Verbesserung des Uebertragungswirkungsgrades durch Richtantennen," Telefunken Mitteilungen, Vol. 21, 1940, pp. 3-8.

57. Simon, J.C., Broussard, G., and Spitz, E. "Sur la Superdirectivite d'une Antenne a Rayonnement Transversal," Comptes Rend. Acad. Sci. Vol. 248, April 1959, pp. 2309-2311.

58. Simon, J.C., Broussard, G., and Spitz, E. "Bemerkungen uber die Absorptionsflache von Richtantennen," Hochfr. u. Elektrakustik, Vol. 61, 1943, pp. 51-53.

59. Bakrakh, L.D. "The Maximal Directivity Coefficient of Linear and Plane Aerials," Kokl. Acad. Nauk SSSR, Vol. 95, March 1, 1954, pp. 45-48.

60. Ishimaru, A., and Held, G. "Analysis and Synthesis of Radiation Patterns from Circular Apertures," Canad. J. Phys., Vol. 38, 1960, p. 78.

61. Bloch, A., Medhurst, R.G., Pool, S.D. "A New Approach to the Design of Super-directive Aerial Arrays," Proc. IRE, Vol. 100, Part III, 1953, p. 303.

62. Bloch, A., Medhurst, R.G., Pool, S.D. "Superdirectivity," Proc. IRE, Vol. 48, 1960, p. 1164.

63. Berman, A. and Clay, C.S. "Theory of Time-Averaged-Product Arrays," J. Acoust, Soc. Amer. Vol. 29, 1957, p. 805.

64. White, W.D. "Limits on the Information Available from Antenna Systems," IRE Nat. Conv. Rec., Part I, 1957, p. 57.

65. Kock, W.E. "Related Experiments with Sound Waves and Electromagnetic Waves," Proc. IRE, Vol. 47, 1959, p. 1192.

66. Seeley, E.W. "Two-and Three-Loop Superdirective Receiving Antennas," J. of Res., Nat. Bur. of Stds, Vol. 67D, 1963, p. 215.

67. di Francia, G.T. "Super Gain Antennas and Optical Resolving Power," Suppl. Nuovo Cimento, Series 9, Vol. 9, 1952, p. 426.

68. Rhodes, D. R. "The Optimum Array for a Single Main Beam," Proc. IRE, Vol. 41, 1953, p. 793.

69. Schildknecht, R. O. "Superdirective Antenna Arrays for Improved VLF (Abstract)" 1962 Int. IRE Con. Part 1, p. 164.

70. Rhodes, D. R. "The Optimum Line Source for the Best Mean-Square Approximation to a Given Radiation Pattern," IEEE Trans. on Ant. and Prop. Vol. AP-11, 1963, p. 440.

71. Pokrovskii, V. L. "The Design of Optimum Aerials Radiating Along the Axis," Radio Engrg. and Electronics, Vol. 2, No. 4, 1957, p. 28.

72. Pokrovskii, V. L. "Optimum Linear Aerials Radiating at a Given Angle to the Axis," Radio Engrg. and Electronics, Vol. 2, No. 5, 1957, p. 61.

73. Tartakovskii, L. B. "The Synthesis of a Linear Radiator and its Analogy in the Wideband-Matching Problem," Radio Engrg. and Electronics, Vol. 3, No. 12, 1955, p. 73.

74. Solymar, L. "On the Optimum Gain of Uniformly Spaced Arrays," Proc. IEEE, Vol. 51, 1963, p. 1258.

75. Yen, J. L. "On the Synthesis of Line-Sources and Infinite Strip-Sources," IRE Trans. on Ant. and Prop. Vol. AP-5, 1957, p. 40.

76. Kashihara, T. K. "On Approach to Superdirectivity through Multiple Beam Processing," Eighth Annual Radar Symposium Record, 1962.

77. Spitz, E. "Supergain and Volumetric Antennas," AFCRC-TR-59-194, 15 June 1959, Final Rept. AF 61(062)-102.

78. Ksienski, A. "Spatial Frequency Characteristics of Finite Aperture Antennas," AFCRL-62-975, July 1962, Sci. Rept. No. 1, AF 19(620)-333.

79. MacPhie, R. "On Maximizing the Signal-to-Noise Ratio of a Linear Receiving Antenna Array," Jan. 1963, AF 33(657)-10474.

80. Ward, H. T., Sterling, C. I., and Wiley, T. W. "Superdirective Antenna Study Task," RADC-TDR-63-3, 1 Nov. 1962, AF 30(602)-2662.

81. Collin, R. E., and Rothschild, S. "Reactive Energy in Aperture Fields and Aperture Q," AFCRL-62-920, Sci. Rept. 34, AF 19(604)-3887.

82. Drane, C. S. "Phase Modulated Antennas" AFCRC-TD-59-138, April 1959.

83. Brown, J. L. "Design of Directional Arrays," J. Acoust. Soc. Amer., Vol. 31, 1959, p. 1638.

84. Price, O. R. "Reduction of Sidelobe Level and Beamwidth for Receiving Antennas," Proc. IRE, Vol. 48, 1960, p. 1177.

85. Fakley, D. C. "Comparison Between the Performances of a Time-Averaged Product Array and an Interclass Correlator" J. Acoust. Soc. Amer., Vol. 31, 1959, p. 1307.

86. Welsby, V. G., and Tucker, D. G. "Multiplicative Receiving Arrays," J. Brit. IRE, Vol. 19, 1959, p. 369.

87. Fel'd, Ya. N. and Bakhrakh, "Present State of Antenna Synthesis Theory", Radio Engineering and Electronic Physics, No. 2, Feb. 1963, p. 163.

SECTION V

ANGULAR DISPERSION-COMPRESSION ANTENNA TECHNIQUES

I Introduction

The concept of angular dispersion and compression was first originated by Urkowitz, Hauer and Koval[1] as an outgrowth of the attempt to formulate the angular ambiguity function of a signal radiated from a scanning antenna. It turned out that for CW or narrow band signals (fractional bandwidth $\delta < 0.2$) the angular ambiguity function could be written as the complex correlation of the antenna pattern. This suggested that directivity could be recovered from any randomly dispersed pattern by simply correlating the received signal with the stored replica of such a pattern. In this respect the angular compression may be regarded as a spatial analogy to the well known principle of pulse compression. Furthermore, it became evident early during the investigation that for narrow band signals the correlation processes defining range and angular resolution are independent of each other and can be implemented in cascade. The same is true, in general, of a six-dimensional processor which includes range, two angles and their respective rates.

There are three main advantages to be realized from application of angular dispersion and compression. The first two--lack of directivity and low average power density in space--make it difficult for the enemy to detect the transmitter. The third advantage results in simplification of array construction by eliminating the requirement of accurate phase control in each of its elements.

Three types of signal processing which could be used to achieve angular dispersion and compression are discussed. These are: electronic processing, spatial processing and optical processing.

Electronic methods are mainly implemented by proper matched filtering or some variations of this basic technique. Spatial processing methods are based on the fact that the received radar signal is proportional to the product of transmitter and receiver antenna patterns. By introducing a relative displacement variable between the two, and integration of the received signal, a pattern autocorrelation function is generated.

Main attractions of the optical method include the two-dimensional character of optical processors, and the virtually unlimited delay and storage capabilities of photographic films. When angular compression is applied to radars with slowly rotating antennas, typical integration times

(1) "Generalized Resolution in Radar Systems", H. Urkowitz, C.A. Hauer J.F. Koval, Proc. IRE, Vol. 50, No. 10, Oct. 1962, pp. 2093-2105.

required to compress the pattern are of the order of seconds. Delays of such magnitude are difficult to obtain by conventional electronic methods but are very simply realized by storing the signals on film for processing by optical correlation.

This paper is not intended to be a rigorous mathematical treatment of angular dispersion and compression. Whenever possible, rigor is sacrificed in favor of descriptive approach. It provides what is believed to be a simple and up-to-date discussion of the state of the art, and provides conjectures for further application as well as suggestions for further research.

II Theoretical Principles

A. Ambiguity Functions

The resolution properties of a signal are contained in its ambiguity function. Thus, in principle, it is possible to resolve two signals in any desired number of dimensions by displaying their appropriate ambiguity functions. Unfortunately, it is difficult to obtain displays of higher than second order by any conventional methods. The multidimensional ambiguity displays are therefore obtained by such subroutine processing techniques as gating and quantization (in time or in frequency domains), these processes generally yielding a number of two-dimensional primary displays, one for each discrete value of every parameter not represented in the primary display. In certain cases the undesirable parameter can be eliminated from the signal by proper compensation (e.g., doppler shifts can be eliminated in this way).

In any case, it is the two-dimensional ambiguity function that is of primary interest in this discussion. Since the application of the angular compression concept seems to be most valuable in range-measuring devices of the radar and sonar type, range will be regarded as one of the essential ambiguity dimensions at all times. The other dimension then must be either elevation or azimuth angle if angular compression is to be demonstrated. Thus the range-azimuth ambiguity function is introduced first as the basic algorithm for signal processing. The extension of this basic function to more than two dimensions (such as elevation angle or range rate) is essentially straight-forward.

Using ambiguity function formulations based on the integrated squared difference of two received complex signals, s_1 and s_2, which differ in range and azimuth, one can show that the required ambiguity function is given by

$$\Phi(\tau, \Delta\theta) = 2\,\mathrm{Re} \iint s_1(t,\theta)\, s_2^*(t+\tau, \theta+\Delta\theta)\, dt\, d\theta \tag{1}$$

where τ and $\Delta\theta$ are range and angle separations between s_1 and s_2, respectively and the integrations are performed over all time and total scanning angle of 2π radians in general.

Assuming the transmitted signal to be

$$s_T = a(t) e^{i\omega_0 t} \tag{2}$$

where a(t) is the complex modulation envelope, the ambiguity function for the case of a continuous linear antenna with a complex illumination function I(x), and length 2a, scanning in the azimuth dimension only, can be written in the following form:

$$\Phi(\tau, \Delta\theta) = \sum_{p=0}^{\infty} \epsilon_p A_p \cos(p\Delta\theta) \tag{3}$$

where

$\epsilon_p = 1$ for $p = 0$

$\epsilon_p = 2$ for $p > 0$

, and the coefficients A_p are given by:

$$A_p = 2\,\mathrm{Re} \int \left| \int A(\omega) I(x) J_p\left(\frac{\omega+\omega_0}{c} x\right) dx \right|^2 e^{i(\omega+\omega_0)\tau}\, d\omega \tag{4}$$

In Eq. (4) $A(\omega)$ is the Fourier transform of the complex signal modulation a(t), J_p is the Bessel function of the first kind and pth order and c is the velocity of light.

Derivation of Eq. (3) involves the plane wave approximation of the far field of the antenna and thus holds for signals which are received from ranges greater than $4a^2\omega_0/\pi c$. At those ranges the antenna field pattern is given by the Fourier transform of the illumination function I(x),

$$G(\omega_0,\theta) = \int_{-a}^{a} I(x)\, e^{i\frac{\omega}{c}x\cos\theta}\, dx \tag{5}$$

, where θ is the azimuth angle measured counter clockwise from the antenna axis. Strictly speaking, Eq. (5) holds only for unmodulated CW signals at frequency ω_0. When the modulation spectral bandwidth is small compared to the carrier frequency (less than 20 percent) Eq. (5), approximates the actual antenna pattern sufficiently close so that it may be used to simplify Eq. (3). After considerable amount of mathematical manipulation Eq. (3) can be written as follows:

$$\Phi(\tau,\Delta\theta) = \frac{2}{\pi} R_e\left[R(\omega_0,\Delta\theta)\, R(\tau)\, e^{i\omega_0\tau}\right] \tag{6}$$

, where

$$R(\omega_0,\Delta\theta) = \int_0^{2\pi} G(\omega_0,\theta)\, G^*(\omega_0,\theta-\Delta\theta)\, d\theta \tag{7}$$

will be recognized as the complex correlation function of the antenna pattern,

$$R(\tau) = \int_{-\infty}^{\infty} a(t)\, a^*(t+\tau)\, dt \tag{8}$$

is the complex correlation function of signal modulation, and R_e denotes "real part of".

The significance of Eq. (6) cannot be underestimated. It states that, regardless of the shape of the antenna pattern, targets can be resolved in angle by forming angular correlation function $R(\omega_0, \Delta\theta)$. Furthermore, it states that the process of angular resolution is independent of range resolution which is contained in the signal correlation function $R(\tau)$. A more rigorous discussion of this relationship was first presented by Urkowitz, Hauer, and Koval[2] using a slightly different formulation of

(2) Urkowitz, et. al., op. cit.

the ambiguity function. Eq. (6) represents the basic processing algorithm for angular and range resolution. Equations (7) and (8) will be recognized as angular and range amgibuity functions, $\Phi(\Delta\theta)$ and $\Phi(\tau)$ respectively, so that Eq. (6) can be written as:

$$\Phi(\tau, \Delta\theta) \propto \Phi(\Delta\theta)\Phi(\tau) \tag{9}$$

, which further emphasizes the independence of the two processes. It must be pointed out that although Eq. (6) was derived for a receiving antenna only, it is equally valid for the transmit-receive case if $G(\omega_o, \theta)$ is defined as the two-way pattern and the transmitting and receiving patterns need not be identical.

As noted before, Eq. (6) can easily be modified to contain more than two dimensions. For example, the combined range and range rate ambiguity function is given by:

$$\Phi(\tau, \omega_d) = \int_{-\infty}^{\infty} a(t)\, a^*(t+\tau)\, e^{i\omega_d t}\, dt \tag{10}$$

This is not an autocorrelation function. In practice, the integral of Eq. (10) is usually calculated in a discrete form, e.g. one autocorrelation integral is evaluated for each discrete value of the range rate. This type of processing is actually based on a much more solid theoretical formulation of maximum likelihood estimation which will not be discussed here. It is important to note, however, that the synthesis of any ambiguity function containing a basic dimension and its rate involves quantization processes which lead to a bank of processors rather than one simple device.

Similarly the ambiguity function for two angles, elevation ϕ and azimuth θ, may be written as a double correlation integral:

$$\Phi(\Delta\theta, \Delta\phi) = \iint G(\omega_o, \theta, \phi)\, G^*(\omega_o, \theta - \Delta\theta, \phi - \Delta\phi)\, d\theta\, d\phi \tag{11}$$

For the very important case of a plane aperture whose illumination function I(x, y) can be factored into a product of two one-dimensional functions, or

$$I(x,y) = I_1(x) I_2(y) \tag{12}$$

the double correlation integral of Eq. (11) can also be factored into two parts

$$\Phi(\Delta\theta,\Delta\phi) = \int G_1(\omega_0,\theta) G_1^*(\omega_0,\theta-\Delta\theta)\,d\theta \int G_2(\omega_0,\phi) G_2^*(\omega_0,\phi-\Delta\phi)\,d\phi \tag{13}$$

$$= R(\omega_0,\Delta\theta)\, R(\omega_0,\Delta\phi)$$

, where $G(\omega_0, \theta)$ and $G(\omega_0, \phi)$ are antenna field patterns in azimuthal and elevation planes, respectively. From Eq. (13) it follows that

$$\Phi(\Delta\theta,\Delta\phi) = \Phi_\theta(\Delta\theta)\,\Phi_\phi(\Delta\phi) \tag{14}$$

Finally, from Eqs. (9) (10) and (14) an expression can be written for the general six-dimensional ambiguity function incorporating range, two angles and their respective rates of change as

$$\Phi(\tau,\omega_d,\Delta\theta,\dot\theta,\Delta\phi,\dot\phi) \propto \Phi(\tau,\omega_d)\,\Phi_\theta(\Delta\theta,\dot\theta)\,\Phi_\phi(\Delta\phi,\dot\phi) \tag{15}$$

where $\dot\theta$ and $\dot\phi$ are azimuthal and elevation rates in radians per second.

B. Ambiguity Function Synthesis

From the discussion above, it is fairly evident that the synthesis of any ambiguity function which involves any of the three basic dimensions of range, azimuth and elevation is accomplished by formation of a complex autocorrelation function of the received signal in the domain of the particular parameter of interest. Eq. (15) indicates that processing in each domain is independent of any other domain and can be done in cascade.

When the ambiguity function includes parameter rates, the resultant six-dimensional processor is a tree-like structure of successive filters and quantizers which at the present time is regarded as uneconomical for practical applications and will not be discussed further in this paper. Within the limitations imposed on derivation of Eq. (15) (narrowband signal and separability of the two dimensional antenna illumination) it can be shown that synthesis of the three-dimensional ambiguity function involving range, azimuth and elevation can be performed directly by operating on the received signal. If the transmitted signal is written as

$$s_T = a(t)e^{i\omega_0 t}$$

, then the signal received by a linear planar aperture from a far-field range R, elevation ϕ, and azimuth θ can be written as:

$$s_R = G_1(\omega_0, \theta) G_2(\omega_0, \phi) a(t - \tfrac{R}{c}) e^{i\omega_0(t - \frac{R}{c})} \qquad (16)$$

To form a three dimensional ambiguity function which resolves two signals of the type represented by Eq. (16) one needs to have stored replicas of the complex conjugates of each of the factors contained in Eq. (16). At each stage of processing the received signal is multiplied by its properly delayed replica and the product is integrated over all values of the particular parameter. This, of course, will be recognized as the processing performed by an ordinary matched filter whose impulse response is the time inverse of the signal, or $h(t) = s_R^*(-t)$. To perform the synthesis of a three dimensional ambiguity function by three cascaded matched filters it is necessary that the antenna patterns be expressed as functions of time. This can be easily accomplished by either scanning the antenna at a uniform rate past the target (mechanically or electronically) or supplying a time-varying illumination function I(x, y, t). In either case the received signal will contain amplitude and phase modulation which represents the antenna pattern as a function of time and can be stored in a matched filter. For a scanning antenna this modulation is given by a time varying pattern $G(\omega_0, \dot{\theta}t - \theta)$ where $\dot{\theta}$ is the constant scan rate, so that the proper matched filter has an impulse response $h(f) = G^*(\omega_0 - \dot{\theta}t)$.

Since every continuous autocorrelation integral has its discrete counterpart, the required matched filters can be implemented by analog or digital methods. The latter become more attractive when one considers

long delay times which are necessary to obtain autocorrelation over the full azimuthal scan of a slowly rotating radar antenna. Perhaps a few additional comments on the general nature of the ambiguity functions are due at this point. One may get a mistaken notion that by processing received signals so as to convert them into their ambiguity functions all problems of resolution are solved in an optimum manner. While this is very nearly true in most cases, there are a few prequisites which the ambiguity function must satisfy in order to produce an unambiguous resolution display.

As was stated before, ambiguity functions are basically derived from maximizing the integrated squared difference of two received signals. For a simple illustration consider formulation of the range ambiguity function for two complex signals which differ in range by an amount τ. The integrated squared difference is:

$$\epsilon^2 = \int \left| s_1\left(t - \frac{R}{c}\right) - s_2\left(t - \frac{R}{c} - \tau\right) \right|^2 dt$$

$$= \int |s_1|^2 dt + \int |s_1|^2 dt - 2 R_e \int s_1 s_2^* dt \qquad (17)$$

, where s_2^* denotes the complex conjugate of s_2 and Re denotes the "real part of". The first two terms of Eq. (17) are constant and equal to the total energy in each of the signals. Hence, if ϵ^2 is to be maximized, the third term of Eq. (17) must be minimized. This integral will be recognized as the definition of the range ambiguity function. For optimum range resolution, this function must be minimum except at the point $\tau = 0$ where s_1 and s_2 are so close together that they may be regarded as one signal. This is equivalent to the requirement that the ambiguity function should have only one maximum in the range interval of interest and this maximum should occur at the range of the target. According to Eq. (8), this requirement will be satisfied if, and only if, the autocorrelation function of the signal modulation has but one maximum in the same range interval. Thus it is through the proper selection of the signal modulation that the optimum ambiguity function may be realized. Similarly, in the course of the angular ambiguity function, it is the modulation imposed on the angular antenna pattern that allows only one correlation peak per each target and thus provides angular resolution.

Mathematically, only purely random functions possess this property. In practice it is difficult to realize and to control a truly random modulation function; hence one must resort to the best available

substitutes. Long, pseudo-random sequences resemble random functions in many respects including the unique correlation property, but their "randomness" takes the form of a certain predetermined sequence which is defined at every point and may be stored in a matched filter. Pseudo-random sequences are also of finite length which makes their use particularly convenient. It is this type of function which is assumed whenever random modulation is referred to throughout the remainder of this report.

C. Angular Dispersion-Compression Concept

The phenomenon of angular compression is a spatial analogy to the well known principle of pulse compression. In a pulse compression system a pseudo-random modulation is imposed upon the transmitted signal and its replica is stored in the receiver. Upon reception the signal is cross correlated with its stored replica so that the receiver output is effectively a one-dimensional range ambiguity function. The location of the peak of the output signal is a measure of the target range while its width at the 3 db points determines the range resolution capabilities of the system. Since the output signal-to-noise ratio of a matched filter is only dependent upon the signal energy, and not upon its shape, long pulses of low peak power can be transmitted and compressed in the receiver into narrow correlation peaks, thus retaining the range resolution properties of narrow pulse systems.

Similarly, if an aperture is excited with a random amplitude and phase illumination with zero average, its far field pattern has a random appearance without indication of a main beam (see Figures 1(a), (b)). If the antenna is allowed to rotate past a stationary target the return signals will be proportional to the random pattern as shown by Eq. (16). A filter matched to this pattern will form a correlation peak at its output; its time position will be proportional to the angular position of the target. When two targets separated in angle exist the output of the matched filter will contain two correlation peaks. The time separation between the correlation peaks will be proportional to the angular separation between the targets; hence targets are resolved in angle without using a strong directive antenna beam. In the case of a pulsed radar the output of the antenna is proportional to the sampled replica of the pattern. The angular correlation in this case is the correlation of the envelope of the samples as shown in Figure 1(d). The number of pulses within the 3 db "beamwidth" of the correlation peak can be adjusted to provide required range sensitivity after integration.

Even though the principle of angular compression was introduced for a rotating radar antenna, this is not the only method of implementation. Antenna rotation becomes unnecessary when the illumination function is

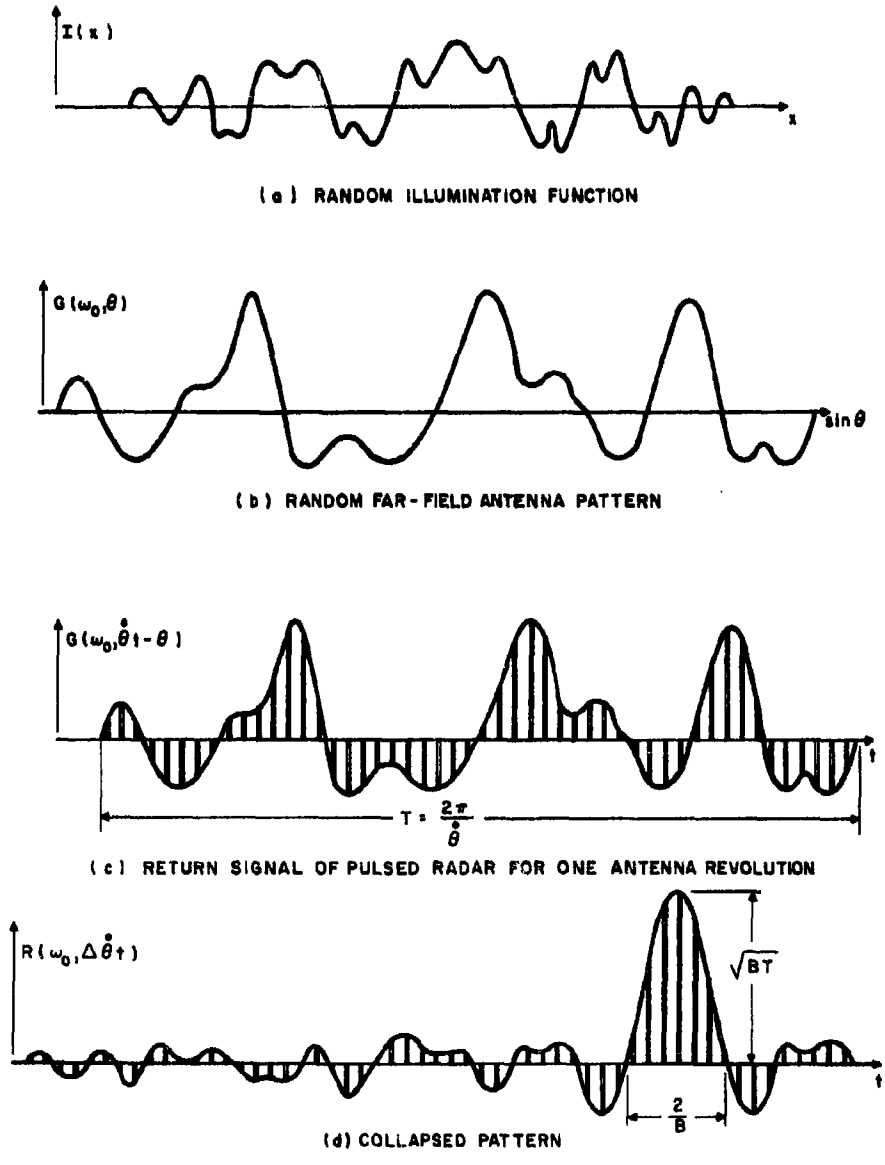

Figure 1 Angular Dispersion and Compression

varied in time. Time variation of the antenna pattern causes a modulation of the transmitted signal. If the illumination function varies rapidly compared with the signal modulation a(t) the signal is dispersed in space. In a discrete array, different pseudo-random sequences can be used to vary the illumination function of each element. The signal received from such a transmitter will depend upon the angle of the receiver with respect to the transmitter, i.e., the receiver will receive different signals depending upon its location. Thus it is possible to transmit different puesdo-random codes at different angles simultaneously.

For a random illumination function the pattern at broadside of an array is given by the average value of the illumination across the aperture. Since it was assumed that this average value is zero, no signal can be transmitted at broadside. If the array is supplied with a uniform average illumination in addition to the random one, a strong non-fluctuating main beam results while the sidelobes continue to vary randomly with time. Thus, a transmitted signal is unmodified in the direction of the main beam, but is modulated randomly elsewhere.

Additional techniques for achieving angular dispersion and compression are discussed in subsequent sections of this paper.

D. Advantages and Limitations

What are the advantages of an angular compression system? For the case of pulse compression, significant simplification of transmitting equipment results due to lower peak power required for transmission. Equipment simplification can be traded for increased sensitivity in a peak power limited system. In addition, pulses can be coded to resemble random noise thus making their detection difficult without the proper matched filter.

Similar advantages result from use of angular compression, only in this case the equipment simplification can become much more significant. To illustrate this advantage, consider an ICBM radar employing a planar array antenna. Now, planar array antennas have several important advantages which make their use very attractive to a radar designer. The most important of these advantages are listed below:(3)

(1) Rapid scanning over the coverage of the antenna without necessity to move the entire antenna structure.

(3) "Introduction to Radar Systems", Merril I. Skolnik, McGraw Hill, Inc., 1962, pp. 318-319.

(2) Simultaneous generation of many independent beams from the same antenna aperture.

(3) Large peak and average powers obtained with separate transmitters at each of the elements of the array.

(4) Electronic, rather than mechanical stabilization for shipboard or airborne radars.

(5) Relative ease with which the aperture illumination may be controlled.

Outside of limited coverage, cost and complexity of a large array antenna are perhaps the biggest limitations to the widespread use of the array antenna in most applications. Within the present state-of-the art the cost of an array is usually proportional to the number of radiating elements which it contains; this in turn determines the angular resolution. Reference (2) states that an array which generates a 1^{o} beamwidth requires roughly 10,000 elements while an array with a 0.1^{o} beamwidth requires almost 1 million elements, assuming that they are spaced a half wavelength apart. When one considers that each array element in fact must contain a low power transmitter and receiver, in addition to beam forming and beam steering circuits, the cost becomes prohibitive. The number of elements is not, however, the only major factor contributing to the cost of an array antenna. Pattern synthesis techniques require that tolerances in element spacings be kept to within a small fraction of the transmitted wavelength. The same requirement also applies to the mechanical tolerances in the plane of the array, i.e., all elements must be located in the same plane.

In addition to mechanical tolerances one has to cope with the problem of accurate control of electrical signals being fed to each element. Specifically, a very important factor which contributes to the cost and complexity of an array is the need to maintain phase stability even under adverse operating conditions. The conventional pattern synthesis requires that the only phase changes in any array element be those deliberately and knowingly introduced by the radar designer. In order to accomplish this, all array components such as transmission lines, mixers, amplifiers, etc., must be kept at constant temperature and humidity and all bias supplies must be heavily regulated. Servo phase-control systems for phased arrays have been designed but they only add to the already high cost of the array. Experience shows that most phased arrays which do not possess automatic phase-control circuits require extensive maintenance to keep them in constant alignment.

Most of the difficulties connected with construction and operation of phased arrays can be eliminated when angular dispersion and compression is used.

Even though the number of elements cannot, in general, be reduced, mechanical and electrical tolerances can be relaxed to the point where their contribution to the total cost becomes insignificant.

With random illumination the spacings between the elements can become random which vastly simplifies mechanical construction. Phase control of the beam forming networks becomes unnecessary since all phases across the array are now random. Similarly, amplitude control of the illumination function is eliminated. This means that elements do not have to be fed by signals at IF frequencies through rigidly controlled lengths of cables but may be fed by wave-guides at microwave frequencies from one central transmitter. This eliminates most of the electronic hardware that is usually associated with each element in a conventional array.

It is unfortunate that no simple method has yet been devised to electronically steer the random pattern of a phased array. Until such a method is found the simplifications resulting from application of random pattern compression must be confined to those arrays which can be scanned mechanically.

Assuming mechanical scanning and time invariant, random illumination the information required to compress received signals in the angular domain is a replica of the antenna pattern which must be stored in a matched filter to perform angular correlation. The pattern replica is easily obtained by scanning the antenna past a stationary reference target in space (such as a balloon with a corner reflector) and recording the received signal after coherent detection. The matched filter is then adjusted to provide the complex conjugate, time inverse of this recorded signal. Even the random phases of the illumination function will eventually drift with change in environmental conditions. Periodic recordings of the random pattern must be made and the matched filter must be readjusted to compensate for long term drifts. Thus it is most convenient to have a matched filter with self-adjusting taps.

When optical signal processing is used the reference pattern is recorded on film from the face of an intensity modulated cathode ray tube. For this type of processor the reference pattern recording and storage becomes rather simple and can be done as often as required.

When this line of reasoning is extended further one comes to the conclusion that any irregularly shaped object which is capable of radiating waves into space can be used as an antenna, providing its angular field pattern is sufficiently random to allow a fairly sharp correlation peak.

This possibility deserves a much more thorough investigation which most certainly will result in some highly flexible and economical antenna designs. Field radar antennas which can be constructed from small parts and easily disassembled for transportation and storage may be one application of this concept.

Simplification of equipment is not the only advantage to be gained from the angular dispersion—compression concept. Another important advantage is the signal masking capability. Because the power is dispersed in space, a significant portion of the antenna gain is effectively "hidden" within the receiver. This means that the radiated power at any point in space will generally be much smaller than the power radiated by a conventional pencil beam antenna of comparable angular resolution properties. The radar which uses the angular compression and dispersion technique is less likely to be detected and is less vulnerable to radar homing missile attack. A typical situation is shown in Figure (2). Two radars transmit the same power P_T into space A radar homing missile is at a range R from both radars. The power density received by the missile detector from the dispersed pattern antenna is $P_T|G_{TD}(\theta)|^2/4\pi R^2$, while from the conventional antenna it is $P_T|G_{TC}(\theta)|^2/4\pi R^2$, where $G_{TD}(\theta)$ and $G_{TC}(\theta)$ are transmitting field patterns of the dispersed and conventional antennas, respectively. Assuming that both radars have the same range sensitivity and angular resolution, $|G_{TD}(\theta)|^2 << |G_{TC}(\theta)|^2$ and

$$G_{TC}(\theta) = \int_0^{2\pi} G_{TD}(\theta) G^*_{TD}(\theta - \Delta\theta)\, d\theta \tag{18}$$

where the right side of Eq. (18) contains a correlation peak at the angular position of the missile. This correlation peak is in all respects identical with the main beam of the conventional pattern. Thus it is obvious that the sensitivity of the missile detector must be increased by an amount equal to the peak value of $G_{TC}(\theta)$ to ensure equally reliable detection of the dispersed pattern at the same range at which the conventional pattern is detected. For a better illustration of this principle, assume that both radars employ identical array antennas with a total of N elements in the plane of the scan. The dispersed pattern radar has a random illumination function and the conventional radar has a uniform illumination function. Then the peak value of the field pattern for the conventional radar is N while the peak value of its power pattern is N^2. Hence the power density present at point R in range due to conventional radar is $P_T N^2/4\pi R^2$. The power pattern of the dispersed radar may be said to consist of two components, the DC or average component which is unity

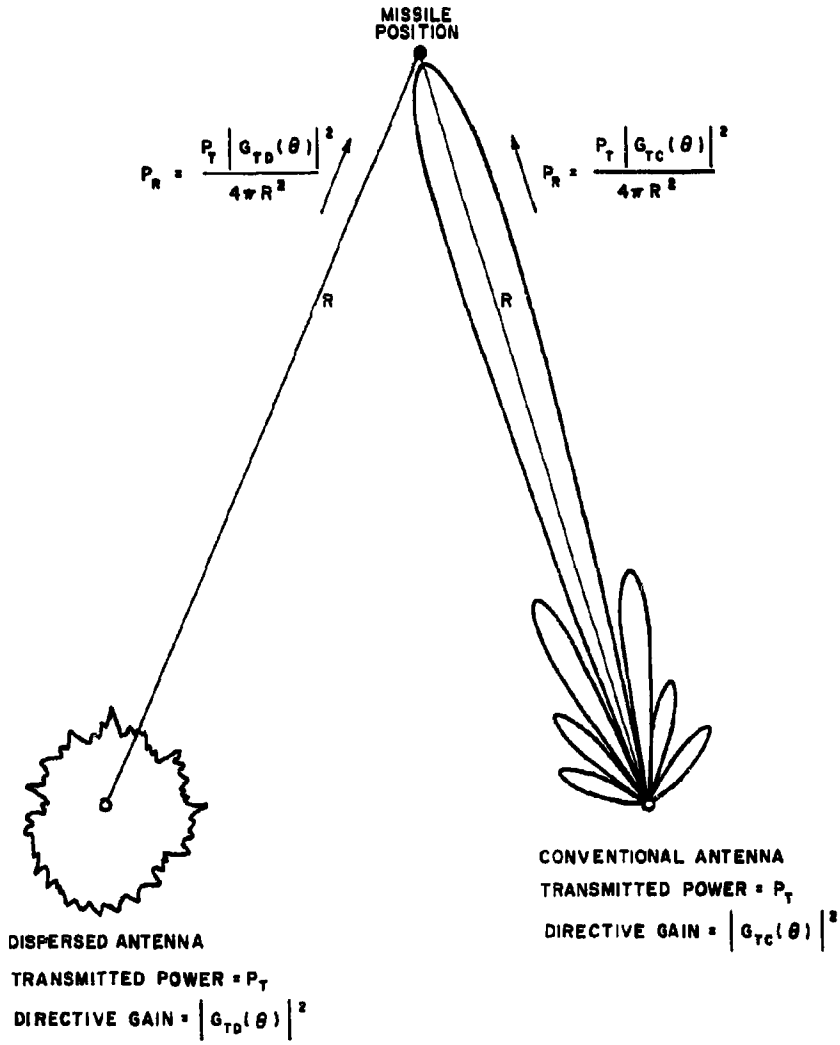

Figure 2 Signal Masking Advantages of Dispersed Pattern Antenna

(average power is uniformly dispersed over all space) and the RMS component which is N. The effective value of the dispersed pattern is the same over all angles and is equal to 1 + N or to N if N is sufficiently large. Thus the power density due to dispersed pattern at point R is $P_T N/4\pi R^2$ which is smaller than the power density due to conventional radar by the factor N or the peak value of the antenna field pattern.

In signal compression theory it is customary to express the increase in the instantaneous peak power of the signal due to compression it terms of the so called "compression ratio" or TW product. If the energy of a band limited signal of time duration T and bandwidth W is compressed in a matched filter, the width of the compressed pulse becomes approximately 1/B and its amplitude is $\sqrt{TW}$. The squared amplitude of this pulse is given by the right hand side of Eq. (18) evaluated at $\Delta\theta = 0$ if the pattern modulation of a scanning antenna is represented as function time.

$$TW = \int_0^{2\pi} |G(\dot{\theta}t - \theta)|^2 d\theta \tag{19}$$

For the case of linear array, TW = N. This quantity represents the net advantage (in power) which the dispersed pattern radar has over a conventional radar of the same sensitivity and resolution properties. Because of this advantage, the radar homing missile must be at a range $R/\sqrt{TW}$ to detect the dispersed pattern with the same reliability as it detects the conventional radar at the range R. With TW products of the order of 10,000 this is indeed a significant advantage, and may provide sufficient time to destroy the missile before it has a chance to detect the radar. Several dispersed-pattern, long range radars can provide an excellent early warning system to protect a network of more conventional tactical radars.

Some additional advantages and applications of angular dispersion and compression are discussed in subsequent portions of this report.

III Electronic Processing

The implementation of an angular compression-dispersion system is most obvious when a matched filter is used to collapse the random pattern. Depending upon the particular method used for pattern dispersion, the matched filters can assume various forms. Three methods discussed below employ electronic hardware to obtain pattern compression in real time.[4] They are directly applicable to radar and sonar systems.

A. Time Coded Antenna

The time domain coding technique consists of a straight forward application of matched filtering to synthesize the range and angle ambiguity function. To make the system more applicable to a realistic situation, doppler compensation is used, which, because of long integration times, results in extremely fine doppler resolution.

Essential parts of the system are shown in Figure 3(a). If the transmitted signal is $s_T = a(t)\, e^{i\omega_0 t}$ the received signal from a target at range R, angle θ, and traveling with a constant radial velocity v_R is:

$$S_R = \int I(x)\, a\left(t - \frac{2R}{c} + \frac{x}{c}\cos\theta\right) e^{i(\omega_0 - \omega_d)\left(t - \frac{2R}{c} + \frac{x}{c}\cos\theta\right)} dx \tag{20}$$

, where ω_d is the doppler frequency corresponding to the target velocity v_R. Letting $\tau = 2R/c$ the outputs of two product detectors are:

In-phase component:

$$S_{RI} = e^{-i(\omega_0 t + \phi)} S_R \tag{21a}$$

, and quadrature component

$$S_{RQ} = i\, e^{-i(\omega_0 t + \phi)} S_R \tag{21b}$$

The matched filter response is

$$h(t) = a^*(t_1 - t) \tag{22}$$

---

(4) "Angular Compression Techniques," C. A. Hauer, Philco Propriety Statement, published by Philco Scientific Laboratory, Blue Bell, Pa., March 5, 1962.

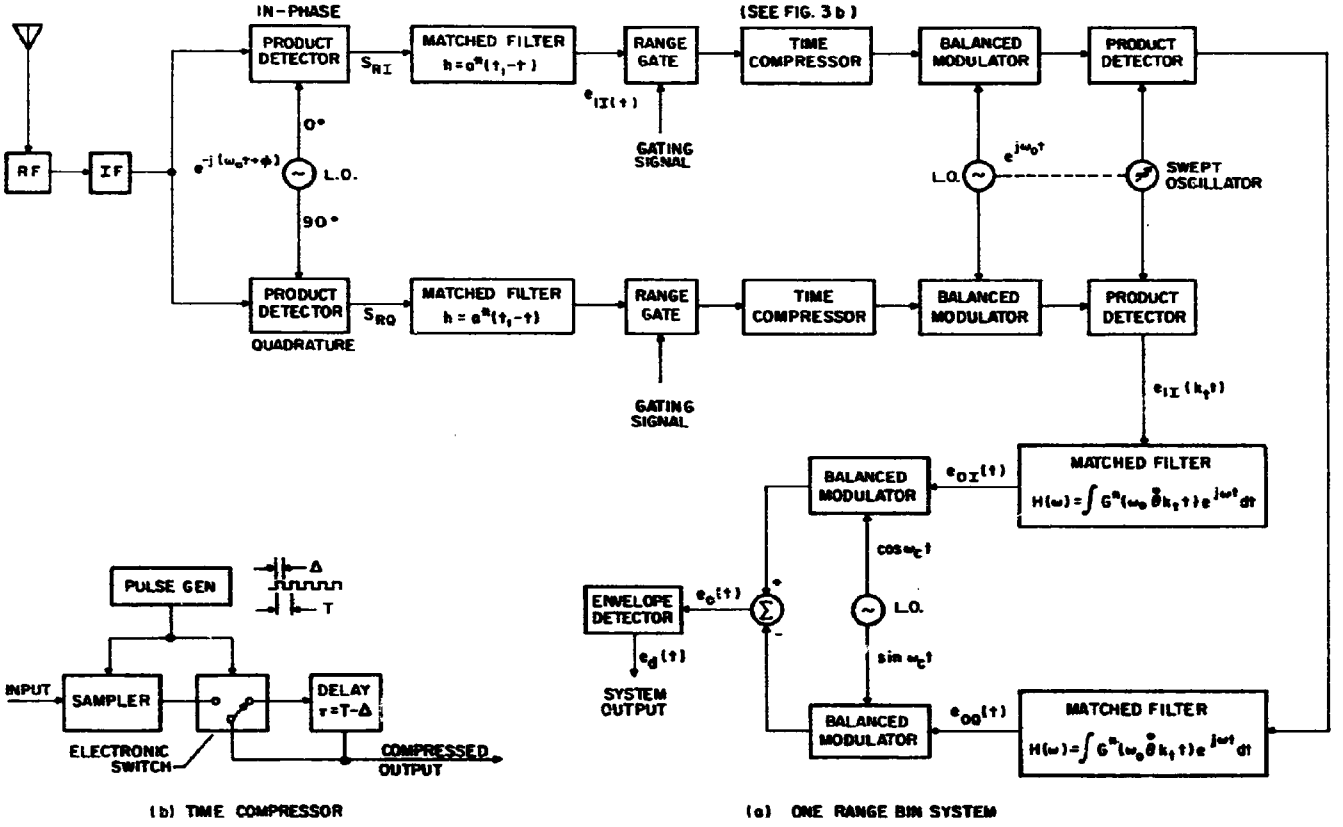

Figure 3 Time Domain Angular Compression System

, and its output is given by

$$e_{12}(t) = \int S_{h2}(t_1)\, a^*(t_1 - t)\, dt_1 \tag{23}$$

Solving for the in-phase component first;

$$e_{12}(t) = \iint e^{i\left[(\omega_o+\omega_d)\left(\frac{x}{c}\cos\theta - \tau\right) - \phi\right]} a\left(t_1 - \tau + \tfrac{x}{c}\cos\theta\right) a^*(t_1 - t)\, I(x)\, e^{-i\omega_d t_1}\, dt_1\, dx \tag{24}$$

Since

$$a(t)e^{i\omega_o t} = \frac{1}{2\pi}\int A(\omega)\, e^{i(\omega+\omega_o)t}\, d\omega \tag{25}$$

Eq. (24) can be written as

$$e_{12}(t) = \frac{1}{4\pi^2}\iiiint e^{i\left[(\omega_o+\omega_d)\left(\frac{x}{c}\cos\theta - \tau\right) - \phi\right]} A(\omega_1) A^*(\omega_2)\, I(x)\, e^{i\left[(\omega_1-\omega_2)t_1 + \omega_2 t - \omega_d t_1\right]}\, e^{i\omega_1\left(\frac{x}{c}\cos\theta - \tau\right)}\, dt_1\, d\omega_1\, d\omega_2\, dx \tag{26}$$

Terms involving t_1 can be separated out,

$$\int_{-\infty}^{\infty} e^{i(\omega_1 - \omega_2 - \omega_d)t_1}\, dt_1 = 2\pi\delta(\omega_1 - \omega_2 - \omega_d) \tag{27}$$

Substituting Eq. (27) into Eq. (26) and using the sifting property of the δ function:

$$e_{12}(t) = \frac{1}{2\pi}\, e^{-i\left[\omega_d(t-\tau) + \omega_o\tau - \phi\right]} \iint A(\omega) A^*(\omega - \omega_d)\, I(x)\, e^{i\left[(\omega_o - \omega_d + \omega)\frac{x}{c}\cos\theta\right]}\, e^{i\omega(t-\tau)}\, d\omega\, dx \tag{28}$$

Equation (28) is considerably simplified by making small bandwidth and small doppler frequency approximations, i.e., $\omega + \omega_o \approx \omega_o$ and $\omega_d / \omega_o << 1$. Another simplification results if $\omega_d < 2\pi/T$ where T is the duration of the transmitted pulse. Using these two approximations Eq. (28) becomes:

$$e_{12}(t) = e^{-i[\omega_d(t-\tau) + \omega_o\tau + \phi]} R(t-\tau) \int I(x) e^{i\omega_o \frac{x}{c}\cos\theta} dx$$

$$= e^{-i[\omega_d(t-\tau) + \omega_o\tau + \phi]} R(t-\tau) G(\omega_o, \theta) \tag{29}$$

, where

$$R(t-\tau) = \int a(t_1)\, a^*(t_1 - t + \tau)\, dt_1$$

$$= \frac{1}{2\pi} \int |A(\omega)|^2 e^{i\omega(t-\tau)} d\omega \tag{30}$$

Up to this point antenna rotation has not been considered. When the field pattern is modified for a rotating antenna, Eq. (29) becomes,

$$e_{12}(t) = e^{-i[\omega_d(t-\tau) + \omega_o\tau + \phi]} R(t-\tau) G(\omega_o, \dot{\theta}t - \theta) \tag{31}$$

The introduction of rotation at this point does not invalidate the results obtained thus far, because the antenna rotation is slow and the system is considered stationary for reception of a given pulse.

The signal next is sampled in a range gate at $t = \tau$ and the resultant wave is time compressed. The time compressor is shown in Figure 3(b). Time compression is used to reduce delay requirements on the second matched filter. The time compressor operates by placing the sampled pulses out of the range gate adjacent to one another by means of a reentrant delay line system. The first sample of the input is fed to the delay line, the length of which is slightly less than the interpulse period of the radar. This sample propagates through the delay line and is fed back to the input just before the second sample arrives. The first and second samples then are recirculated around the delay line loop, after which time the third sample is added. This process continues until the delay line is completely filled.

At this point, the oldest sample in the line is dropped to make way for the arriving sample. The total number of pulses stored in the delay line should correspond to the number of pulses required to adequately sample the antenna pattern through one full revolution. Note that the time compressor produces a time compressed signal which is repeated many times at the output. The time compressed output of the range gate is:

$$e_{1I}(t) = e^{-i[\omega_d k_t t + (\omega_o - \omega_d)\tau + \phi]} R(o) G(\omega_o, \dot{\theta} k_t t - \theta) \qquad (32)$$

, where k_t is the time compression scale factor. Because the input signal is sampled at the pulse repetition rate, doppler ambiguities result for $\omega_d > \pi / T_r$ where T_r is the interpulse period. For example, a signal with a doppler of $\omega_d = 2\pi / T_r$ will appear as a signal without doppler. These ambiguities cannot be eliminated by any simple method.

The time compressor produces the output many times in succession. This output is fed to a balanced modulator after which it is detected again by a product detector. The detector is fed by a deviable oscillator whose frequency is swept at a slow increasing or decreasing rate. Because the signal is effectively repeated many times, each repeated signal is demodulated with a slightly different frequency. Sooner or later, the frequency sweep compensates for doppler. When the signal is fed to the pattern matched filter, correlation occurs only when the frequency error is small. Thus, an output will occur only when the injection frequency to the demodulator compensates for the doppler shift to within specified limits. The doppler shift can be determined by observing the frequency of the injection signal at the instant of correlation. Typically, a doppler resolution of 0.1 to 1.0 cps can be achieved by this technique. The number of doppler bins available is equal to the number of pulse circulations in the time compressor. Using analog techniques, 50 to 100 circulations can be achieved. Many more circulations are possible if digital signals are circulated with pulse reconstitution after each circulation.

At the time when the error frequency is small, the output of the product detector can be written as

$$e_{1I}(t) = e^{-i[\omega_d k_t k_d t + (\omega_o - \omega_d)\tau + \phi]} R(o) G[\omega_o, \dot{\theta} k_t (t - t')] \qquad (33)$$

where k_d is a number less than unity and $t' = \theta/\dot{\theta}k_t$ is the time of observation of the target in angle.

Defining the Fourier transform of the pattern as

$$P(\omega) = \int G(\omega_0, \dot{\theta} k_t t) e^{-i\omega t} dt \tag{34}$$

, the transfer function of the filter matched to the pattern is

$$H(\omega) = P^*(\omega) = \int G^*(\omega_0, \dot{\theta} k_t t) e^{i\omega t} dt \tag{35}$$

If the Fourier transform of the input signal $e_{1I}(k_t t)$ is $E_{1I}(\omega)$, the output voltage of the matched filter is given by

$$\begin{aligned} e_{oI}(t) &= \frac{1}{2\pi} \int H(\omega) E_{1I}(\omega) e^{i\omega t} d\omega \\ &= \frac{R(0)}{2\pi} e^{-i[(\omega_0 - \omega_d)\tau + \phi]} \iiint G[\omega_0, \dot{\theta} k_t (t_1 - t')] \\ &\qquad G^*(\omega_0, \dot{\theta} k_t t_2) e^{-i\omega_d k_d k_t t_1} e^{i\omega(t_2 + t - t_1)} dt_1 dt_2 d\omega \end{aligned} \tag{36}$$

Integration with respect to ω can be separated

$$\int_{-\infty}^{\infty} e^{i\omega(t_2 + t - t_1)} d\omega = 2\pi \delta(t_2 + t - t_1) \tag{37}$$

Substituting (37) into (36) and utilizing the sifting properties of the δ - function,

$$\begin{aligned} e_{oI}(t) &= R(0) e^{-i[(\omega_0 - \omega_d)\tau + \phi]} \int G[\omega_0, \dot{\theta} k_t (t_1 - t')] \\ &\qquad G^*[\omega_0, \dot{\theta} k_t (t_1 - t)] e^{-i\omega_d k_d k_t t_1} dt_1 \\ &= R(0) R[\omega_0, \dot{\theta} k_t (t - t')] e^{-i[(\omega_0 - \omega_d)\tau + \phi]} \end{aligned} \tag{38}$$

This equation is true if, and only if, $k_d = 0$, or when there is a complete doppler compensation.

The actual signal output will be the real part of Eq. (38), or

$$e_{oI}(t) = R(0)\, R_e\left\{ R[\omega_o, \dot{\theta} k_t (t-t')] \right\} \cos[(\omega_o - \omega_d)\tau + \phi] \tag{39}$$

The output of the quadrature channel is derived in exactly the same manner, and is:

$$e_{oQ}(t) = R(0) R_e\left\{ R[\omega_o, \dot{\theta} k_t (t-t')] \right\} \sin[(\omega_o - \omega_d)\tau + \phi] \tag{40}$$

The remainder of the processing serves to combine the in-phase and quadrature components. The in-phase signal is multiplied by $\cos \omega_c t$ and the quadrature signal is multiplied by $\sin \omega_c t$ (ω_c purely arbitrarily), and the two are subtracted. The output of the subtractor is

$$\begin{aligned} e_o(t) &= R(0) R_e\left\{ R[\omega_o, \dot{\theta} k_t (t-t')] \right\} \left\{ \cos[(\omega_o - \omega_d)\tau + \phi] \cos \omega_c t \right. \\ &\qquad \left. - \sin[(\omega_o - \omega_d)\tau + \phi] \sin \omega_c t \right\} \\ &= R(0) R_e\left\{ R[\omega_o, \dot{\theta} k_t (t-t')] \right\} \cos[\omega_c t + (\omega_o - \omega_d)\tau + \phi] \end{aligned} \tag{41}$$

The envelope detector gives the magnitude of the signal in Eq. (41), or

$$e_d(t) = \left| R(0) R_e\left\{ R[\omega_o, \dot{\theta} k_t (t-t')] \right\} \right| \tag{42}$$

, which is precisely the angular ambiguity function. The angle of the target is determined by observing the time $t' = \theta / \dot{\theta} k_t$ when the correlation peak occurs, and the doppler frequency is found by observing the heterodyning frequency of the deviable oscillator at the time of correlation. Range is determined by gating.

The system described above essentially overcomes the two major problems inherently present in realization of the time domain technique. These are the doppler desynchronization and the amount of

delay medium required to collapse the pattern of a slowly rotating antenna. If time compression were not used, the matched filter, which typically takes the form of a tapped delay line, would have to have a delay of the order of seconds or longer. This is hard to realize in practice. Also, Eq. (38) shows that angular correlation will not take place unelss doppler frequency shift is eliminated. In-phase and quadrature processing is used to eliminate the effect of unknown doppler and range delay phases as well as any other phase delays (target aspect, etc.) not considered in the analysis.

It must be noted that time compression is only possible in conjunction with range gating. This immensely complicates the entire system because it means that a processor such as shown in Figure 3 must be used for each radar range resolution element. Thus the time coded antenna approach to angular compression may be applicable to radars whose range interval of interest is not too large and whose range resolution requirements are not too stringent.

B. Frequency Coded Antenna

A somewhat simpler approach to angular dispersion and compression which also uses electronic processing is based on a frequency equivalent of the time domain technique. The method eliminates the requirement for antenna scanning and thus is applicable to array antennas where electronic scanning of a random pattern is difficult to accomplish.

The frequency domain coded antenna achieves angular resolution by establishing a correspondence between the spectral content of a signal and its angle of arrival. The basic principle of operation can be explained with the aid of Figure 4. Imagine that a number of similar beams are formed by the antenna, each separated from the other by a small angular increment and each formed at a particular frequency; three beams of this group are shown. Now examine signal reflected by targets located in directions θ_A and θ_B. For direction θ_A, amplitudes A_1, A_2, A_3 are received at frequencies $f_o + f_1$, $f_o + f_2$, $f_o + f_3$, respectively, from beams 1, 2, and 3. For direction θ_B amplitudes B_1, B_2, B_3 are received also at frequencies $f_o + f_1$, $f_o + f_2$, $f_o + f_3$. Because of signal separation in the frequency domain, outputs from beams 1, 2, and 3 can be filtered out into separate channels. Amplitudes A_n and B_n will have either positive or negative signs, depending on whether they were derived from an in-phase or out-of-phase portion of the field pattern. In this technique, the signal sequences A_n or B_n are arranged so that they form a coded ensemble which will pass preferentially through one coded filter instead of another. Coded Filter "A" will receive and collapse, or coherently add, the signal ensemble A, whereas coded filter "B" will receive the signal ensemble B. If the filter codes are chosen properly, there will be minimum cross coupling between filters and sidelobes of the filter response will be low.

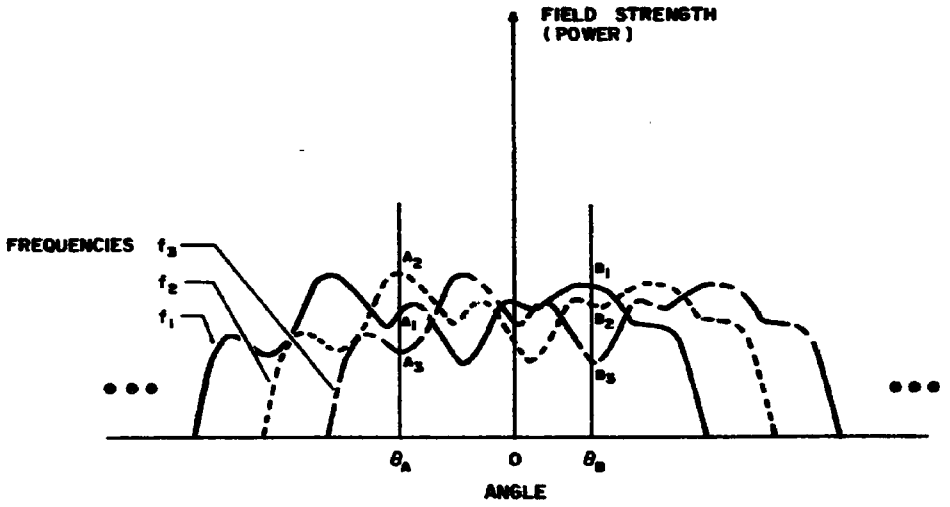

Figure 4 Component Beams Operating At Separate Frequencies

The form of the received signal will be clarified now, the receiving filter will be described later. Some insight into the principle of the technique can be gained by inspecting Figure 5. Because the beams are similar, the form of the spectral function received from each angular direction will be the same. But the spectrum is shifted in frequency for progressively greater angles, as shown in Figure 5. The rate of fluctuation evidenced in the spectral distributions usually is proportional to the characteristic beamwidth of the antenna (λ/L) and the frequency difference between beams. The individual beams, illustrated in Figure 4 need not be regular in shape, nor contain any strong central lobe as in a conventional antenna. The next step in this technique is to construct a set of filters which will accept the spectral distribution derived at one angle, and reject those derived at other angles. Basic elements of such a receiving system are shown in Figure 6.

Signals from the radiation beams are filtered into separate channels and then mixed with a local oscillator to achieve the i-f frequencies $f_o - f_x \pm f_1$, $f_o - f_x \pm f_2$, ..., $f_o - f_x \pm f_N$. The signals at these i-f frequencies form the spectral components of the transmitted pulse but with their amplitudes and phases coded in some prescribed manner. Each i-f signal is amplitude and phase weighted in accordance with the code. The signals then are added and detected to produce an output pulse with a spectral bandwidth extending from f_1 to f_N. If the individual beams (shown in Figure 4) have been chosen to have the proper shape, i.e., a sequence of positive and negative lobes, and if the filter taps are properly adjusted to match the plus-minus configuration of beam amplitudes derived from a given angular direction, then an effectively narrow beam will be formed by the filter configuration shown in Figure 6. Moreover, if a proper pseudo-randomly coded-beam shape is chosen, a beamwidth proportional to the "conventional" beamwidth of the aperture (approximately equal to λ/L) can be formed with low sidelobe level.

The technique described achieves simultaneous coding of the beam shape and the pulse shape, and the compression in both domains is achieved simultaneously. To restrict the field of view so that beams will not be formed in all directions, directive radiators can be used and patterns can be coded within the element beamwidth.

It is clear from the description above that the amount of hardware required for implementation of the frequency coded antenna is considerably smaller than for its time domain counterpart. The number of beams required for synthesis of any given pulse is determined from the sampling theorem. A band limited signal of bandwidth B and duration T is represented adequately by 2TB samples. Since $B = f_N - f_1$, $N = 2T(f_N - f_1)$ which shows that wide-band signals may be processed with a relatively small number of beams.

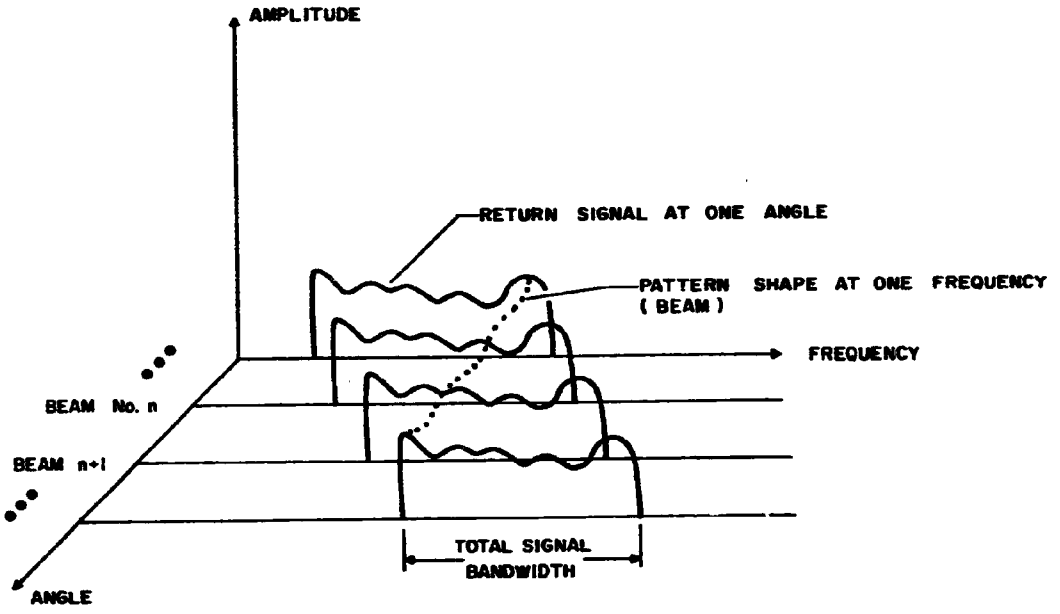

Figure 5 Return Signals In the Frequency-Angle Domain

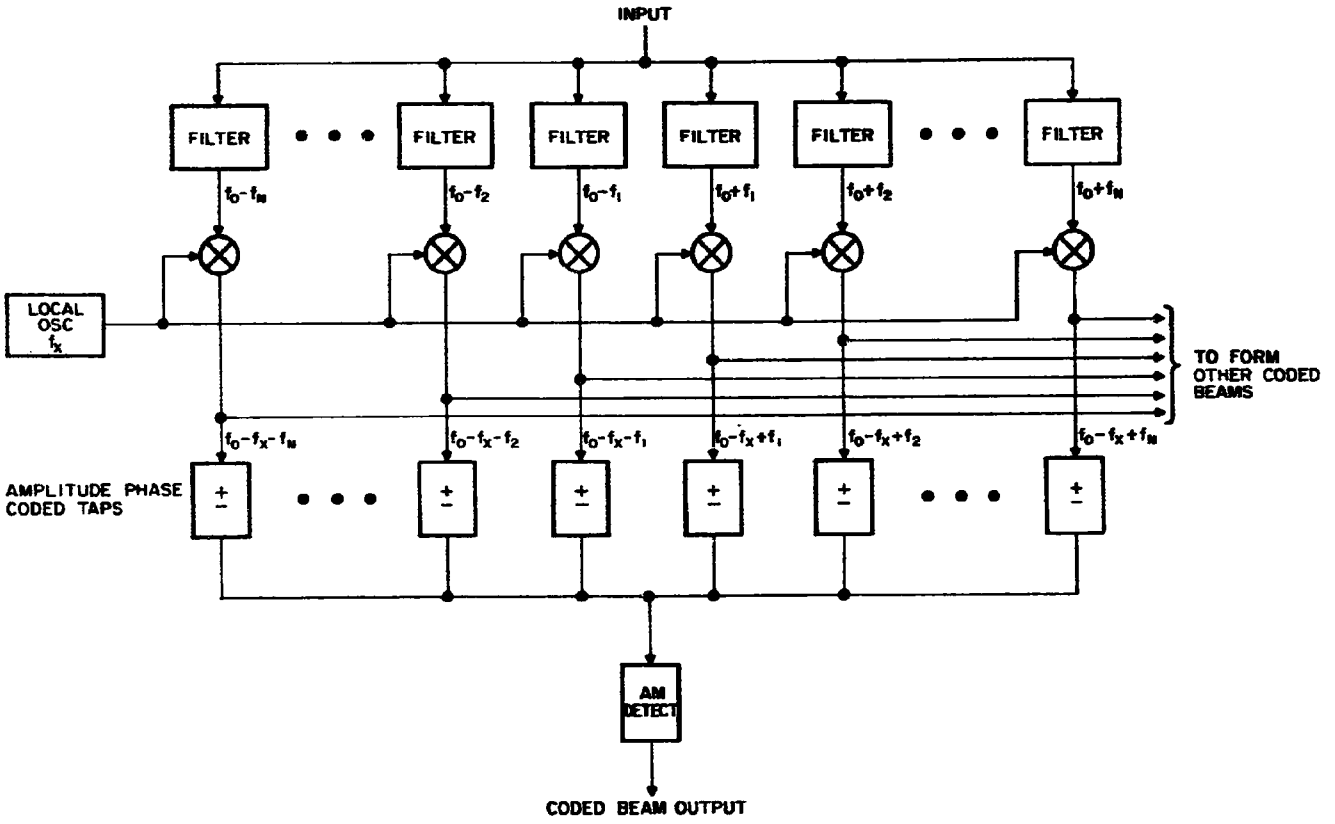

Figure 6 Frequency Domain Angular Compression Techniques

It is also possible to generate the pseudo-random pattern shape with an array of randomly placed radiators, positioned in three-dimensional space and fed by random-length transmission lines. In this case, large arrays of radiators can be constructed to be free of the difficulties involving dimensional tolerance and phase accuracy. Beams formed by an array of this type can be plotted, and the amplitude and phase variations, in turn, can be recorded in the "memory" represented by the coded taps. Alternately, the memory code can be formed automatically by placing a target in the far field and then allowing the taps of the filter bank to be set properly by "photographing" or sensing the form of the incoming signal. If a number of frequencies are fed into a random antenna, random-pattern shapes would be different for each frequency; the various shapes obtained must be consistent to achieve minimum cross coupling between the various beam filters.

C. Time-Frequency Coded Antenna

The third electronic angular compression system is a hybrid of time and frequency approaches.

This antenna operates through a combination of time-varying and frequency-varying aperture illuminations. The operating principle can be understood best by examining Figure 7. A transmitter emitting energy at frequency f_1 is connected sequentially to radiators 1, 2, 3,...N, 1, 2,... on signal transmissions 1, 2, 3,...N, N+1, N+2..., respectively. Returns from these transmissions are coherently added, pulse by pulse, in an integrator (e.g., a real-time reentrant loop filter, a coherent optical storage processor, etc.). Pulse-to-pulse coherence can be achieved with a coherent localoscillator or a fully coherent transmitter. Integration of signals at frequency f_1, received from radiator positions 1, 2, 3...N will form a beam approximately $\lambda_1/2L$ wide where λ_1 is the wavelength corresponding to frequency f_1, and L is the spatial extent of the N transmissions. If successive signal receptions are properly phased, the resulting beam can be pointed in any desired angular direction.

Transmissions at frequency f_2 follow those at f_1 in sequence. When transmitter f_1 has reached radiator 2, transmitter f_2 has reached radiator 1, when f_1 has reached radiator 3, f_2 has reached radiator 2, etc.; the remaining N-2 frequencies follow, as illustrated in Figure 7. When frequency f_1 has reached radiator N, it cycles back to the first radiator on the next pulse, and frequencies f_2, f_3... follow. Transmissions at the different frequencies can take place simultaneously; reception at various frequencies also can take place simultaneously, because isolation is effected by filters. A single set of N transmitters emitting signals at the various frequencies can be used. Each is connected in time sequence to the various radiators with a switching circuit.

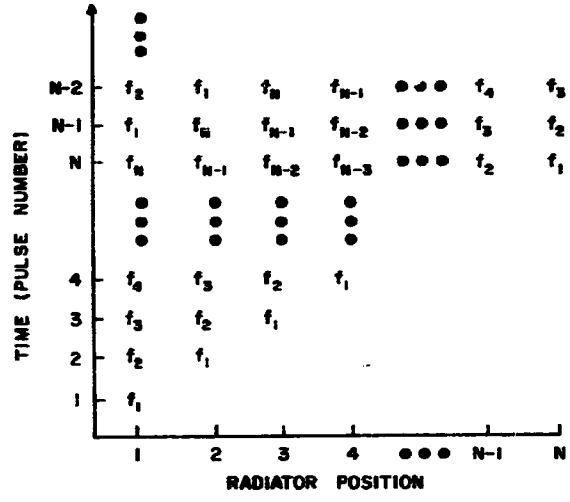

Figure 7 Transmission Frequency As A Function of Time and Radiator Position

The total frequency band covered by frequencies f_1 to f_N, will be limited to some degree by the spacing of radiators. Usually it is necessary to limit the total frequency band to prevent the formation of multilobes caused by radiator spacings somewhat greater than a half-wavelength. Individual beams formed at the several frequencies can be pointed in independent angular directions; the direction of each is controlled only by its own pulse-to-pulse phasing program. Hence, the antenna technique can be used to produce multiple simultaneous beams at different frequencies.

Within the time period of the pulse, transmissions can be coded as in ordinary pulse-compression techniques. Decoding is performed before coherent integration. On a pulse-to-pulse basis, coding can be achieved by phase-reversal techniques; received signals can be decoded during the integration process. The signal level in the far field at any one frequency is low during any transmission, which makes it difficult for the enemy to detect the radiation.

D. Applications

Some applications of angular compression-dispersion techniques became obvious during the previous discussion of the advantages of dispersed antenna patterns. The possibility of significant equipment simplifications in a planar array radar was pointed out. The signal masking advantages of a dispersed pattern were discussed from the point of view of radar homing missile protection. All of these seem to emphasize the fact that radar and sonar devices will probably benefit from angular dispersion techniques more than other types of systems.

Signal masking is of extreme importance in sonar applications. For example, doppler navigation techniques are very useful in properly guiding submarines by sonar signals. One of the major deterrents to widespread application of doppler navigation techniques in submarines, however, is the fact that they cannot be used at times when sonar silence must be maintained. In most cases submarines must rely on purely passive listening devices to avoid detection. Pulse coding and compression may be used in active systems to conceal the message content. Attempts to use pulse compression alone to prevent signal detection are not adequate since the enemy sonar will detect the signal as a sudden increase in noise level. Complete masking requires that the signal level at the enemy receiver site be at least equal to the ambient noise level. In principle, this can be easily achieved by combination of the angular dispersion technique and pulse coding and this can be achieved without any significant sacrifices in range sensitivity. Within bandwidth limitations imposed by the propagating medium, the frequency coded antenna may be used to achieve sound pattern

dispersion. This method of processing avoids problems connected with long integration times normally encountered in sonar due to the low velocity of propagation of sound in water. Other techniques, more directly adoptable to the peculiar propogation properties of ocean water may be devised.

As an outgrowth of angular dispersion and compression, a technique for producing randomly varying antenna sidelobes was described. This may be used in communications to enhance message security and to provide additional protection against jamming.

When sidelobes fluctuate randomly any receiver not located in the main beam is denied access to the message. This can be done without encryption or decryption devices in the transmitter and receiver.(5)

Assume a message consisting of M binits which are phase modulated onto the carrier (phase reversal modulation). The antenna consists of an array of N radiating elements which are excited at random for each binit of the message. If each element is excited at random with some probability, p, the amplitude of the main beam fluctuates with a binomial distribution. For the particular modulation system assumed, amplitude fluctuations may be limited out, but the effects of a fading signal still will be experienced. This will cause errors when the signal-to-noise is low. To avoid this, a constant number of elements may be chosen at random, as one chooses balls from an urn (without replacement). In this way, the signal observed at the center of the beam will not fluctuate in amplitude or phase.

However, an observer who is not in the main beam will see a sequence of vectors with randomly fluctuating amplitudes and phases and hence is denied the message content. If the condition

$$\binom{N}{\frac{N}{2}} >> M \tag{43}$$

holds, the probability of obtaining the same antenna pattern during the message is very small.

(5) C.A. Hauer, op. cit., pp. 8-11.

One might ask, if the message can be received perfectly at the center of the main beam, but cannot be received at all on the sidelobes, where does the transistion take place, and what causes it? As the receiver departs from the center of the beam, the quadrature noise increases quite rapidly, causing phase perturbations. Therefore, in the main beam, the phase vectors will be clustered around 0 and π radians. As the angular deviation increases, the distributions gradually merge, and it becomes increasingly difficult to distinguish marks from spaces. At the point which corresponds to the first null of the full array, all phases are equally probable, and the signal does not disclose the transmitted signal. As the receiver moves into the first sidelobe, certain phases are more probable than others.

The signal to noise ratio for a given sidelobe is given by

$$\left(\frac{S}{N}\right)_j = A_j\sqrt{\frac{2Np}{1-p}} \tag{44}$$

where A_j is the level of the jth sidelobe.

For best performance, A_j, N, and p should be small. Hence, performance can be improved by using aperture tapering to decrease the sidelobe level. Three tapering methods can be used: amplitude, space and probability. Amplitude taper is the conventional approach, but it makes the problem of eliminating main beam noise more difficult. Space tapering is accomplished by spacing elements further apart at the edges of the aperture. In a probability taper, the edge elements are excited less frequently than the central elements.

This technique can be also used as an adjunct to a simple spread-spectrum system. A spread spectrum-system provides resistance to jamming by using a much wider transmission bandwidth than the information bandwidth. In a simple system, binary codes would be used for mark and space, which would phase modulate the carrier. Thus, the signal is the same as before, except it is faster and there are repeated sequences. Now for each mark and space, the antenna illumination will be changed at random, and each code sequence will use a random phase. The object of this is to prevent the enemy from determining the codes which would increase his jamming effectiveness by spoofing or repeater jamming.

In this case, the jammer has a slight advantage because of the repetitive nature of the codes. He can take advantage of this in the following manner: Assume a knowledge of the code length. (It can be obtained by trial and error if not known.) There are four distinct ways to arrange two adjacent code elements, say one and two; in the mark code they

may be the same or different, and the same is true for the space code. Now take the inner product (AB cos θ) of vectors one and two and add a large number of such products together. There are three possible results for this sum. If elements one and two are the same in both mark and space, the bit will be positive. If elements one and two both are different in mark and space, it will be negative. If one and two are the same in one code and different in the other, the sum will be near zero. By performing this computation between all possible elements, the framing and the codes themselves can be determined.

The inner product detection process is basically noncoherent, and for small signal-to-noise ratios the signal is suppressed. Therefore, they require an extremely long sequence before the separation into the three classes becomes apparent. In fact, for small S/N, the number of code sequences required is:

$$n = \frac{\left(\frac{S}{N}\right)_o}{\left(\frac{S}{N}\right)_i} \tag{45}$$

where $(S/N)_o$ and $(S/N)_i$ are the output and input power signal-to-noise ratios, respectively. If the required $(S/N)_o$ is + 10 db and $(S/N)_i$ is -20 db, then a message at least 5×10^4 bits long is required to break the codes. All these bits must be from one message, because it would be difficult to combine the information from more than several messages.

One of the most promising applications for these secure sidelobe generation techniques is to provide secure command control signals for military satellites. In this application, it is important to withhold information about the command signals from the enemy to prevent him from acquiring control of the satellite. The desirability of A/J protection also is obvious. However, the equipment in the satellite should be as simple and reliable as possible. Therefore, the decrypting and decoding devices in the satellite should be minimized. The secure sidelobe generation technique is ideal because almost all the complexity is on the ground.

IV Spatial Processing

A. Counter Rotating Antennas

For certain restricted applications, it is possible to perform the angular correlation directly in space and thus eliminate the necessity of pattern storage in a matched filter. This type of processing takes advantage of the fact that the voltage of the narrow band radar echo signal is proportional to the product of transmitter and receiver angular patterns (Eq. 16). If one pattern is a complex conjugate of the other and a continuous angular displacement variable is introduced between them, the integration of the received signal over all angles of interest yields the true value of angular autocorrelation function and thus compresses the signal in angle.

The method is best introduced by an example of two counter-rotating, randomly dispersed angular patterns shown in Figure 8. Power patterns are shown. These are identical in shape even though their fields are complex conjugates of each other.

Practical difficulties connected with generation of two identical conjugate patterns in space will be temporarily ignored. In Figure 8, the receiving pattern $|G_R(\theta)|^2$ is a mirror image of the transmitting pattern $|G_T(\theta)|^2$ with respect to the $\theta = 0$ axis. Both patterns are pseudo-random in angle but constant in time and they rotate in the opposite directions at a constant angular rate of $\dot{\theta}$ radians per second, as shown. The distance L between their centers is assumed insignificant when compared with the target range, R, of interest. Thus in the far field both patterns are effectively superimposed on top of each other and can be measured in the same set of angular coordinates.* The rotation rate $\dot{\theta}$ is assumed to be small with respect to the interpulse period so that each target in space generates a sufficient amount of samples to reproduce the pattern shape as a function of time. For many revolutions the signal returns will be a periodic function of θ, e.g., $s(\theta_T) = s(\theta_T \pm 2n\pi)$, where θ_T is the target angle. Three cycles of such signal are shown for each pattern in Figure 9, where rectangular coordinates have been used. The analysis assumes a continuous envelope rather than the sampled version which does not in any way invalidate the results. Voltage returns from any target at an angle θ with respect to broadside will be proportional to $G_T(\theta)\, G_R(\theta)$; where θ is

---

* The same condition is obtained in the near field if L = 0.

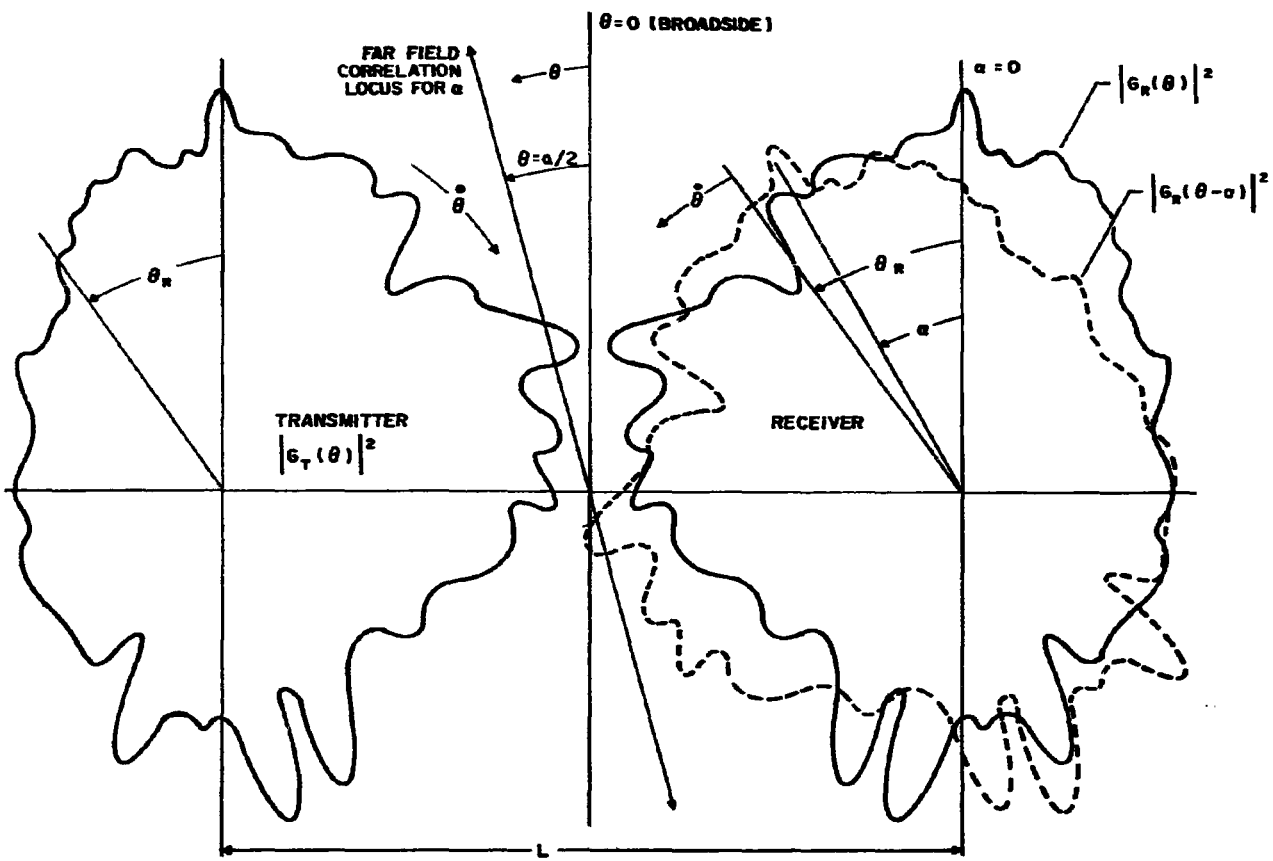

Figure 8 Counter-Rotating Antenna Patterns

considered positive counterclockwise from broadside ($\theta = 0$). When the relative angular displacement, α, between the two patterns is zero, (Figures 9(a) and 9(b)), transmission takes place over pattern $G_T(\theta)$ and the signal is received over $G_R(\theta)$, where

$$G_R(\theta) = G_T^*(\theta) \tag{46}$$

An arbitrary reference point, θ_R, is selected on each antenna so that it rotates together with the antenna. With respect to this point, Eq. (46) can be written as

$$G_R(\theta - \theta_R) = G_T^*(\theta_R - \theta) \tag{47}$$

and the corresponding point on the transmitting pattern becomes $G_T(\theta - \theta_R)$. When the receiving pattern is given a positive angular displacement α with respect to the transmitting pattern, where α is constant over one full revolution, (see Figure 8 and 9(c)), Eq. (47) becomes,

$$G_R(\theta - \theta_R - \alpha) = G_T^*(\theta_R + \alpha - \theta) \tag{48}$$

, while the corresponding transmitting gain expression does not change. Since the two patterns move in opposite directions, the patterns are represented in the time domain by letting $\theta_R = -\dot{\theta}t$ in the transmitting pattern and $\theta_R = \dot{\theta}t$ in the receiving pattern. Thus, in the time domain the transmitting gain is $G_T(\dot{\theta}t + \theta)$ and the receiving gain is:

$$G_R(\theta - \dot{\theta}t - \alpha) = G_T^*(\dot{\theta}t + \alpha - \theta) \tag{49}$$

The output of the receiving antenna is proportional to the product of both patterns, or to

$$G_T(\dot{\theta}t + \theta)\, G_T^*(\dot{\theta}t + \alpha - \theta)$$

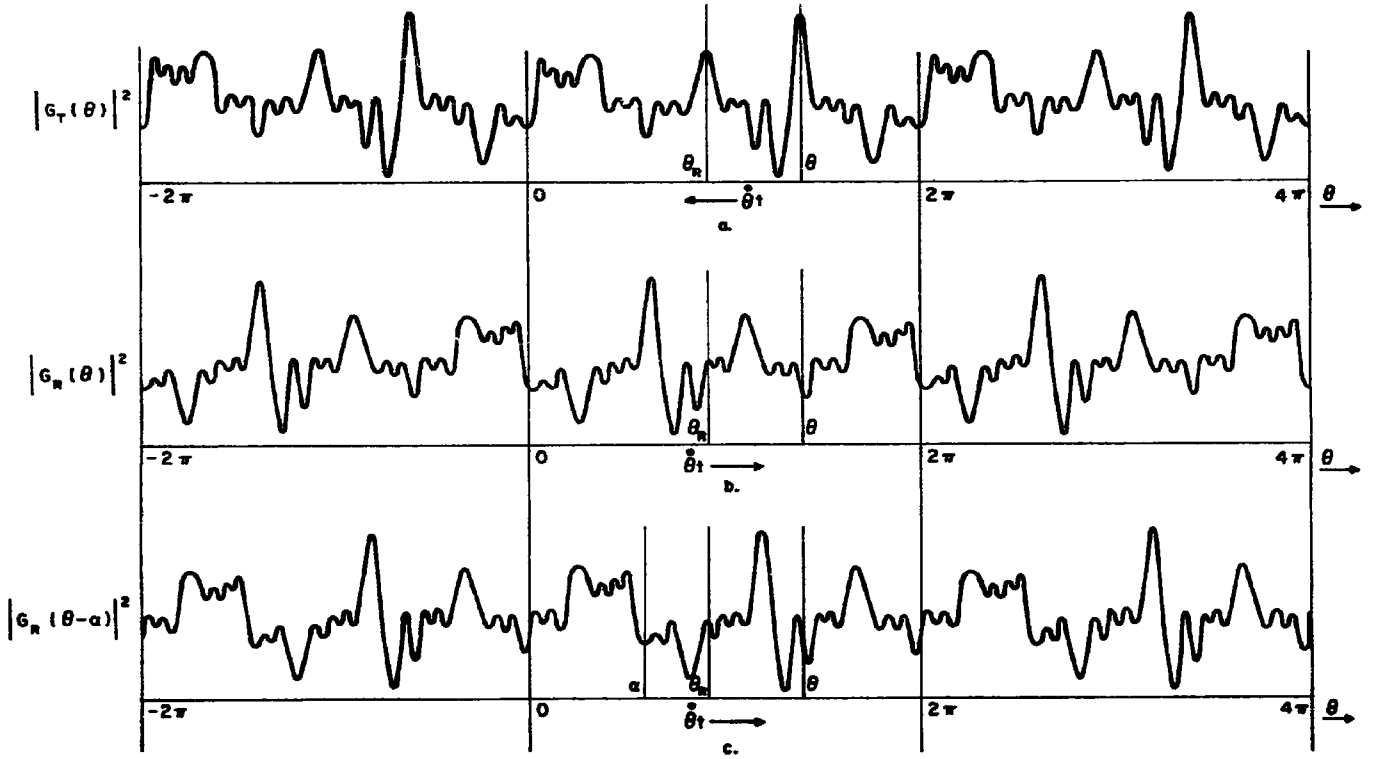

Figure 9 Spatial Correlation Techniques

Integration in time over one full revolution gives

$$S_R(\tau) = \frac{\dot{\theta}}{2\pi} \int_0^{\frac{2\pi}{\dot{\theta}}} G_T(\dot{\theta}t + \theta) G_T^*\left[\dot{\theta}(t+\tau) - \theta\right] dt \tag{50}$$

, where $\tau = \alpha/\dot{\theta}$ is the angular displacement represented in the time domain. At first glance, Eq. (50) does not resemble the angular ambiguity function in the sense that it is not a complex correlation integral. The equivalence of the function represented by Eq. (50) to the desired ambiguity function can, however, be demonstrated rather simply. The desired angular ambiguity function in the time domain can be written as:

$$\Phi(\Delta\theta) = \frac{\dot{\theta}}{2\pi} \int_0^{\frac{2\pi}{\dot{\theta}}} G(\dot{\theta}t + \theta_0) G^*\left[\dot{\theta}t + \theta_0 - \Delta\theta\right] dt \tag{51}$$

, where θ_0 is the target angle and $\Delta\theta$ is the angular displacement variable. Let $\theta_0 = \theta_0' + \Delta\theta/2$ where θ_0' is the location of the correlation peak and $\Delta\theta$ is an arbitrary angular deviation from this peak. Eq. (51) becomes

$$\Phi(\Delta\theta) = \frac{\dot{\theta}}{2\pi} \int G(\dot{\theta}t + \theta_0' + \tfrac{\Delta\theta}{2}) G^*(\dot{\theta}t + \theta_0' - \tfrac{\Delta\theta}{2}) dt \tag{52}$$

Similarly, in Eq. (50) let $\theta = \alpha/2 + \Delta\theta/2$ so that

$$S_R(\alpha) = \frac{\dot{\theta}}{2\pi} \int G_T(\dot{\theta}t + \tfrac{\alpha}{2} + \tfrac{\Delta\theta}{2}) G_T^*(\dot{\theta}t + \tfrac{\alpha}{2} - \tfrac{\Delta\theta}{2}) dt \tag{53}$$

, which is equivalent in form to Eq. (52) if $\alpha/2$ is the angle at which the correlation peak occurs. Thus in a counter-rotating antenna system, the correlation peak can only occur at $\theta = \alpha/2$ for any particular value of α. At this point, Eq. (50) becomes

$$S_R(\tfrac{\alpha}{2}) = \frac{\dot{\theta}}{2\pi} \int \left| G_T(\dot{\theta}t + \tfrac{\alpha}{2}) \right|^2 dt \tag{54}$$

$$= \Phi(\tau)_{MAX}$$

The operation of the system now becomes clear. A value of displacement α_1 is chosen usually to be one angular resolution bin. For this value of displacement the system is rotated one full revolution and the received signals are integrated in time. This yields one point on the angular ambiguity curve.

Next, the receiving antenna is shifted to another value of angular displacement, α_2, and the received signals are again integrated over one full revolution, giving another point on the ambiguity curve. The process is repeated continuously so that full ambiguity function can be displayed for each target. Note that the result is equivalent to a conventional scanning antenna.

Unfortunately, $\theta = \alpha/2$ is not the only maximum that occurs within the period of the antenna pattern. Another maximum is at $\theta = \alpha/2 + \pi$ at which Eq. (50) becomes

$$\begin{aligned} S_R\left(\tfrac{\alpha}{2}+\pi\right) &= \frac{\dot\theta}{2\pi}\int G_T\left(\dot\theta t + \tfrac{\alpha}{2}+\pi\right) G_T^*\left(\dot\theta t + \tfrac{\alpha}{2} - \tau\right) dt \\ &= \frac{\dot\theta}{2\pi}\int \left|G\left(\dot\theta t + \tfrac{\alpha}{2}\right)\right|^2 dt \\ &= \Phi(\tau)_{MAX} \end{aligned} \tag{55}$$

since the pattern is a periodic function of θ with period 2π. Thus the counter-rotating pattern correlation has two angular ambiguity peaks in the sense that any two targets at points (R, $\alpha/2$) or (R, $\alpha/2 + \pi$) cannot be resolved in angle. Note that the targets must be at the same range for this to occur. The information obtained from the lower half of the scanning plane (Figure 8) is thus redundant. This redundancy can be eliminated if only one half of each pattern is used, or if the signal is radiated only over π radians instead omnidirectionally.

The requirement of changing displacement angle after each revolution may pose some significant mechanical difficulties. If the receiver antenna consists of many patterns superimposed on top of each other in such a way that each pattern is displaced from the transmitter by a different value of α, all points on the ambiguity curve are obtained during one revolution of the antenna system. The number of stacked receiver patterns is, of course, equal to the number of angular resolution bins required in the prescribed angular coverage of the antenna. To keep mechanical complexity at a minimum, a compromise must be reached between the amount of desired coverage and the angular resolution.

B. Implementation and Implications

The semicircular pseudo-random pattern can, of course, be easily achieved by a linear array of directive elements illuminated by a pseudo-random illumination function and scanned mechanically in angle. An omnidirectional pattern results when the array elements are omnidirectional. The array, however, is not the most economical random pattern antenna, especially because its main advantage, that of electronic scanning, cannot be easily implemented. Figure 10 shows another concept which may be utilized to construct a random pattern antenna. It consists of a solid dielectric disc which has random cut-outs around its circumference. The disc is mounted between two metal plates and the signal is fed to the center of the disc by an open-ended coaxial cable or other convenient method. At the center of the disc the energy is radiated equally in all directions but is confined between two metal plates. The total phase shift imposed upon the radiated wave by the dielectric material is $2\pi n + \beta$, where β can assume any value between 0 and 2π, depending on the direction of radiation. Therefore, β effectively represents a random phase of the antenna illumination function. To achieve random amplitude control, the disc can be sprayed with a thin film of absorbing material whose thickness is random around the circumference of the disc and whose phase shifting properties are negligible.

The question may arise as to what type of random cut-outs should be used to give a desired pseudo-random pattern in the far field. Even though the dielectric disc antenna is sufficiently inexpensive to permit extensive experimentation, a rigidly controlled synthesis procedure is possible. It is beyond the scope of this report to give a detailed example of such procedure because of rather lengthy computations involved. Otherwise, the method is essentially straight forward. A desired pseudo-random sequence having proper correlation properties (minimum sidelobe level and beamwidth) is chosen for the antenna pattern. The length of the sequence may be rather large since it must contain all of the desired angular resolution elements of the antenna. If the antenna were a linear array, a Fourier transform of this sequence would give the desired value of the illumination function. In principle, however, a proper integral transformation of the sequence will give the illumination function on a circular arc, instead of a linear array. The phase and amplitude of the illumination function are sampled along the arc and each phase sample is represented by a proper cut-out in the dielectric disc while each amplitude sample is represented by the proper thickness of the absorbent film around the disc circumference.

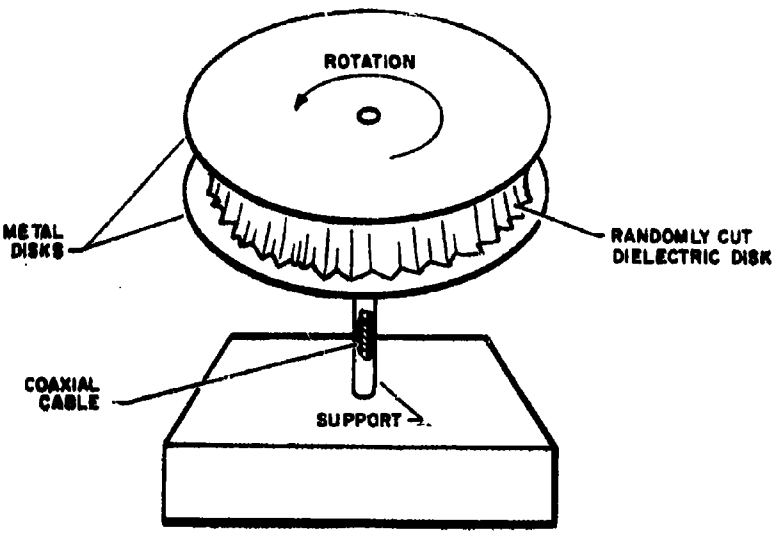

(a) ASSEMBLY

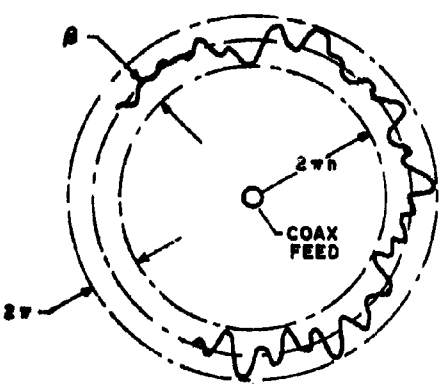

(b) DISK CUT-OUT

Figure 10 Dielectric Disk Antenna

According to sampling theory, the number of samples taken around the arc must be at least twice the number of angular resolution elements and the diameter of the disc will be of the order of the ratio of λ divided by the angular resolution $\Delta\theta_o$, which for 1^o resolution at X-band gives about 7 meters. Hence the discs can be quite large but comparable in size to ordinary parabollic antennas.

To obtain the complex conjugate pattern in the receiver, the receiving disc is cut out in an exactly opposite manner with respect to the transmitting disc so as to present a phase shift of $2n\pi - \beta$ to the signal which was transmitted with a phase shift of $2n\pi + \beta$. In-phase and quadrature processing is possible if the receiver antenna is made of two discs, one having a phase shift which is everywhere $\pi/2$ radians larger than the other. Details are shown in Figure 11. In this way, signals containing unknown input phases can be processed by in-phase and quadrature techniques with substantial simplifications in the electronic equipment.

There is no basic reason why the principle of spatial correlation could not be applied to provide three-dimensional radar volume resolution. The mechanical problems associated with application of dielectric disc antennas to this problem may become complex, but further study may uncover simpler techniques.

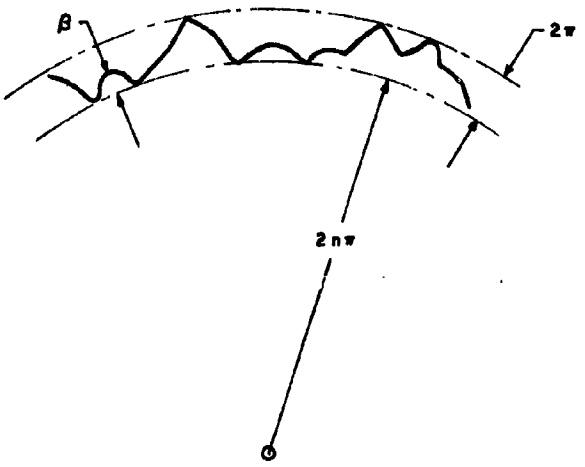

(a) TRANSMITTER CUT-OUT

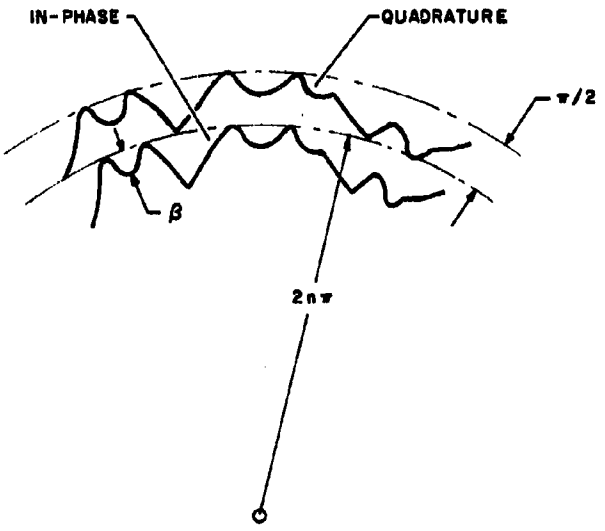

(b) RECEIVER CUT-OUT

Figure 11 Complex Conjugate and In-Phase and Quadrature Antennas

V. Optical Processing

One of the principal difficulties encountered in the systems discussed thus far was the requirement for excessive delays to either design a proper matched filter or to provide sufficient integration time for one full revolution of the pattern. Some of these problems may be solved by application of digital processing. Long time digital integrators are not necessarily simple or economical, however. Also, for a truly six-dimensional processing many such integrators or filters may be required. It is for these reasons that attention is now focused on optical signal processing as a means to simplify the overall equipment complexity.

The paragraphs which follow are not intended to offer the ultimate solution to six dimensional processing. Their intent is to briefly summarize the most important characteristics of the state-of-the art and to point out some of the immediate applications as well as the necessity for continued research effort.

A. Processing Philosophy

In many respects there exists a close analogy between optical and electronic systems. Except for the magnitude of the frequencies involved, both deal with essentially the same phenomenon of wave radiation.

If microwave processing were used, the equipment involved would be exactly the same as that used in optics except for the physical size. Thus the main difference between the two types of systems is due to properties of the particular domain in which the processing takes place. Transmissions of electronic signals through a network can be only represented as function of only one variable - time. Propagation of a light wave through space may be described as a function of two spatial coordinates in the plane perpendicular to the propagation path. Thus, if the light wave serves the purpose of a carrier it is possible to modulate this carrier simultaneously in two dimensions. This additional degree of freedom is the main advantage of the optical system. Other advantages are due to the simplicity with which operations such as integration, correlation, and spectral analysis can be performed The understanding of optical systems is vastly simplified for the reader who has an extensive background in microwave antennas. When a transparency representing a complex signal is inserted in the path of coherent light the emerging field pattern is completely analogous to that formed by a CW microwave antenna. The coherent light represents the CW carrier the transparency is the antenna illumination function and its size represents the antenna aperture. All usual near and far field properties hold, including the existence of a spatical Fourier transform relating the transparency and the far field pattern.

In the discussion above mention was made of the coherent properties of light. This is perhaps a convenient starting point in summarizing the properties of optical systems, since it is usually one that presents the most problems.

An electronic signal originating from a microwave oscillator is coherent in the sense that a simple phase relationship exists between any two points on a sinusoidal wave. If a bank of such oscillators producing all possible frequencies were added together (a physical impossibility), coherency would be completely destroyed and the resultant signal would be what is generally regarded as white noise in electronics. In practice noise does not contain all frequencies and is band limited by frequency selective properties of nature. This is exactly the characteristic of white light.

Thus incoherent optical systems can only be discussed in terms of intensity rather than amplitude and phase just as noise is discussed in terms of mean-squared power.

Coherent light consists of only one frequency (color) and has a simple phase relationship between any two points in a pair of planes perpendicular to the axis of propagation.

Coherency can be achieved by projecting non-coherent light through a narrow slit (one dimensional) or a pinhole (two dimensional) which is located in the focal plane of a collimating lens. This arrangement is completely equivalent to filtering out one sinusoidal frequency from a complex noise spectrum. Generally for processing purposes, light is regarded as coherent if the simple phase relation exists for a distance of at least 3 meters from the source. For communication purposes coherency requirements are much more stringent and distances as large as 3000 kilometers have been achieved with laser beams.

Optical systems suitable for signal processing must be linear. Thus their input-output relationship can be represented by the usual convolution integral of their impulse response and the input signal, except that the convolution is in two dimensions.[6] This is shown in Figure 12. A signal transparency having a complex amplitude transmission $A(x_o y_o)$ is inserted into the path of light at the signal plane (x_s, y_s). If the light emanating from the source plane (u, v) is incoherent the output in the image plane is given by the intensity convolution integral

---

6. "Spatial Filtering in Optics," E. L. O'Neill, IRE IT No. 2, June 1956, pp. 56-65.

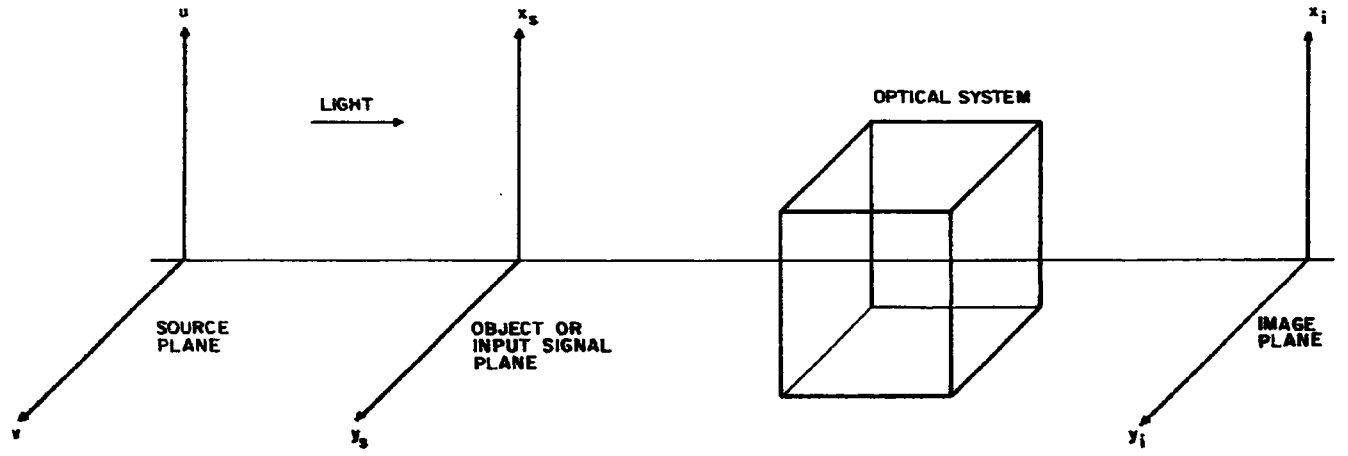

Figure 12 General Optical System

$$I(x_i, y_i) = \iint_{-\infty}^{\infty} |h(x_i - x_o, y_i - y_o) A(x_o, y_o)|^2 dx_o dy_o \qquad (56)$$

which states that incoherent systems are linear in intensity but nonlinear in amplitude. In Equation (56), $h(x_i, y_i)$ is the spatial impulse response of the optical system. If the light is coherent, however, the output intensity is given by

$$I(x_i, y_i) = \left| \iint h(x_i - x_o, y_i - y_o) A(x_o, y_o) dx_o dy_o \right|^2 \qquad (57)$$

Equation (57) shows that coherent systems are linear in amplitude but nonlinear in intensity. Since most optical recording devices are sensitive to intensity only, Equation (57) provides a very valuable relationship for interpretation of the recorded outputs of optical processors. It must be noted that both Equations (56) and (57) could be written in the spatial frequency domain as products of two-dimensional Fourier transforms.

The impulse response of an optical system can be measured experimentally but is not easily obtained by analytical methods. For this reason, other, less general properties of optical systems are investigated to provide simpler methods of analysis. Such properties exist in coherent optical systems and are very ably demonstrated in a recent paper by Cutrona.[7] Using Cutrona's notation these properties are:

(1) If a coherent optical wave, represented by a complex function $E = A(x, y)e^{i\phi(x, y)}$ is incident upon a thin transparency represented by an intensity transmission function $t^2(x, y)$ and a thickness function $\alpha(x, y)/2\pi(n-1)$ (in wavelengths) then the emergent light wave can be written as

$$E_o = A(x, y)t(x, y)e^{i[\alpha(x, y) + \phi(x, y)]} \qquad (58)$$

Equation (58) states that the incident light was modulated in amplitude and phase by the transparency or signal function.

---

7. "Optical Data Processing and Filtering Systems," L. J. Cutrona, E. N. Leith, C. J. Palermo, L. J. Porcello, IRE-IT, June 1960, pp. 386-400.

(2) The intensity of a coherent light wave is proportional to the product of the complex conjugates of its amplitude,

$$I(x,y) = k\,E(x,y)E^{*}(x,y) \tag{59}$$

(3) If the signal transparency is placed in the focal plane of a converging (idealized) lens than the output wave observed at the other focal plane is the exact spatial Fourier transform of the transparency amplitude. If the transparency is not located in the focal plane then the output is the Fourier transform to within a phase factor. With reference to Figure 13, if f is the focal distance of the Lens, L_1, and a transparency whose amplitude function is $E(x, y)$ is inserted into the path of coherent light of uniform intensity I_o at the plane P_1, then

$$\frac{E(x_3,y_3)}{\sqrt{I_o}} = e^{i\left(1+\frac{g}{f}\right)\left(\frac{x_3^2+y_3^2}{f}\right)} \iint E(x_1,y_1)\,e^{-i(x_1\omega_x + y_1\omega_y)}\,dx_1\,dy_1 \tag{60}$$

where g is arbitrary ($g > f$) and $\omega_x = -\frac{2\pi x_3}{\lambda f}$, $\omega_y = -\frac{2\pi y_3}{\lambda f}$, λ being the wavelength of the incident light. Both ω_x and ω_y have dimensions of inverse distance or spatial frequency and the phase factor outside of the brackets vanishes for $g = f$, or when the transparency is in the focal plane of lens L_1 (plane P_2 in Figure 13). Thus for $g = f$, Equation (60) becomes a true two-dimensional Fourier transform except that frequency coordinates ω_x and ω_y are reversed in direction with respect to the spatial coordinates x_3, y_3 (see Figure 13). This reversal in coordinates is due to the fact that lens L_1 actually introduces a kernel $\exp[i(x_2x_3 + y_2y_3)2\pi/\lambda f]$ in passing from plane P_2 to P_3 and not its conjugate as required by the conventional Fourier transform. A cascaded lens system takes successive Fourier transforms rather than the transform and its inverse. Since $\mathcal{F}\{\mathcal{F}[f(x)]\} = 2\pi f(-x)$, a two lens optical system will map all points in x_1 into $-x_4$ and those in y_1 into $-y_4$. For systems in which light travels from left to right an automatic coordinate reversal system can be adopted so that a nominal sign convention can be used throughout.

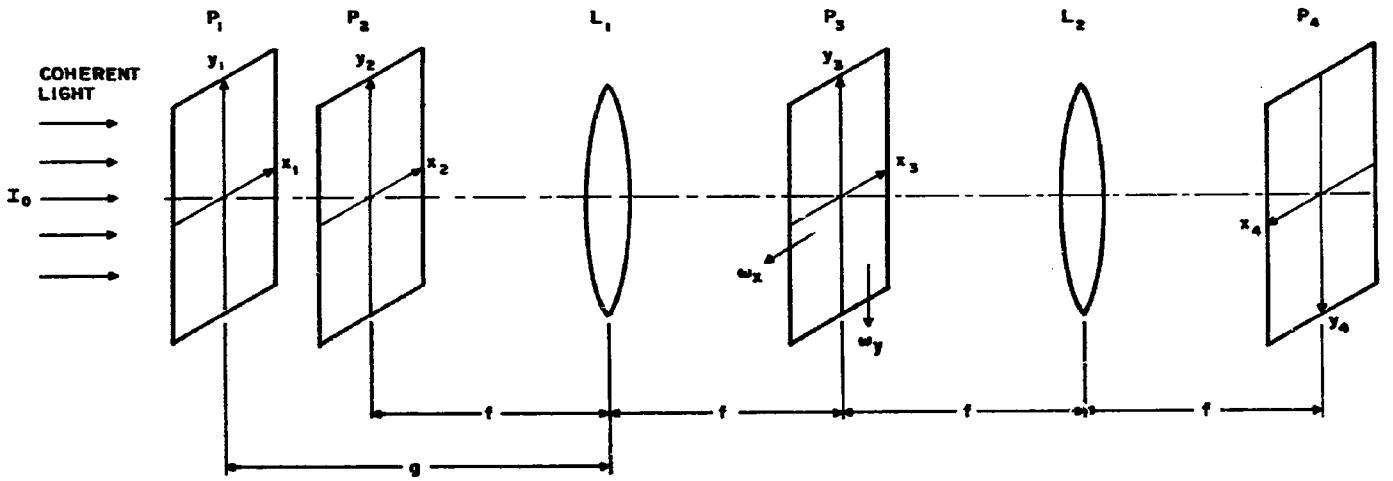

Figure 13 Fourier Transform Relationship In A Coherent Optical System

The integration over a plane (x_2, y_2) can now be performed by a photo-detector at plane P_4 whose resolution elemental size is greater than the image of the transparency $E(x_2, y_2)$ at plane P_4 (e.g., $E(x_4, y_4)$.

Figure 13 immediately suggests several applications to signal processing. First of all, filtering of the signal can be accomplished by physically blocking any frequency component in the P_3-phase. A matched filter may be synthesized by placing a transparency in the P_3-phase which is a complex conjugate of the signal spectrum. A cross-correlation integral may be generated by superimposing two transparencies in the P_2-plane and moving one with respect to the other. The value of the cross-correlation can be obtained directly at plane P_2 without resorting to an integrating device. If $s(x_1, y_1)$ and $r(x_1, y_1)$ are the two transparencies and x' and y' are the values of relative displacement among them then the signal at plane P_2 will be of the form $\mathcal{F}\{s(x_1 - x', y_1 - y')\, r(x_1, y_1)\}$. When the output is taken only at $\omega_x = \omega_y = 0$ the signal becomes a correlation integral

$$E_1(x', y') = \iint s(x_1 - x', y_1 - y')\, r(x_1, y_1)\, dx_1 dy_1 \tag{61}$$

When the coordinates of $s(x_1, y_1)$ are reversed prior to recording, Equation (61) becomes a convolution integral. Hence two types of synthesis procedures are available - the spatial domain and the frequency domain. The combination of these two offers great flexibility in design of optical processing systems.

It may be often desirable to perform correlation or filtering operations in one dimension only. In this case the other dimension may be utilized to provide multiple processing channels. This can be accomplished with the aid of a cylindrical lens placed in the system as shown in Figure 14. Signal plane and spectral plane are located at two focal planes of the spherical lens L_s. Nominally this lens would provide a double Fourier transform at plane P_2. When a cylindrical lens L_c is inserted between L_s and plane P_2 in such a way that its focal length f_c coincides with the plane P_2, an additional Fourier transform will be taken in the x-dimension only. Thus the output at P_2 has spatial coordinates in the x-dimension and frequency coordinates in the y-dimension, and is a one dimensional Fourier transform. When the x-dimension of plane P_1 consists of many discrete channels the output gives a Fourier transform of each channel separately and thus enables multichannel processing. The number of channels is limited only by the size and resolution properties of the optical aperture. The function of cylindrical lens L_c may be understood more clearly by considering Equation (60) and application of simple geometric optics. Plane P_1 is located at the focus of the spherical lens L_s. Thus the cylindrical lens L_c "sees" an object

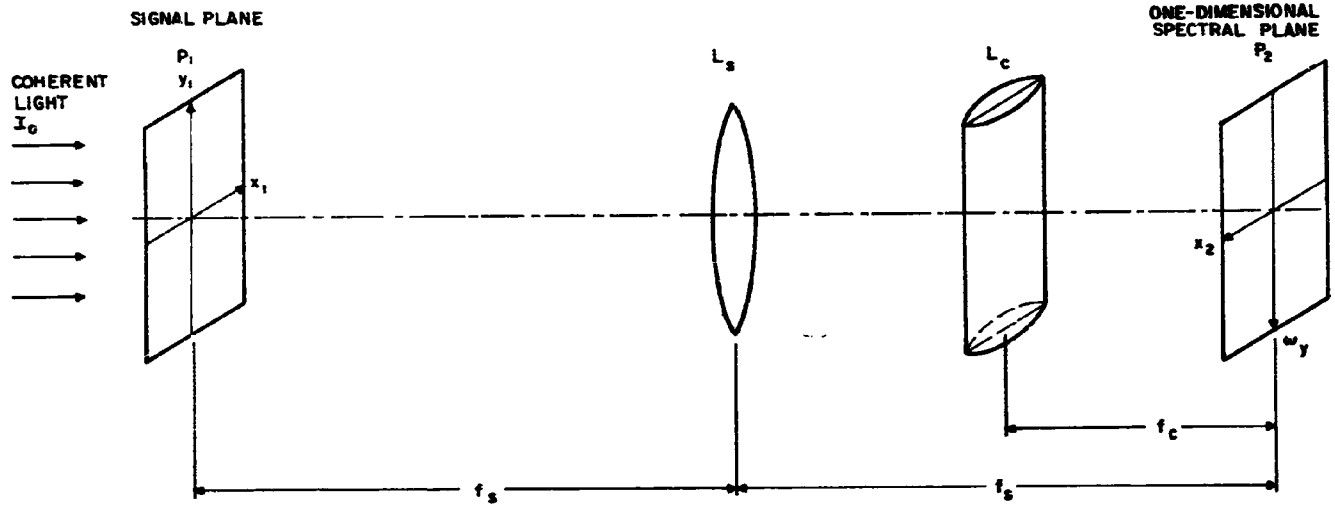

Figure 14 One-Dimensional Multiple-Channel Optical Processor

effectively located at infinity. When $g \to \infty$ in Equation (60) the phase factor goes to zero giving an exact Fourier transform at the output focal plane of the cylindrical lens.

B. Signal Recording

In theoretical discussion it was very convenient to introduce a hypothetical signal transparency possessing both amplitude and phase. In practice, however, this may not be very convenient since an accurate phase modulation of the incident light beam requires that the thickness of the transparency be controlled to within a fraction of a light wavelength over the entire aperture plane. While phase modulation of light is generally possible by ultrasonic cell techniques * it is very difficult to achieve on a permanent transparency such as film. The thickness of an ordinary film is usually nonuniform to begin with, so that special precautions (such as an oil bath) must be introduced to prevent random phase modulation of incident light and to achieve a more or less uniform phase shift over the aperture. The resultant film transparency may be of the form $E(x, y) = A(x, y)\, e^{i\phi}$ where ϕ is a constant.

There is one other major difficulty involved in recording of electronic signals on film. As a recording medium, film is only sensitive to light intensity and not to amplitude. Hence in order to record a signal on the film it must be converted to intensity modulated light. This is usually accomplished by photographing the face of an intensity modulated cathode ray tube where the signal is used to modulate the intensity of the electron beam. The intensity, however, is a positive quantity while an electrical signal is usually bipolar. This difficulty may be resolved when the signal is recorded around an intensity bias which is chosen so as to accommodate the largest positive and negative excursions of the signal. This procedure limits the dynamic range of recording but does offer a simple and practical solution to the problem. The maximum bounds of a film transmission function are 0 and 1. When the transmission is zero, the film is completely opaque and when it is unity it is completely transparent. Thus a function of time $f(t)$ can only be recorded on film as $f_o + f(x)$ where f_o is the bias value such that $0 < f_o + f(x) < 1$ for all values of x(or t). When two such transparencies are superimposed in an optical correlator the output signal contains not only the desired signal product but also the cross-products between the two signals and their biases as well as the bias itself. The bias term may be removed optically by placing an appropriate stop in the Fourier transform plane to block the dc term of the transparency spectrum. This can only be done when the portions of the spectrum due to the bias and those due to the signal are separable in space, e.g., when the signal is a band pass function. The higher the center frequency

* See Subsection C of this report.

of the signal spectrum the better the separation. Unfortunately, however, high signal frequencies require large optical apertures with good resolution. The final design is usually a matter of compromise between all of these factors.

To illustrate a common method of signal recording and some of the problems connected with the bias elimination consider the example of Figure 15. A coherently detected video signal with some modulation is recorded on a film as a column of N samples in the y-dimension in P_1-plane This signal may for example, be a series of doppler modulated radar returns obtained from a target at a certain range R (x-dimension on the film) or a series of pattern modulated signals obtained during one resolution of a pseudo-random dispersed antenna, etc. If the signal is at video it must be assumed that the shortest modulation period is much larger than the signal duration τ (τ = d, the diameter of the dot on film). Thus the signal train on the film represents a sampled replica of the modulation function and can be written as

$$s(y_1) = A_0 + \sum_{m=0}^{N-1} A(mT_r)\cos\left[\psi(t - mT_r) + \theta\right] \tag{62}$$

where A_0 is the bias level, $A(m\,T_r)$ is the value of amplitude modultation at the m^{th} sample, T_r is the sampling period $\psi(t - m\,T_r)$ is an arbitrary phase modulation, and θ is a constant phase shift. To obtain meaningful results consider the simplest case when $s(y_1)$ is a sampled sinusoid of frequency ω with an arbitrary phase shift θ, e.g.,

$$s(y_1) = A_0 + \sum_{m=0}^{N-1} A\cos(\omega m T_r + \theta) \tag{63}$$

The net effect of the lens system of Figure 15 will be a Fourier transform of the pulse train of Equation (63).

$$\begin{aligned} s(\omega_y) &= \int s(y_1)\, e^{-i y_1 \omega_y}\, dy_1 \\ &= \sum_{m=3}^{N-1} \int_{md}^{(m+1)d} \left[A_0 + \cos(\omega m T_r + \theta)\right] e^{-i y_1 \omega_y}\, dy_1 \end{aligned} \tag{64}$$

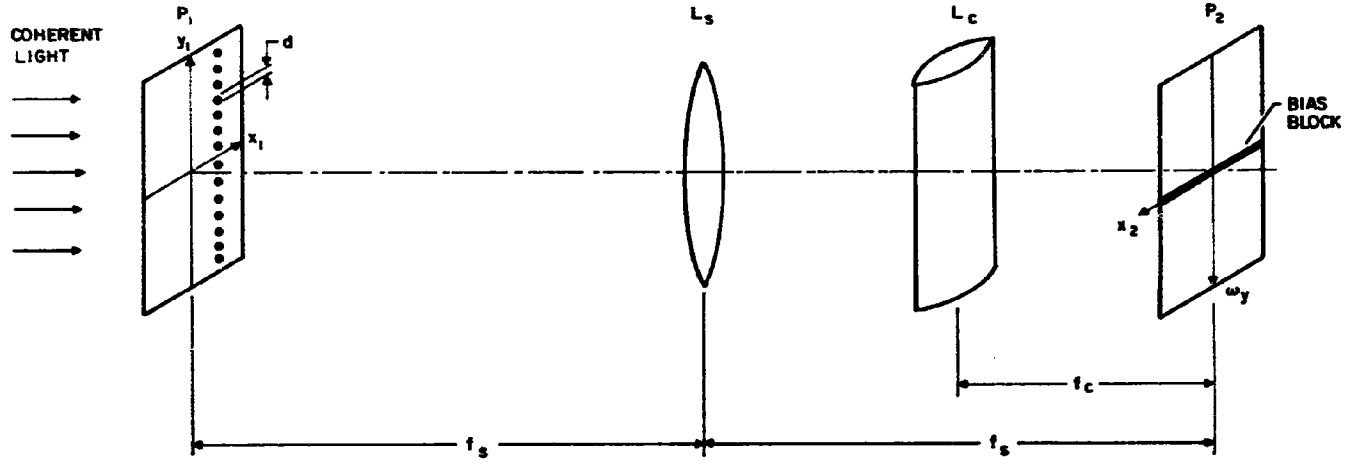

Figure 15 Bias Elimination In the Frequency Plane

Using the relationship

$$\sum_{m=0}^{N-1} e^{-im\psi} = \frac{\sin\left(N\frac{\psi}{2}\right)}{\sin\frac{\psi}{2}} e^{-i(N-1)\frac{\psi}{2}}$$

Equation (64) is evaluated to give

$$S(\omega_y) = Nd\left\{ A_0 + \frac{\sin\left(\frac{N\omega_y d}{2}\right)}{\frac{N\omega_y d}{2}} e^{i\frac{N\omega_y d}{2}} \right. \tag{65}$$

$$+ \frac{A}{2} \frac{\sin\left(\frac{\omega_y d}{2}\right)}{\frac{\omega_y d}{2}} \frac{\sin\left[\frac{N}{2}(\omega_y d + \omega T_r)\right]}{N\sin\left[\frac{1}{2}(\omega_y d + \omega T_r)\right]} e^{i\left[\frac{N\omega_y d}{2} + (N-1)\frac{\omega T_r}{2} + \theta\right]}$$

$$\left. + \frac{A}{2} \frac{\sin\left(\frac{\omega_y d}{2}\right)}{\frac{\omega_y d}{2}} \frac{\sin\left[\frac{N}{2}(\omega_y d - \omega T_r)\right]}{N\sin\left[\frac{1}{2}(\omega_y d - \omega T_r)\right]} e^{i\left[\frac{N\omega_y d}{2} - (N-1)\frac{\omega T_r}{2} - \theta\right]} \right\}$$

Equation (65) clearly consists of 3 components. The first component is due to transparency bias and the other two are due to signal. A sketch of Equation (65) is shown in Figure 16. In order to be able to block out the DC component the center frequency of the modulation, ω, must be sufficiently large so that all spectral components of the signal are removed from the origin ($\omega_y = 0$). If ω is constant this can usually be accomplished without excessive losses in intensity of the spectrum. Suppose now that the sinusoidal frequency is at IF, i.e., several cycles of ω are contained within the dot size d. The signal on the film can then be represented by [7]

$$S(y_1) = \sum_{m=0}^{N-1} \left\{ A_0 + \cos\left[\frac{2\pi k}{d}(y_1 - md) + \omega m T_r + \theta\right] \right\} \tag{66}$$

---

7. "Processing of Simulated IF pulse Doppler Signals," W. G. Hoeffer, IRE Trans., MIL-6, No. 2, Apr. 1962.

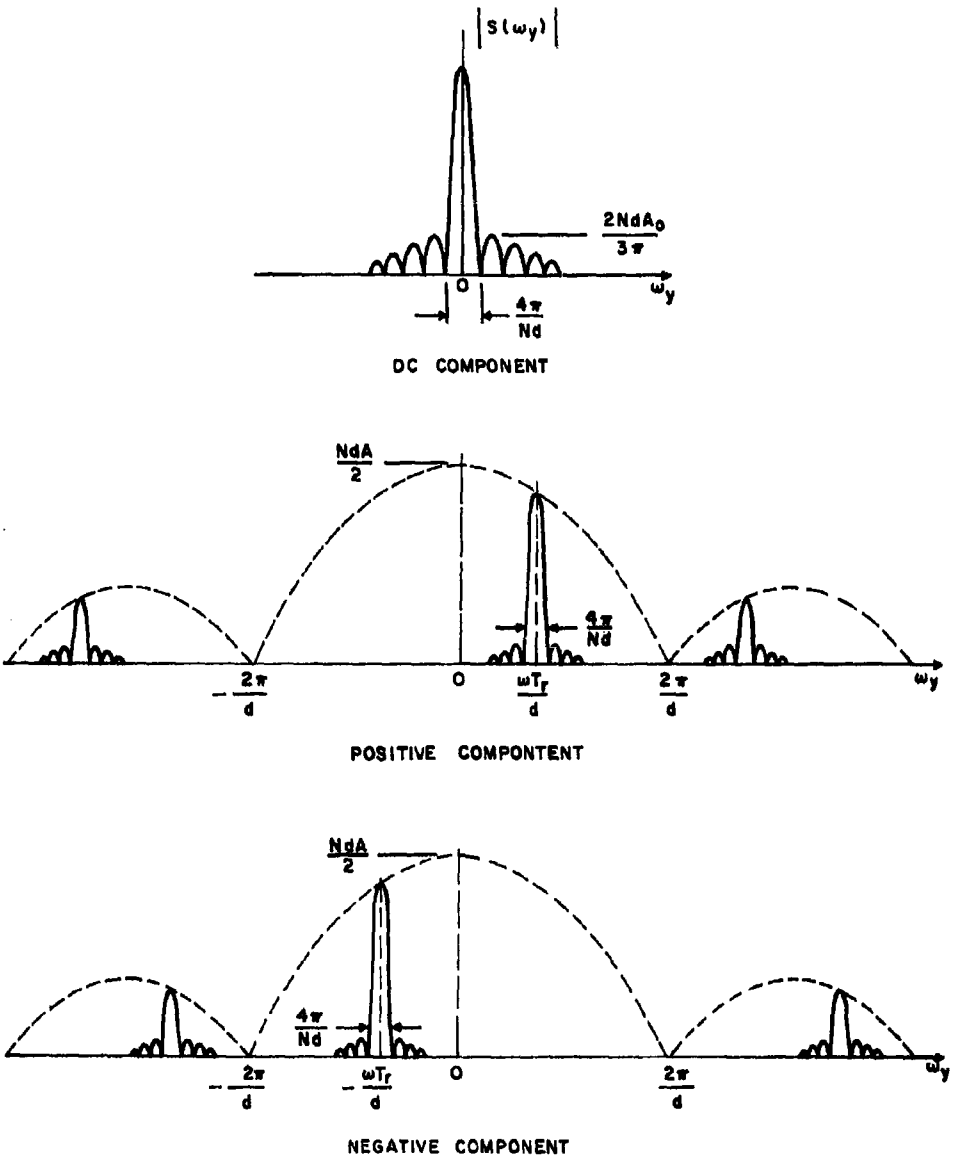

Figure 16 One-Dimensional Amplitude Spectrum of Video Signal of Sampled Sinusoid

where k is the number of cycles of IF contained in the sample of length d (not necessarily an integer). Hoeffer shows that the spectrum of this signal is identical to Equation (65) except that the envelope terms $\frac{\sin(\omega_y \frac{d}{2})}{\omega_y \frac{d}{2}}$ of the positive and negative signal spectrum components are now centered at $\omega_y = \pm \frac{2\pi k}{d}$ instead at $\omega_y = 0$. This method of recording assures complete separation of the spectrum with minimum intensity losses.

Even though the bias filtering principle was illustrated for a sampled sinusoid . it will hold for any other type of modulation. Specifically it also holds for a pseudo-random pattern modulation. If the pattern modulated signal is not heterodyned all the way down to video but is left at some low offset frequency prior to recording there will be no spectral components present at $\omega_y = 0$ other then those due to the bias term.

The use of an IF frequency in signal recording increases the requirements of aperture resolution and size. This will be demonstrated by a rather simplified argument for both video and IF recordings.

Assume that the signal is recorded on a moving film from a stationary spot (or trace) on the face of a cathode ray tube. Assuming linearity throughout the system the process is roughly equivalent to low-pass filtering operation in the sense that the CRT output is given by the convolution of the signal and the spot impulse response while the film record can be written as a convolution of the CRT output and the film impulse response, plus appropriate bias levels. The increase in required film space can be obtained approximately without detailed evaluation of the convolution integrals. Considering video recording first, if a time interval T is represented on a CRT trace of length L and the time and phosphor resolution elements are τ and ℓ, respectively, then

$$\frac{T}{\tau} = \frac{L}{\ell} \tag{67}$$

Suppose that the smallest film resolution spot is fixed to the size d,

$$d = M\ell$$

where M is the image size reduction factor between the CRT and the film. Thus

$$d = \frac{LM\tau}{T} \tag{68}$$

But LM = A, the required film aperture size and $\frac{T}{\tau}$ is the number of time resolution elements which must be accomodated in this aperture. Also $\frac{1}{\tau}$ is approximately equal to the video bandwidth W. If $\frac{1}{\delta}$ is regarded as an equivalent film bandwith B_f then

$$B_f = \frac{TW}{A} \tag{69}$$

Equation (69) states that for recording of video signals with high TW products on a film with fixed bandwidth B_f the aperture size increases directly with the signal TW product.

Consider now the same signal at IF frequency f_o. The highest significant spectral component is of the order of $f_o + 1/\tau = f_o + W$. Thus the new required time resolution element is at least $\tau' = \frac{1}{f_o+W}$. The film bandwidth to accommodate this resolution is $B_f' = \frac{(f_o+W)T}{A}$.

If the film bandwidth is fixed, i.e., $B_f' = B_f$ the new aperture dimension must be A' or

$$\frac{(f_o+W)T}{A'} = \frac{TW}{A}$$

Solving for the ratio A/A',

$$\frac{A}{A'} = \frac{W}{f_o+W} = 1 + \frac{2}{\delta} \tag{71}$$

where $\delta = \frac{2W}{f_o}$ is the signal fractional bandwidth. For narrow band signals $\delta << 1$ and

$$A' = \frac{2A}{\delta} \tag{72}$$

This shows that with an increase in f_o (or decrease in δ) the required aperture size increases as $1/\delta$. To ensure spectrum separation δ must be at most unity which means that A' = 3A. Thus an offset frequency of only twice the video bandwidth requires a three-fold increase in aperture dimensions. It must be pointed out that the required aperture increase can always be traded off for signal duration, T, e.g., smaller amount of discrete channels (or samples) can be recorded in the same aperture.

C. Processing Time

One of the standard objections to the use of a moving film correlator in continuous processing of radar signals is the high cost of film used for signal recording. Since an ordinary photographic film cannot be re-used after development and if the system apertures require non-standard film dimensions this can indeed become objectionable.

Another standard objection is excessive time delay required to expose and develop the film before it can be processed. The time delay problem may become very serious in case of a ballistic missile radar but some modern films have reduced this time to the point where it may be acceptable for ordinary radar. For example, ANSCO Radar Copy Type 450 film,[8] designed especially for correlator processing can be processed (wet) only 0.2-0.3 seconds after exposure. The development is done with the film moving through a monobath spray. This processing speed approaches very nearly the real time processing for most ordinary radar applications. There is no reason to doubt that future research may shorten this time interval even further.

One recent development which may provide a solution to film waste is the method of photoplastic recording.[9] A thermoplastic photoconductive polymeric material is used. The film is grainless, dry and re-usable. It is sensitized by a uniform electrical charge in the dark, immediately prior to exposure. Positive or negative potential using corona discharge can be applied. The film is then exposed to the light image. To develop the image in the form of deformations or grooves, the photoplastic film is heated to its melting point rapidly. The inert support to which the film is attached remains essentially at room temperature and serves as an efficient heat sink to cool the film quickly and freeze-in the deformations. On remelting, the surface is smoothed over and is ready for re-use. The resolution properties of photoplastic films are claimed to be of the order of 0.4 microns for a 1 mil film with 100 volts charge at room temperature. Since the information recorded on such film appears in the form of thickness modulation its behavior in the beam of coherent light must be investigated. As far as is known such investigation has not yet been undertaken but is certainly warranted when one considers obvious advantages of photoplastic films for use in radar signal correlators.

---

8. "Rapid Processing Black and White Films of High Resolving Power," J. Duffy, Photographic Engineering, Vol. 6, No. 2, 1955, p. 130

9. "Photoplastic recording," J. Gaynor and S. A. Aftergut, Photographic Science and Engineering, Vol. 7, No. 4, July-August 1963, pp. 209-213.

As already mentioned, film is not the only method to modulate coherent light. Other standard methods, suitable for short time correlation techniques, utilize stress modulation in a solid or liquid transparent medium produced by application of signal in the form of ultrasonic waves. The stress changes in the medium modulate its index of refraction which, in turn, can provide phase modulation to a beam of coherent light shining through the medium. Various types of such modulators, using both liquid and solid media, and different physical processes, have been described in the literature. Although they dispense completely with signal recording requirements their application to dispersed pattern correlation problem is not possible because of insufficient delays available (For example, 1 ft. of quartz can provide roughly 100 μsec delay at ultrasonic frequencies). Ultrasonic cells are particularly suitable for pulse compression filters and have been often used for that purpose.

D. Application to Angular Dispersion and Compression

Before discussing actual application of an optical correlator to compression of a pseudo-random pattern, a few general remarks about the operation of a moving film correlator must be made.

Refering to Figure (14) it is seen that if the system is to be used as a correlator then both signal and reference transparencies cannot be superimposed in plane P_1 because of resulting bias-signal cross products appearing at its output. If the plane P_1 is used for moving the signal film alone, then a bias stop can be inserted at plane P_2 (see Figure 15) and the signal may be recovered by a subsequent Fourier transform. This arrangement is illustrated in Figure 17. The reference mask is placed in the plane P_3. This mask consists of identical signal recordings placed side by side for each incremental value of x. Since the mask is on film it will also have a bias value. The effect of this bias must be eliminated before the true correlation function can be recorded. This is nominally accomplished by utilizing specific properties of the input signal.

When the signal film in plane P_1 moves with a velocity V_f the signal output at plane P_2 after bias removal is*

$$S_{2,out}(x_0, y-y') = S_1(x_0, y-y')$$

* If the system is designed corrrectly all dimensions in space are equal and the subscripts can be omitted.

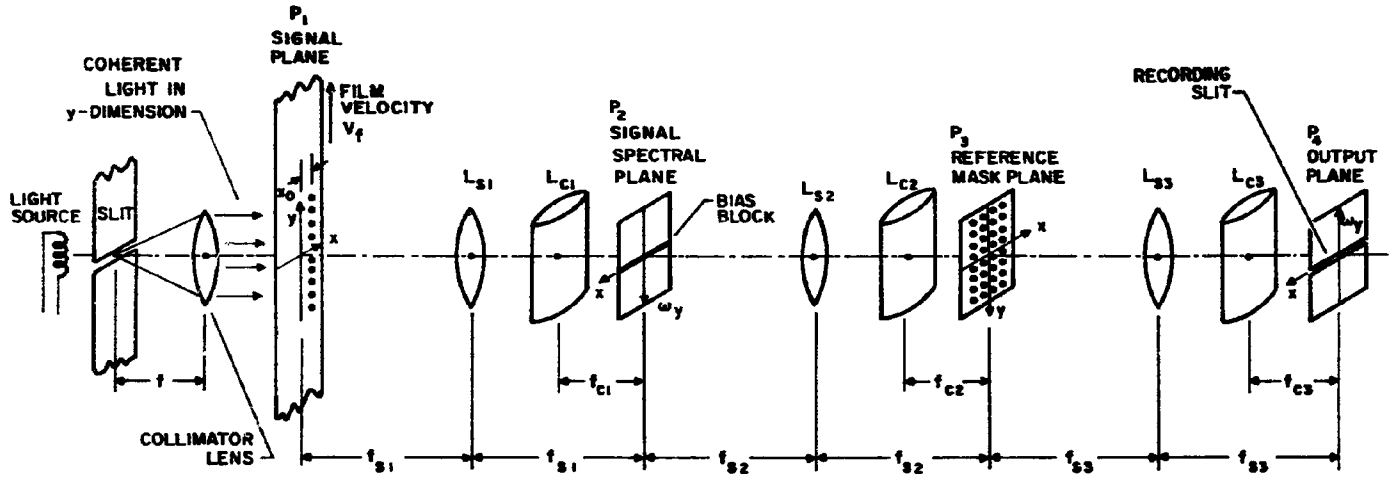

Figure 17 One-Dimensional Multi-Channel Optical Correlator Using Moving Film

where $y' = V_f t$ and t is the time variable. The mask signal is of the form $A_o + s_1^*(x, y)$ so that the output at the plane P_3 is

$$S_{3,out}(x_o, y, y') = S_1(x_o, y-y')\left[A_o + S_1^*(x_o, y)\right] \tag{74}$$

The combination of lenses L_{s3} and L_{c3} takes a one-dimensional Fourier transform (in the y-dimension) of Equation (74). Consequently the output signal at plane P_4 is,

$$S_{4,out}(x_o, \omega_y, y') = \int \left[A_o S_1(x_o, y-y') + S_1(x_o, y-y') S_1^*(x_o, y)\right] e^{-iy\omega_y} dy \tag{75}$$

When the output at plane P_4 is read through a narrow slit placed at $\omega_y = 0$ (along the x - axis), Equation (75) will change to:

$$S_{4,out}(x_o, 0, y') = A_o \int S_1(x_o, y-y')dy + \int S_1(x_o, y-y') S_1^*(x_o, y)\, dy \tag{76}$$

The second integral in Equation (76) will be recognized as the desired autocorrelation function. This autocorrelation can only be obtained if the first integral of Equation (76) is zero for all values of y'. Now, if the signal $s_1(x_o, y)$ represents one revolution of a pseudo-random antenna pattern with zero average value the first integral will be zero. If, however, $s_1(x_o, y)$ contains some additional modulation (target scintillation, etc.) its value integrated around the pattern in time may not be zero. At this point it may be convenient to recall that all signals and masks in this system are recorded on an off-set frequency ω_c. In the plane P_4 there will be two Fourier spectra on the left side of the slit as given by Equation (75). The first of these is due to be the product $A_o s_1(x_o, y-y')$. It will actually be a "running" spectrum because y' is constantly changing with time; when the film speed is slow it will be the same as a stationary spectrum. Since the signal is recorded on an offset frequency the spectrum $\int A_o S_1(x_o, y-y') e^{-iy\omega_y} dy$ will never have a d-c component and hence will not interfere with the recording of the autocorrelation function through the slit at $\omega_y = 0$. This will be true regardless of the modulation on the input signal and its average value. Thus the offset frequency recording of the input signal will automatically eliminate the mask bias term.

The system shown in Figure 17 represents a "brute force" method of synthesizing a correlator. Yet, as will become evident later, when the signals to be correlated extend over appreciable time intervals it may be the

only system which is immediately applicable with present day techniques. Its main disadvantages are its length and excessive film usage for signal and output recordings. Another disadvantage may be the time delay required for film processing. This, however can be cut down considerably with contemporary techniques. Since the system uses only processing in y-dimension, the light beam must be coherent only in the y-coordinate. This can be accomplished with a slit perpendicular to the y-axis and passing through x = y = 0 at the focus of a collimating lens as shown in Figure 17. The use of a slit increases light intensity throughout the system but even then the physical length involved may require that a low power laser be used as the light source.

Figure 17 represents the essential features of an optical correlator suitable for angular compression and dispersion. A few comments on some specific problems connected with this particular application may be appropriate. First of all, to achieve proper angular correlation in time, the film velocity V_f in plane P_1 must be closely synchronized with the antenna rotational speed $\dot{\theta}$. The time at which the correlation occurs will then indicate the target angle, and the width of the peak at the 3 db points will give the angular resolution. The processor is capable of angular correlation in one angle and at all ranges. In order for this to happen the aperture must be sufficiently large to accomodate all required range bins in the x-dimension and all signal pulses received during one full antenna resolution in the y-dimension. A common variety field radar has a range resolution of the order of 0.5 nautical miles or 6 μsec. A film with a resolution of 100 lines per mm can conveniently accomodate at least 50 range bins or 25 n. miles in one mm. If a standard 35 mm film is used a range interval of 875 nautical miles can be processed in the x-dimension. This may be regarded as sufficient for most applications. For an angular resolution of 0.5 degrees the pulse train which represents one antenna revolution will consist of about 720 pulses. If only half of the film resolution properties are used this train can be recorded in a total distance of 14.4 mm, or less than 50% of the aperture. Thus the storage properties of the film can hardly be compared with those of ordinary electronic devices. It is mainly this availability of practically unlimited delay on film that makes its use so attractive for purposes of angular pattern compression. One signal pulse train in any range bin can be represented on film as

$$S_1(x_0,y) = \sum_{m=0}^{N-1} \left\{ S_0 + a(\sigma) \left| G(\omega_0, \dot{\theta} m T_r - \theta) \right| \cos(\omega_c m T_r + \psi_{Gm} + \gamma) \right. \qquad (77)$$

when the film is stationary. If the film is moving with a velocity V_f as indicated in Figure 17 a time displacement variable proportional to $\dot{\theta}/2\pi$ is introduced into all modulation terms. In Equation (77) S_0 is the bias level, T_r is the prf period, ω_c is the offset frequency, $a(\sigma)$ contains only the target modulation (e.g., the signal is doppler compensated and already compressed in range), ψ_{Gm}

is the pattern phase associated with the particular m^{th} sample and γ is an arbitary phase which accounts for all other possible phase shifts. The mask recording contains a pulse train which represents a complex conjugate of Equation (77). In the real signal domain this means that the argument of the cosine term in Equation (77) is reversed in sign, e.g., the term is cos ($\omega_c m T_r - \psi_{Gm}$). This type of recording can be made with a special type of processor which is described next.

Consider a fully coherent radar, transmitting RF pulses at frequency ω_0 and phase α. The received signal (at RF) in any pulse may be written as

$$Re\, S_R = |Ga| \cos(\omega_0 t + \alpha + \beta) \tag{78}$$

where Ga is the product of the product of the properly delayed antenna pattern and signal modulation functions, and β is the phase associated with G and a (combined). "Re" stands for real part of the otherwise complex signal S_R. Observe that

$$Re\, S_R^* = |Ga| \cos(\omega_0 t + \alpha - \beta) \tag{79}$$

The purpose of the processor is to convert the signal of Equation (78) into (79). In a coherent radar there are two convenient CW reference sources

$$\begin{aligned} Re\, S_i &= \cos(\omega_0 t + \alpha) \\ Re\, S_q &= \sin(\omega_0 t + \alpha) \end{aligned} \tag{80}$$

Using two product detectors one gets

$$(Re\, S_R)(Re\, S_i) = \frac{|Ga|}{2}\left[\cos\beta + \cos(2\omega_0 t + 2\alpha + \beta)\right] \tag{81}$$

and

$$(Re\, S_R)(Re\, S_q) = \frac{|Ga|}{2}\left[\sin(2\omega_0 t + 2\alpha + \beta) - \sin\beta\right]$$

Upon filtering out of the 2 ω_0 terms two coherent video signals are obtained

$$S_1 = \frac{|Ga|}{2}\cos\beta$$

$$S_2 = -\frac{|Ga|}{2}\sin\beta \tag{82}$$

When the signal S_2 is shifted in phase by π radians

$$S_2' = \frac{|Ga|}{2}\sin\beta \tag{83}$$

Signals S_1 and S_2' are used to modulate the in-phase and quadrature reference CW signals in two balanced modulators. This gives

$$S_1 \, Re S_I = \frac{|Ga|}{2}\cos\beta\cos(\omega t + \alpha)$$

$$S_2' \, Re S_Q = \frac{|Ga|}{2}\sin\beta\sin(\omega t + \alpha) \tag{84}$$

Addition of both terms of (84) results in

$$S_o = \frac{|Ga|}{2}\left[\cos(\omega t + \alpha)\cos\beta + \sin(\omega t + \alpha)\sin\beta\right]$$

$$= \frac{|Ga|}{2}\cos(\omega_o t + \alpha - \beta) \tag{85}$$

$$= Re\, S_R^*$$

The block diagram of the processor is shown in Figure 18. When the output of the processor is heterodyned down to the offset frequency ω_c, and if the signal phase modulation is removed from β by range compression the resultant signal is recorded as a mask in plane P_3. The output recording will only register the squared absolute value of the angular autocorrelation function. Thus, there still remains the problem of the unknown phase angle γ in Equation (77). This angle incorporates all unknown signal phase shifts acquired in space and during the processing. It can make some of the signal samples go to zero when there is actually signal present at the antenna. For this purpose another processor working in quadrature with the first one (including the mask) must

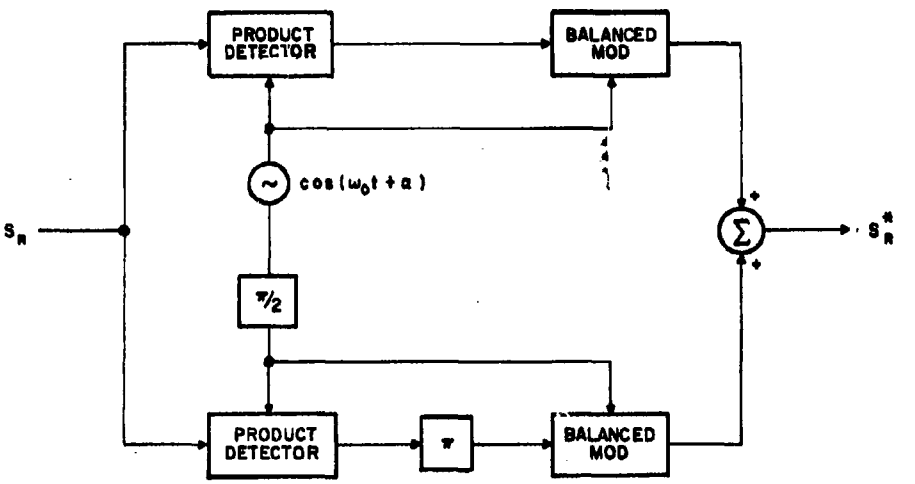

Figure 18 Complex Conjugate Processor

be used. When the outputs of both processors are monitored by photomultiplier tubes instead of film they can be added to produce the final signal. Note that if the input signal contains doppler shift it will manifest itself in the spectral planes P_2 and P_4. Positive and negative signal spectrum components will have their peaks shifted by an amount proportional to the doppler frequency. This will prevent proper signal multiplication in the plane P_3 since the mask is recorded for zero doppler. Thus a different set of masks must be used to process each doppler frequency. This, of course, complicates the system immensely. An alternative method may be to record the signal for two full antenna revolutions and utilize one revolution to monitor the doppler frequency at the plane P_2. Observed signals can be used to activate a deviable oscillator located ahead of the optical processor at IF; this would compensate for the doppler shift during the next antenna revolution. Since doppler shifts in all range bins are not necessarily equal, a separate compensation for each range bin must be generally employed.

The description above has been rather suggestive than rigorous in the sense that little mathematical analysis of the system has been presented. Many practical details such as the effect of the finite aperture size on the inverse Fourier transforms, the presence of noise in the system, and the degradation of resolution due to cascading of optical components, were completely neglected. Nevertheless the example above served to point out that the two dimensional nature and availability of large storage delays in the optical systems makes them useful in applications such as antenna dispersion and compression. If the system of Figure 17 is regarded as a stepping stone toward the implementation of a six-dimensional radar rather than as an ultimate and practical signal processor then, perhapes, some of the omissions and lack of rigor may be justified.

E. Extension to Multiple Dimensions

In the last section a rather crude method to achieve pattern compression in one angular dimension and at all ranges was discussed. It was shown that presence of doppler shift in the received signal may complicate the required processing very significantly. It is conceivable that with a cleverly designed scanning pattern a two dimensional optical correlator may perform a simultaneous pattern compression in both angles; with present state-of-the-art, however, one such processor would be required for each range bin. Hence the extension of optical processing to more than two dimensions seems to encounter all the usual problems of excessive equipment complexity.

There are many problems in optical signal processing still awaiting solution. It may be possible that extension to more than two dimensions can be achieved by synthesis of proper pattern and signal modulation functions in order to obtain signal recordings with the self-focusing properties of a zonal plate.

The art of light modulation by methods which would permit long delays without requirement of film storage is still in the beginning of its development. Efficient methods for combination of several modulated light beams either by addition, subtraction or multiplication are still not available. Finally, utilization of such properties of light as color modulation and polarization for purposes of signal processing are not fully explored. The potential use of fiber optics as a means of multiple channel processing should be investigated.

Answers to all of these problems may eventually provide the techniques for synthesis of a truly six-dimensional correlator.

SECTION VI

MULTIPLE FREQUENCY ANTENNA TECHNIQUES

I. Introduction

The term "multiple frequency array," as used in this paper, will refer to antenna arrays in which each radiator operates at a single frequency. Analysis of the properties of these antennas will be restricted to one dimensional, linear arrays; consequently, the radiator frequencies can be represented as a function of one position variable. The geometrical configuration of the array is like that illustrated in Figure 1, where the array appears as a line segment. A simple example of a multiple frequency array is one in which the operating frequency varies linearly with the array coordinate. The operating frequency in this case can be represented by the graph in Figure 2. Frequency distributions of this type, in which no frequency is repeated, are of primary concern in this paper.

Study of multiple frequency arrays originally was motivated by the search for high bandwidth antennas in which the element transmitters were limited to narrowband, CW operation. The multiple frequency array defined in Figure 2, for example, is capable of transmitting wideband signals despite the fact that each element is excited by a CW transmitter. Total bandwidth of the emitted signal is limited only by the number of radiators in the array, and the frequency separation between adjacent elements. In fundamental concept, the spectral components of the desired radiated signal are assigned to the individual radiators of the array. The frequency difference between adjacent radiators therefore determines the repetition rate of the transmitted signal.

One of the main problems associated with multiple frequency arrays is an apparent loss in angular directivity. Because of the spreading of individual spectral components among the array radiators a range-angle ambiguity pattern results, i.e., appreciable beam energy can be found at a number of range-angle values, instead of one range-angle value as in the case of a simple pulse emitted through a narrow beam. This loss in directivity can be circumvented, however, by varying the multiple frequency array illumination such that each frequency appears at each radiator, in sequence, as a function of time, - and then integrating the received signals. The output of the integrator in this case resembles that obtained from a conventional antenna system in which the entire pulse spectrum is emitted from each radiator. The obvious disadvantage of this process is the loss of time

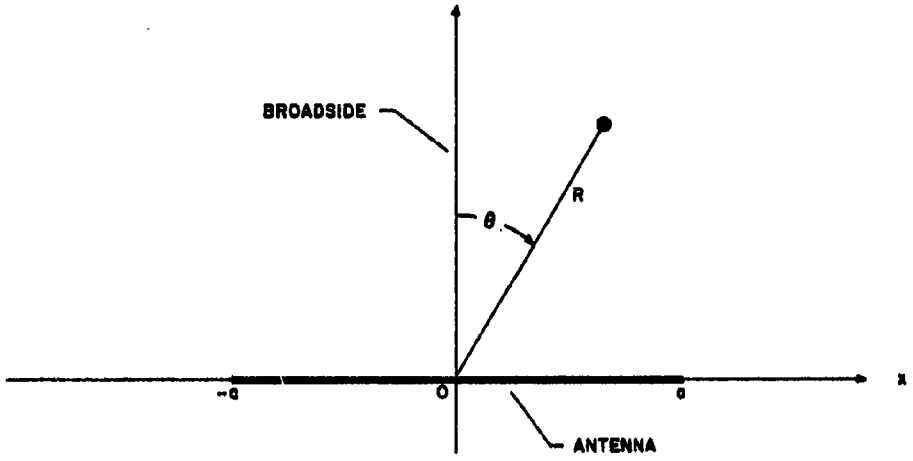

Figure 1 Antenna Geometry

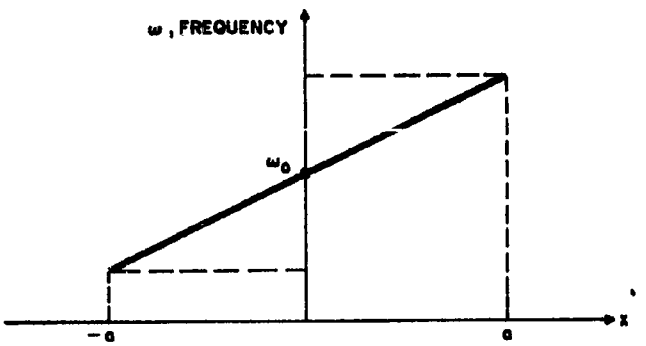

CONTINUOUS ARRAY

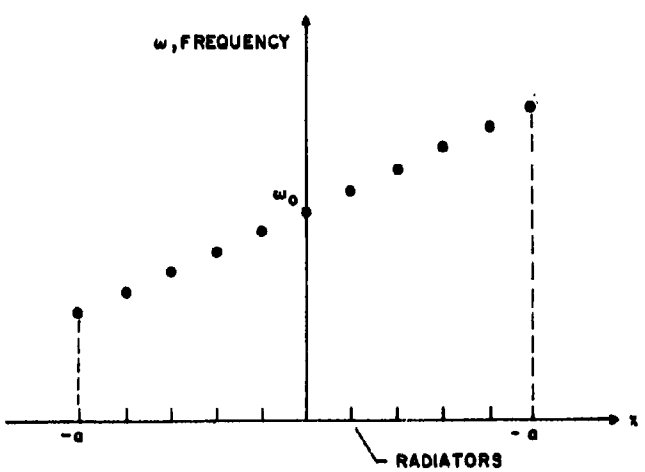

DISCRETE ARRAY

Figure 2 Linear Frequency Distribution

involved in cycling each spectral component so that it can radiate for a period from each radiator in the array. However, the advantage gained is one which is usually found in pulse compression systems - high peak powers are obtained with low power CW transmitters. Moreover, high bandwidth signals are easily generated since the large bandwidth is created through addition of a large number of narrow bandwidth signals. A less obvious advantage of the multiple frequency array technique is its relative immunity to mutual coupling effects. Since each radiator operates at a different frequency, narrowband filters can be used to attenuate coupled energy. The transmission of the multiple frequency array can also be modified to overcome the classical transit time problem usually associated with large radiating apertures. In conventional arrays transient buildup of the radiated signal is incurred (equivalent to a pattern distortion) when the spatial extent of the signal is small compared to the aperture size and when the aperture beam is scanned off broadside. As will be shown in later sections this transient effect can be eliminated through use of a time-varying multiple frequency illumination in which the phases at the radiators are changed as a function of time.

A knowledge of the propagated energy distribution in space and time is required to quantitatively analyze the properties of multiple frequency arrays. For this reason equations relating the radiated field and the aperture excitation will be reviewed first.

II. Field Equations

The classical diffraction problem is concerned with finding the radiation distribution caused by a known current distribution over a plane aperture. The nature of the radiation distribution must be such as to satisfy the wave equation. Suppose the aperture, A, containing the excitation currents is described by the coordinates shown in Figure 3. The aperture coordinates are x and y, z is the coordinate perpendicular to the aperture, and (R, θ, ϕ) is the usual spherical coordinate system. When the current operates at the frequency ω, and when it has an amplitude and phase given by the function $F(x, y)$, the radiation field is given by[1]

$$U = \frac{i\omega e^{i\omega(t-\frac{\rho}{c})}}{4\pi c R} \iint F(x,y)[\cos\theta + i_z \cdot S] e^{i\frac{\omega}{c}\sin\theta(x\cos\phi + y\sin\phi)} dx dy \qquad (1)$$

---

(1) S. Silver, Microwave Antenna Theory and Design, Radiation Laboratory Series, McGraw Hill, 1949, p. 173, Equation (8).

involved in cycling each spectral component so that it can radiate for a period from each radiator in the array. However, the advantage gained is one which is usually found in pulse compression systems - high peak powers are obtained with low power CW transmitters. Moreover, high bandwidth signals are easily generated since the large bandwidth is created through addition of a large number of narrow bandwidth signals. A less obvious advantage of the multiple frequency array technique is its relative immunity to mutual coupling effects. Since each radiator operates at a different frequency, narrowband filters can be used to attenuate coupled energy. The transmission of the multiple frequency array can also be modified to overcome the classical transit time problem usually associated with large radiating apertures. In conventional arrays transient buildup of the radiated signal is incurred (equivalent to a pattern distortion) when the spatial extent of the signal is small compared to the aperture size and when the aperture beam is scanned off broadside. As will be shown in later sections this transient effect can be eliminated through use of a time-varying multiple frequency illumination in which the phases at the radiators are changed as a function of time.

A knowledge of the propagated energy distribution in space and time is required to quantitatively analyze the properties of multiple frequency arrays. For this reason equations relating the radiated field and the aperture excitation will be reviewed first.

II. Field Equations

The classical diffraction problem is concerned with finding the radiation distribution caused by a known current distribution over a plane aperture. The nature of the radiation distribution must be such as to satisfy the wave equation. Suppose the aperture, A, containing the excitation currents is described by the coordinates shown in Figure 3. The aperture coordinates are x and y, z is the coordinate perpendicular to the aperture, and (R, θ, ϕ) is the usual spherical coordinate system. When the current operates at the frequency ω, and when it has an amplitude and phase given by the function $F(x,y)$, the radiation field is given by[1]

$$U = \frac{i\omega e^{i\omega(t-\frac{\rho}{c})}}{4\pi c R} \iint F(x,y)[\cos\theta + i_z \cdot S]\, e^{i\frac{\omega}{c}\sin\theta(x\cos\phi + y\sin\phi)}\, dx\,dy \qquad (1)$$

(1) S. Silver, Microwave Antenna Theory and Design, Radiation Laboratory Series, McGraw Hill, 1949, p. 173, Equation (8).

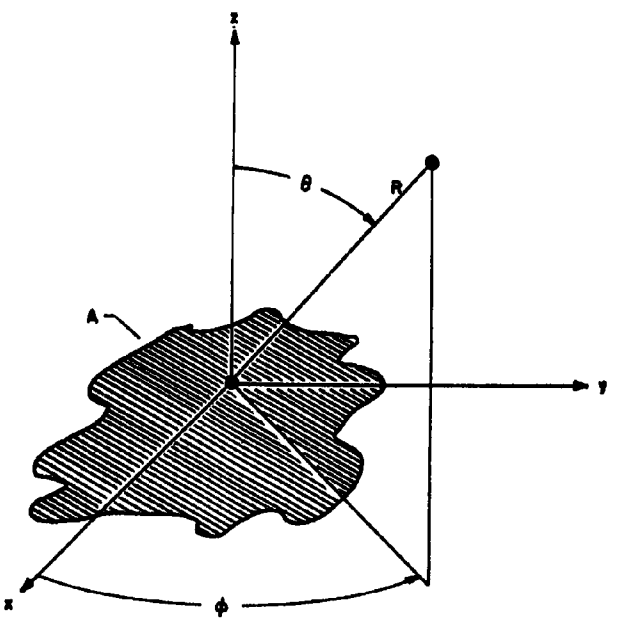

Figure 3 Aperture Geometry

The quantities, t and c, represent the time and the propagation velocity, respectively. The quantity S is a unit vector normal to an equiphase surface. This surface becomes the aperture itself when the phasing is uniform, in which case $i_z \cdot S = 1$.

The radiation expression is based on three assumptions, usually found in array theory. These are: (1) uniform polarization of the currents, (2) small wavelength compared to the aperture dimensions, and (3) the far field approximation in which R is assumed much greater than the aperture dimensions. The assumption is also made that only one frequency component is radiated. The purpose here is to derive the radiation distribution when the more general excitation, $a(x, y, t)$, appears on the aperture. Provision is made in this formulation for more than one frequency to exist at a point in the aperture. A Fourier transform of the excitation $a(x, y, t)$ can be defined as $A(x, y, \omega)$, which denotes the excitation spectrum for each aperture point.

Application of the expression (1) to a particular spectral component of the excitation, $a(x, y, t)$, yields

$$U(\omega) = \iint \frac{i\omega e^{i\omega(t-\frac{R}{c})}}{4\pi c R} A(x, y, \omega)(\cos\theta + i_z \cdot S_\omega) e^{i\frac{\omega}{c}\sin\theta(x\cos\phi + y\sin\phi)} dx\,dy \qquad (2)$$

Notice here that the equiphase surface, S, generally depends on the frequency. To consider all the frequencies in the excitation spectrum, apply the superposition principle to Equation (2) to obtain the total radiation distribution. This is

$$u = \int_{-\infty}^{\infty} U(\omega)\, d\left(\frac{\omega}{2\pi}\right) \qquad (3)$$

$$= \iiint \frac{i\omega}{4\pi c R} (\cos\theta + i_z \cdot S_\omega) A(x, y, \omega) e^{i\omega(t - \tau_{x,y})} dx\,dy\, d\left(\frac{\omega}{2\pi}\right)$$

where several terms have been consolidated into the quantity,

$$\tau_{x,y} = \frac{R}{c} - \frac{x}{c}\sin\theta\cos\phi - \frac{y}{c}\sin\theta\sin\phi \qquad (4)$$

This represents the time delay of a disturbance traveling between the point (x, y) on the aperture and the point (R, θ, ϕ) in space. It is possible to transform (3) so that the quantity, $\tau_{x,y}$, has more conceptual value. Interchange the order of integration in Equation (4) to obtain

$$U = \frac{1}{4\pi c R}\iint i\omega(\cos\theta + i_z \cdot S_\omega) A(x, y, \omega)\, e^{-i\omega\tau_{x,y}}\, e^{i\omega t}\, d\left(\frac{\omega}{2\pi}\right) dx\, dy \tag{5}$$

The integration, here, with respect to frequency, ω, is recognized as the inverse Fourier transform of the quantity, $i\omega(\cos\theta + i_z \cdot S_\omega)\, A(x, y, \omega)\, e^{-i\omega\tau_{x,y}}$. Assume first, as will be later justified, that $i_z \cdot S_\omega$ equals some constant, η. A well-known transform relation can now be applied:

$$T^{-1}\left[i\omega F(\omega) e^{i\omega t_o}\right] = \frac{\partial}{\partial t} f(t - t_o) \tag{6}$$

where T^{-1} represents the inverse Fourier transform and the function $F(\omega)$ is the Fourier transform of the function, $f(t)$. The quantity t_o is just a constant. In the expression the excitation spectrum $A(x, y, \omega)$ is analogous to the function $F(\omega)$ in (6). Therefore (5) becomes

$$U = \frac{1}{4\pi c R}(\cos\theta + \eta)\iint \frac{\partial}{\partial t}\left[a(x, y, t - \tau_{x,y})\right] dx\, dy \tag{7}$$

This is the radiation distribution for the general aperture excitation, $a(x, y, t)$. The assumption made during the derivation, that $i_z \cdot S_\omega$ equals a constant holds in the two cases of interest here. The first case occurs when the phasing is uniform, implying that $i_z \cdot S_\omega = 1$. The second case, applicable to electronic scanning techniques, occurs when the phase varies linearly with the aperture coordinates, x and y, and the frequency ω. The fact that $i_z \cdot S_\omega$ is constant in this second case follows on inspection of the equation for $i_z \cdot S_\omega$,[2]

$$i_z \cdot S_\omega = \left\{1 - \frac{c^2}{\omega^2}\left[\frac{\partial}{\partial x}\psi(x, y, \omega)\right]^2 - \frac{c^2}{\omega^2}\left[\frac{\partial}{\partial y}\psi(x, y, \omega)\right]^2\right\}^{1/2} \tag{8}$$

---

(2) S. Silver, op. cit., p. 162, Equation (107).

where ψ is the phase distribution. In cases where the quantity $i_z \cdot S_\omega$ is not constant, slightly more complicated radiation expressions ensue.

A noteworthy aspect of the expression (7) is the appearance of a time derivative. This operation may be interpreted as the effect of proceeding from the aperture disturbance to the disturbance in space. The other effects described in (7) are the usual range diminution, the obliquity factor which accompanies all flat arrays, and finally the time delay of the disturbance traveling from the array into space. This latter effect of time delay is the only factor which gives information as to the interaction of the radiators; consequently attention will be focused on the quantity

$$P \equiv \iint a(x,y,t-\tau_{x,y})\,dx\,dy \tag{9}$$

which is defined as the space pattern. The effects of range diminution, obliquity factors, and time differentiation will be taken for granted.

III. Typical Patterns

A. Linear Frequency Distribution

Since the arrays of interest are one dimensional, the multiple frequency array can be represented by the form, $a(x)\, e^{i\omega(x)t}$. The quantity $\omega(x)$ denotes the frequency component as a function of the array coordinate; $a(x)$ denotes the array illumination, which specifies the amplitude and phase of the disturbance for every array position. Referring to (9) and making the necessary dimensional adjustments, the space pattern for the general multiple frequency array is given by:

$$P = \int_{-a}^{a} a(x)\, e^{i\omega(x)\left[t - \frac{\beta}{c} + \frac{x}{c}\sin\theta\right]}\,dx \tag{10}$$

This expression assumes the array is located between $x = -a$ and $x = a$. The multiple frequency array having constant illumination ($a(x) = 1$) and having the frequency distribution,

$$\omega(x) = \omega_0\left(1 + \frac{\delta}{a}x\right) \tag{11}$$

where ω_o is the center frequency, $2\omega_o\delta$ is the bandwidth, and 2a is the array length, has a representative space pattern. The problem here is to put the resulting integral, Equation (10), in terms of tabulated or common functions. Substituting,

$$P = \int_{-a}^{a} e^{i\omega_o\left(1+\frac{\delta}{a}x\right)\left(t-\frac{R}{c}+\frac{x}{c}\sin\theta\right)}\,dx \tag{12}$$

$$= e^{i\omega_o\left(t-\frac{R}{c}\right)}\int_{-a}^{a} e^{i\frac{\omega_o}{c}x\left[\frac{\delta}{a}(ct-R)+\sin\theta\right]}\, e^{i\frac{\omega_o\delta}{ac}x^2\sin\theta}\,dx$$

When

$$A = \frac{a}{2\delta} - \frac{R-ct}{2\sin\theta} \quad , \qquad B = \frac{\omega_o\delta}{ac}\sin\theta$$

the expression becomes

$$P = e^{i\omega_o\left(t-\frac{R}{c}\right)}\int e^{iB(x^2+2xA+A^2)}\, e^{-iBA^2}\,dx \tag{13}$$

A change of variables, y = A + x, reduces the expression to

$$P = e^{i\omega_o\left(t-\frac{R}{c}\right)}\, e^{-iBA^2}\int_{-a+A}^{a+A} e^{iBy^2}\,dy \tag{14}$$

$$= e^{i\omega_o\left(t-\frac{R}{c}\right)}\, e^{-iBA^2}\int_{-a+A}^{a+A}\left[\cos(By^2)+i\sin(By^2)\right]dy$$

Expressions of the form

$$\int_0^u \sin\left(\tfrac{\pi}{2}t^2\right)dt \quad , \qquad \int_0^u \cos\left(\tfrac{\pi}{2}t^2\right)dt$$

are known as Fresnel integrals, and they have been tabulated.[3] Denoting these S(u) and C(u), respectively, the space pattern is finally:

(3) E. Jahnke and F. Emde, Tables of Functions, Fourth edition, Dover Publications, New York, 1945, p. 34-37.

$$P = e^{i\omega_0(t-\frac{\beta}{2})} e^{-i\beta A^2} \sqrt{\frac{\pi}{2|B|}} \left\{ C\left[(a+A)\sqrt{\frac{2|B|}{\pi}}\right] + C\left[(-A+a)\sqrt{\frac{2|B|}{\pi}}\right] \right. \tag{15}$$

$$\left. \mp S\left[(a+A)\sqrt{\frac{2|B|}{\pi}}\right] \mp S\left[(-A+a)\sqrt{\frac{2|B|}{\pi}}\right] \right\}^*$$

This expression includes all cases except B = 0, (i.e., the broadside case) but this case may be handled separately. Set $\theta = 0$ in (12) to obtain

$$P = \int_{-a}^{a} e^{i\omega_0(1+\frac{\delta x}{a})(t-\frac{\beta}{2})} dx \tag{16}$$

$$= 2a\, e^{i\omega_0(t-\frac{\beta}{2})} \frac{\sin\left[\delta\omega_0(t-\frac{\beta}{2})\right]}{\delta\omega_0(t-\frac{\beta}{2})}$$

Thus the Equations (15) and (16), jointly determine the energy distribution in space and time, caused by the particular antenna excitation described above.

In order to interpret the space pattern, described by (15) and (16), one must first understand the nature of the Fresnel integrals. These have been plotted in Figure 4. Both functions are antisymmetric, e.g., C(-u) = -C(u), and as a result their graphs go through the origin. Also, depending on the sign of their arguments, they have a damped oscillatory behavior about the values of 1/2 or -1/2. In fact, the functions approach these values asymptotically. The exact asymptotic forms (for large x) are

$$C(x) = \tfrac{1}{2} + \tfrac{1}{\pi x}\sin\left(\tfrac{\pi}{2}x^2\right) + O\left(\tfrac{1}{x^2}\right)$$

$$S(x) = \tfrac{1}{2} - \tfrac{1}{\pi x}\cos\left(\tfrac{\pi}{2}x^2\right) + O\left(\tfrac{1}{x^2}\right) \tag{17}$$

---

* Use upper signs when δ is positive and lower signs when δ is negative.

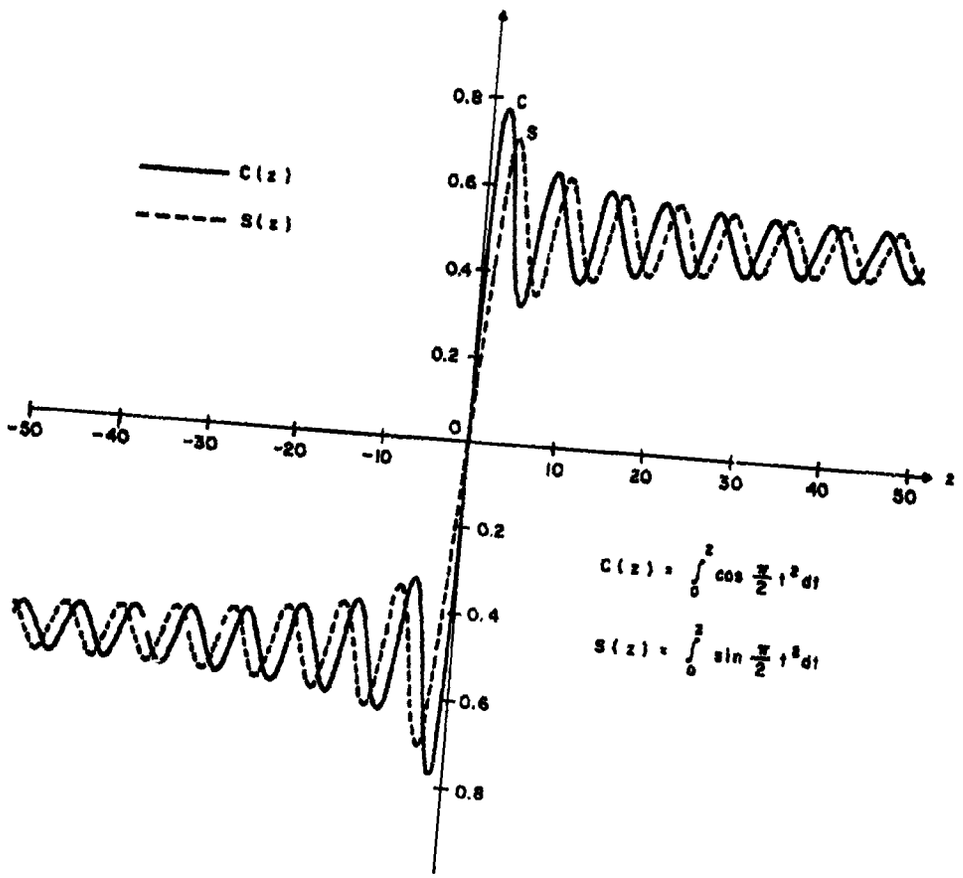

Figure 4 Fresnel Integrals

From these properties, the qualitative behavior of the space pattern can be determined; but as a conceptual aid the space pattern is plotted for the parameters, $a\omega_n\delta/c = 40\pi$ and $\delta = 0.2$. This plot appears in Figure 5. The fact that the quantity, R-ct, is an independent variable in the figure instead of R, means that the pattern propagates from the antenna with the speed, c. Consequently, the plot is one which an observer, moving with the velocity c, would see.

There are four descriptive aspects associated with the space patterns of Equation (15) and (16), three of which are conveniently described by introducing the concept of the radial pulse. Indeed any pattern may be thought of as a set of radial pulses whose forms depend on the angle. Usually, the form is the same for all angles, so that each pulse is connected to the others by proportionality constants. The situation here is different in that the pulse forms will vary with angle. The outstanding feature of the pattern is the set of the radial pulse maxima which form a ridge about the antenna. Referring to Equation (12), it is seen that, for a fixed angle θ, P is maximized when

$$\frac{\delta}{a}(ct - R) + \sin\theta = 0$$

Hence, the locus of the maximal ridge is

$$R = ct + \frac{a}{\delta}\sin\theta \tag{18}$$

This locus is known as the Limaçon of Pascal, and is plotted in Figure 6. Notice that the parameter a/δ affects the shape of the ridge, such that small a/δ implies a more circular shaped Limaçon.

The next aspect is the field strength on the Limaçon itself. An expression for this is found by substituting A = 0 into Equation (15). The result is

$$P_m = 2a\, e^{i\omega_0(t-\frac{R}{c})}\sqrt{\frac{\pi}{2a^2|B|}}\left[C\left(\sqrt{\frac{2a^2|B|}{\pi}}\right) \mp i\,S\left(\sqrt{\frac{2a^2|B|}{\pi}}\right)\right] \tag{19}$$

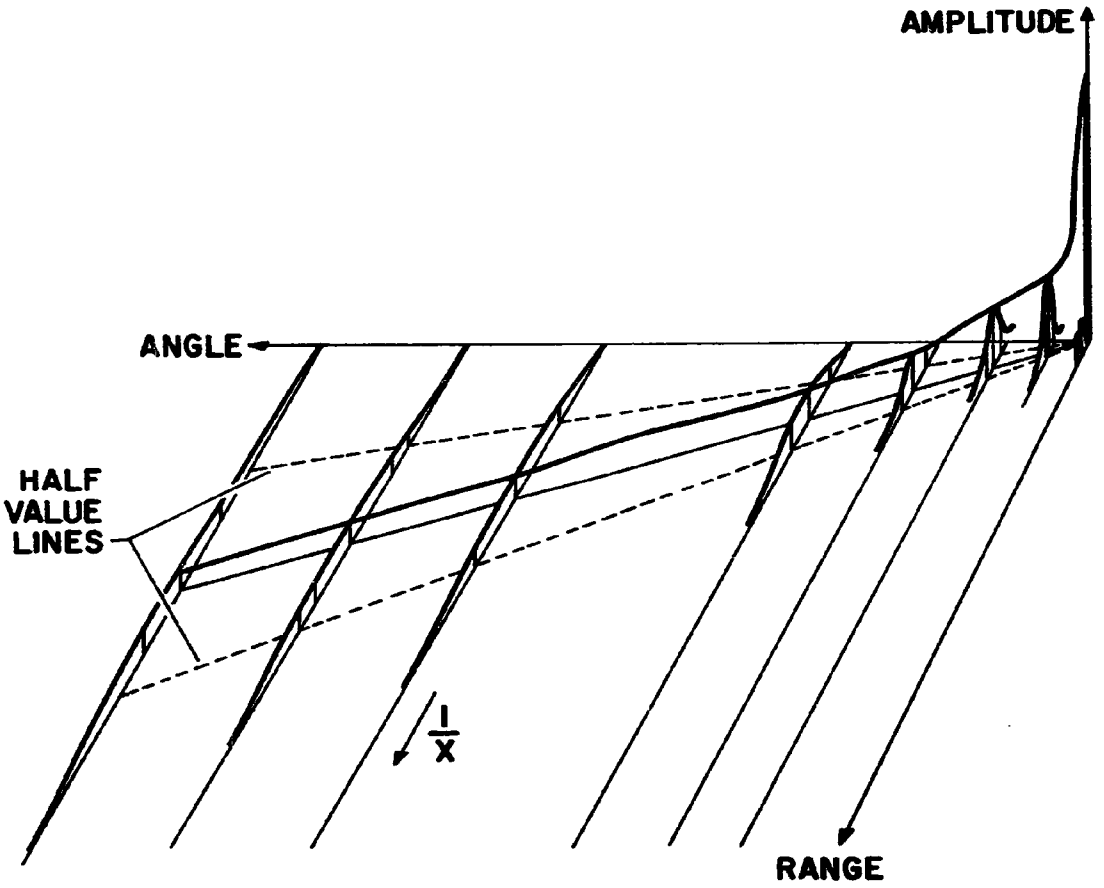

Figure 5 Field Pattern - Wideband Linear Frequency Distribution (20% BW)

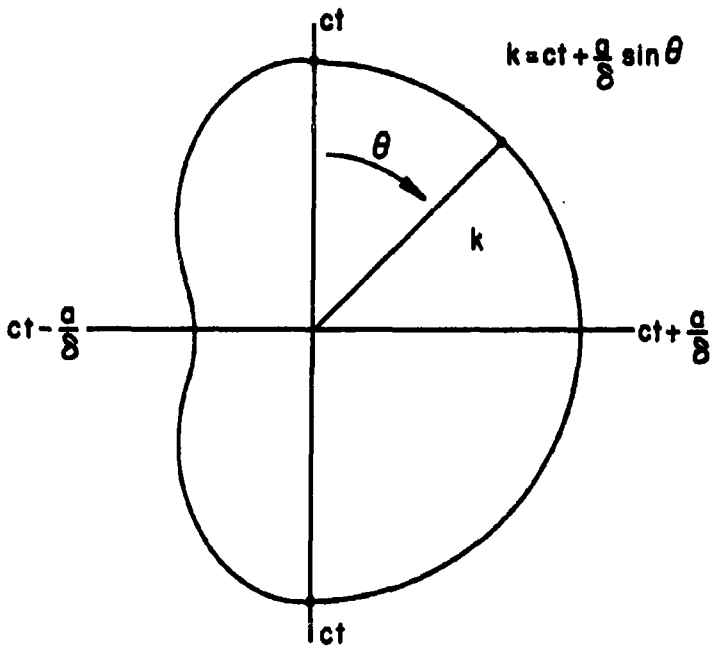

Figure 6 Limacon of Pascal

The point to be seen here is that the field is peaked about B = 0, the broadside direction, where it has the value 2a. At other positions on the Limaçon,

$$\frac{2a^2|B|}{\pi} = \frac{2a\omega_o \sin\theta}{\pi c} \tag{20}$$

Therefore, when

$$\theta = \frac{\pi^2 c}{2a\omega_o \delta} ,$$

since $2\theta/\pi \leq \sin\theta$ for all values of θ, the following inequality ensues,

$$\frac{2|B|a^2}{\pi} \geq 2$$

Applying this inequality to (19) yields

$$|P_H| \leq 2a\sqrt{\frac{\pi}{2}} \left| C(\sqrt{2}) + iS(\sqrt{2}) \right| \leq \frac{a}{\sqrt{2}} \tag{21}$$

Thus the half power point on the Limaçon occurs between the angles $\theta = 0$ and $\theta = \pi^2 c/2a\omega_o\delta$. By either increasing the bandwidth $\omega_o\delta$ or the array length, the half power points approach closer to the broadside direction. In this way, the Limaçon field becomes more peaked.

Although the field level of the radial pulses decreases for increasing angle, θ, the pulses broaden; and as a result all the pulses contain the same amount of power. The fact that the pulses do broaden can be seen by finding two "half-value ridges." These are defined as the ridges which, for any angle θ, have half the field strength as that on the maximal ridge. It will be shown that these two ridges separate more for larger angles, which implies of course that the pulses broaden. When neither θ nor $\omega_o\delta\, a/c$ is small, the half value ridge can be shown to be given by $A = \pm a$ or $R = ct + (a/\delta \pm a)\sin\theta$. By (15) the field on these loci is given by

$$|P_H| = \sqrt{\frac{\pi}{2|B|}} \left[C\left(\sqrt{\frac{8a^2|B|}{\pi}}\right) - iS\left(\sqrt{\frac{8a^2|B|}{\pi}}\right) \right] \tag{22}$$

Since the Fresnel integrals vary little for arguments removed from zero, P_H will indeed be half of P_M, despite the fact that the arguments of C and S are different in (19) and (22). The radial distance between the two ridges is $4a \sin\theta$ which, as claimed previously, increases as the angle increases.

The remaining consideration is the asympotic behavior of the field strength on the radial pulses. On broadside the behavior is clear from expression (16). For angles off the broadside, the radial dependence of the pattern is obtained through the use of the asympotic forms of the Fresnel integral in (17). When θ and R-ct are not small, it follows from (15) and (17) that

$$|P| \leq \frac{2}{R_0 A} \approx \frac{4ac}{d\omega_0 (R-ct)} \tag{23}$$

Hence the space pattern asymptotically decreases, radially, faster than $1/R-ct$ as R-ct increases; and most of the energy in the radial pulses will be located between the half-value loci.

Under certain circumstances, the expression for the space pattern can be simplified. When $a\omega_0\delta/c$ is small a simplified expression is obtained by making the approximation,

$$e^{i\frac{\omega_0\delta}{ac}x^2\sin\theta} = 1 + i\frac{\omega_0\delta}{ac}x^2\sin\theta \tag{24}$$

Substitution into (12), when $b = \omega_0\delta/ac\ (R-ct)$, yields for the space pattern

$$I = 2e^{i\omega_0(t-\frac{R}{c})}\int_0^a (1+i\beta x^2)\cos(bx)\,dx \tag{25}$$

Evaluation of the integral produces the final result,

$$I = 2ae^{i\omega_0(t-\frac{R}{c})}\left\{\frac{\sin(ab)}{ab} - \frac{i\beta}{ab}\left[\left(\frac{2}{b^2}-a^2\right)\sin(ab) - \frac{2a}{b}\cos(ab)\right]\right\} \tag{26}$$

In the limit of very small bandwidth, B becomes small, and the pattern is

$$I = 2a\, e^{i\omega_0(t-\frac{\rho}{c})} \left\{ \frac{\sin\left[\delta\omega_0(t-\frac{\rho}{c}) + \frac{\omega_0 a}{c}\sin\theta\right]}{\delta\omega_0(t-\frac{\rho}{c}) + \frac{\omega_0 a}{c}\sin\theta} \right\} \tag{27}$$

This is a situation where the field is constant over the Limacon. Also the pulse will be relatively wide since $\omega_0\delta$ is small. A plot of the narrowband case appears in Figure 7.

The continuous array, just analyzed, is an approximation to the actual array with discrete elements. When the discrete array is analyzed, however, only the concept of a "pulse repetition rate" is introduced. As for the form of the space patterns, they are very similar to the corresponding continuous array. Suppose the frequency of the n-th radiator is given by

$$\omega_n = \omega_0\left[1 + \frac{x_0 n}{N}\delta\right] \tag{28}$$

where x_0 is a constant. Assuming $a_n\omega_n$ is constant, the pattern can be written

$$I = \sum_{n=-N}^{N} e^{i\omega_n(t-\frac{\rho}{c} + \frac{na}{Nc}\sin\theta)} \tag{29}$$

When the substitution for ω_n is made, when the small bandwidth approximation is made, and when well known summation formulas are applied, the pattern becomes:

$$I = e^{i\omega_0(t-\frac{\rho}{c})} \frac{\sin\left\{(2N+1)\frac{\omega_0}{2N}\left[(t-\frac{\rho}{c})\delta + \frac{a}{c}\sin\theta\right]\right\}}{\sin\left\{\frac{\omega_0}{2N}\left[(t-\frac{\rho}{c})\delta + \frac{a}{c}\sin\theta\right]\right\}} \tag{30}$$

This expression assumes a maximum value, 2N + 1, whenever

$$\frac{\omega_0}{2N}\left[(t-\frac{\rho}{c})\delta + \frac{a}{c}\sin\theta\right] = L\pi\,, \qquad L = \text{INTEGER} \tag{31}$$

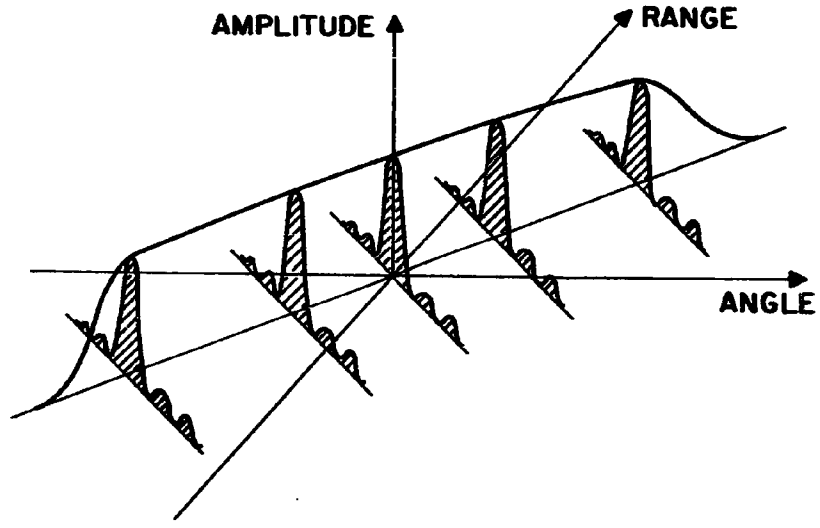

Figure 7 Field Pattern - Linear Frequency Distribution

Hence the pattern is a succession of constant field ridges which, for a fixed range, occur at time increments, $\Delta t = 2\pi N/\omega_o\delta$. In other words, the pulse repetition rate is $\omega_o\delta/2\pi N$ per second.

The analysis here has uncovered several differences between the multiple frequency array space pattern and the patterns of conventional antennas. The radial pulses have different forms for different angles; the energy in the radial pulses is independent of direction; the locus of the set of radial maximas is no longer a circle, but instead a Limacon; a pulse repetition rate is achieved without radiator modulation. The major drawback of these arrays is the large amounts of sidelobe energy which they produce; the advantage is in their bandwidth capability. A possible instrumentation might make use of the bandwidth capability on transmission, then a conventional array could add directivity to the system on reception. In this way, the advantages of both arrays would be utilized.

B. Symmetrical Distribution

A modified version of the linear frequency distribution is the symmetrical distribution given by

$$\omega(x) = \omega_o\left(1 + \frac{\delta}{a}|x|\right) \tag{32}$$

The distribution is illustrated in Figure 8, and there it is shown that the bandwidth is $\omega_o\delta$, the array length is 2a, and the minimum frequency is ω_o. The space pattern of this array is similar to that of the last section; however, an improvement in directivity exists, and the array is important for that reason. Furthermore, much of the analysis of the previous section can be used to derive the space pattern.

The pattern expression, when $a(x)\,\omega(x) = 1$, is

$$I = \int_{-a}^{a} e^{i\omega\left(1+\frac{\delta}{a}|x|\right)\left(t-\frac{R}{c}+\frac{x}{c}\sin\theta\right)}\,dx \tag{33}$$

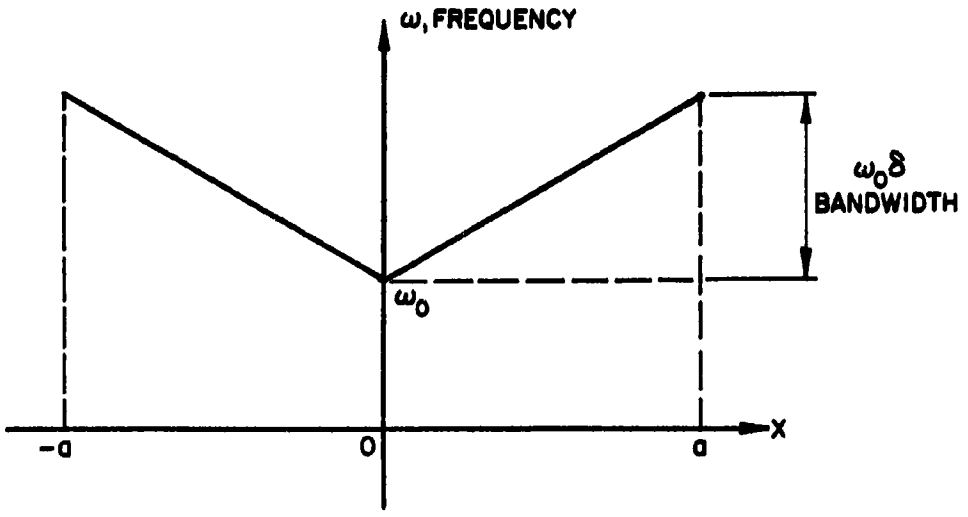

Figure 8 Symmetrical Frequency Distribution

which is most conveniently written as two integrals:

$$I = \int_0^a e^{i\omega_0\left(t+\frac{\delta}{a}x\right)\left(t-\frac{R}{c}+\frac{x}{c}\sin\theta\right)} dx + \int_0^a e^{i\omega_0\left(t+\frac{\delta}{a}x\right)\left(t-\frac{R}{c}+\frac{x}{c}\sin\theta\right)} dx \qquad (34)$$

From the last section, borrow the notation:

$$A = \frac{a}{2\delta} - \frac{R-ct}{2\sin\theta}$$

$$B = \frac{\omega_0 \delta}{ac}\sin\theta$$

and let

$$A' = \frac{a}{2\delta} + \frac{R-ct}{2\sin\theta}$$

Then by arguments identical to those of the preceding derivation, the space pattern becomes

$$I = e^{i\omega_0\left(t-\frac{R}{c}\right)}\left[e^{-iBA^2}\int_A^{a+A} e^{iBy^2}dy + e^{iBA'^2}\int_{A'}^{a+A'} e^{-iBy^2}dy\right] \qquad (35)$$

Using the triangle inequality, i.e., $|p+q| \leq |p| + |q|$ for any p and q, an upper bound for (35) will be:

$$|I| = \left|\int_A^{a+A} e^{iBy^2}dy\right| + \left|\int_{A'}^{a+A'} e^{-iBy^2}dy\right| \qquad (36)$$

Referring to (14) and denoting the space pattern of the previous section, $I_L(A, B, a)$, (36) can be rewritten as

$$|I| \leq \left|I_L\left(A+\tfrac{a}{2}, B, \tfrac{a}{2}\right)\right| + \left|I_L\left(A'+\tfrac{a}{2}, B, \tfrac{a}{2}\right)\right| \qquad (37)$$

This is the desired result. It means that an envelope for the symmetrical distribution space pattern is the sum of two space patterns for a linear frequency distribution. The envelope is shown in Figure 9.

The envelope is characterized by two intersecting maximal ridges, Limaçons, whose loci are given by $R-ct = (a + a/\delta) \sin \theta$ and $R-ct = -(a + a/\delta) \sin \theta$. The important parameters are $(a + a/\delta)$, which affects the shape of the Limaçons, and $a\omega_o\delta/c$ which affects the rate of field strength descent on the Limaçons with distance from the broadside direction. As for the sidelobe energy, it is approximately half that of the array in the previous section. This is a result of the fields adding linearly on the broadside to give twice the amplitude as that on either ridge. This means the power level here is four times that of either ridge. Although this is only a crude argument, actual computations have shown close correspondence to the prediction. Actually the new sidelobe energy is 3/4 the amount of the old sidelobe energy. This is true regardless of the parameter values.

Since the symmetrical array has greater directivity it may be desired to combine this array with a directive receiver achieving even better directivity. The bandwidth of this array, however, is half that of the array in the previous section. It has been shown that the symmetrical array can have increased bandwidth only by increasing the number of radiators or by changing the pulse repetition rate. It is also possible to extend the symmetrical array as is done in the cases illustrated in Figures 10 and 11. These have an even greater amount of directivity, but the bandwidth will be limited to greater extent. The mechanism for these multiple frequency arrays is described below.

Frequency duplication along the array increases directivity, but it also eliminates the possibility of increasing total bandwidth. This tradeoff is based on two factors. First each frequency component must be separated from adjacent components by the same frequency increment to keep a specified pulse repetition rate. Secondly, each radiator emits only one frequency component. When either of these conditions are eliminated the tradeoff will disappear.

IV. General Representation

A. Matrix Representation

This section is concerned with arrays whose radiators are not limited to a single frequency. The only restrictions are that the array be

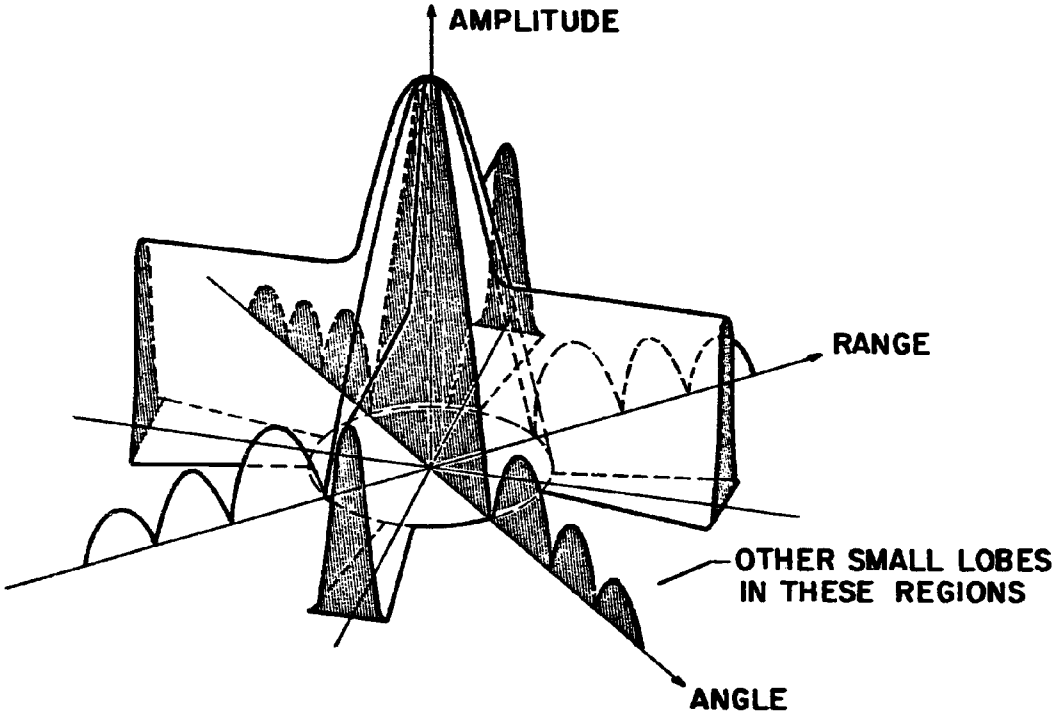

Figure 9 Field Pattern - Linear Symmetrical Frequency Distribution

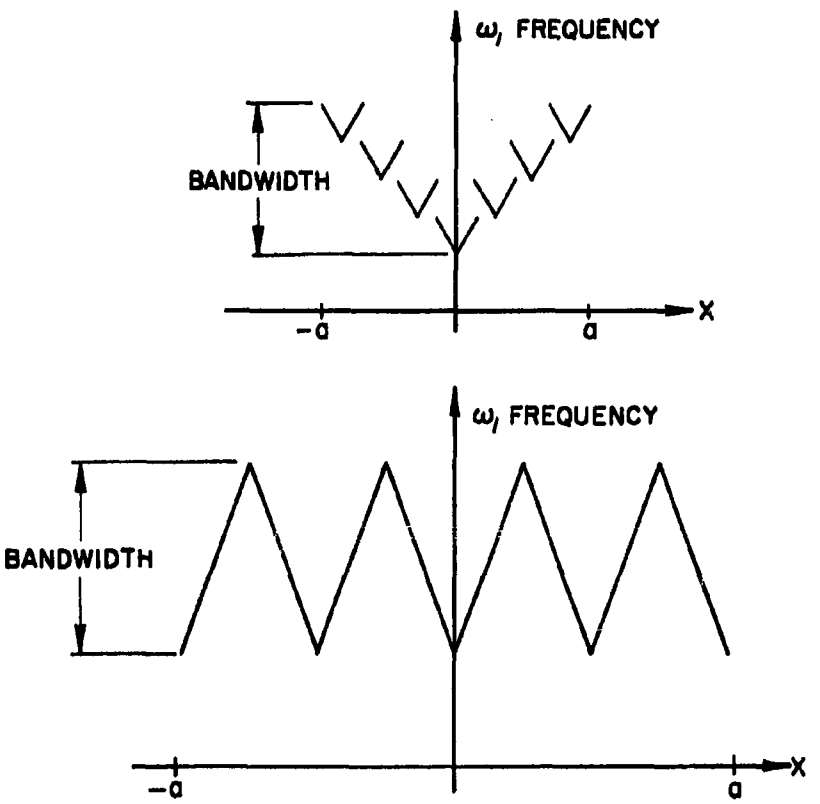

Figure 10 Multi-Symmetrical Frequency Distributions

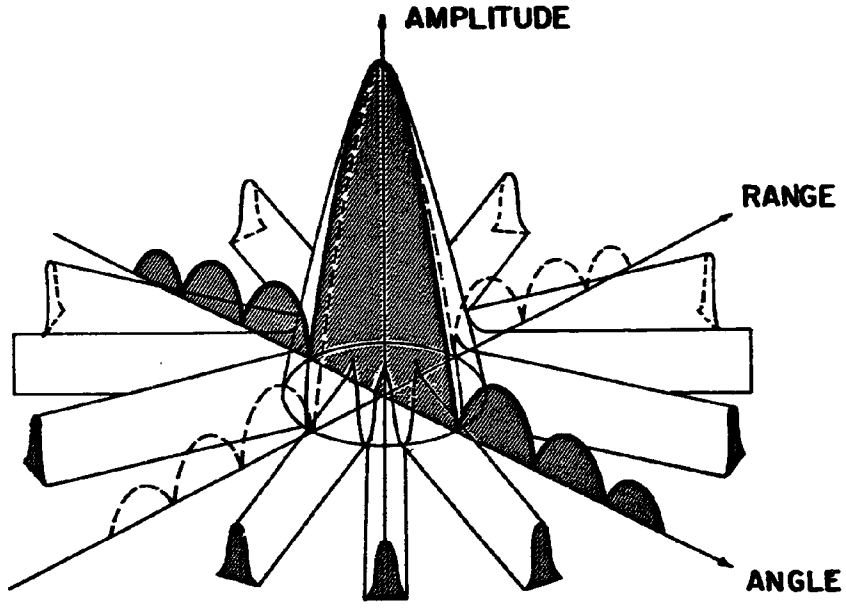

Figure 11 Field Pattern - Multi Linear Symmetrical Frequency Distribution

band limited and that the array extend from x = -a to x = a. If the center frequency is denoted by ω_o and the bandwidth is 2α, these arrays can be represented by a matrix rectangle extending from x = -a to x = a in one dimension and from $\omega = \omega_o - \alpha$ to $\omega = \omega_o + \alpha$ in the other dimension. The array is then completely specified when a magnitude and phase is associated with each point in the rectangle. An example of this representation appears in Figure 12, where the entire bandwidth is emitted from each radiator. When the amplitude and phase are assumed to be the same for all radiator positions and for all frequencies, this example defines the continuous uniformly illuminated conventional array. The space pattern for this array is

$$I = \int_{\omega_o-\alpha}^{\omega_o+\alpha} \int_{-a}^{a} e^{i\frac{\omega x}{c}\sin\theta} e^{i\omega(t-\frac{\beta}{c})} dx\,d\omega \tag{38}$$

After the array integration has been performed,

$$I = 2a \int_{\omega_o-\alpha}^{\omega_o+\alpha} \frac{\sin\left(\frac{\omega a}{c}\sin\theta\right)}{\frac{\omega a}{c}\sin\theta} e^{i\omega(t-\frac{\beta}{c})} d\omega \tag{39}$$

By a simple substitution this becomes

$$I = 2a\, e^{i\omega_o(t-\frac{\beta}{c})} \int_{-\alpha}^{\alpha} \frac{\sin\left[\frac{a}{c}(\omega+\omega_o)\sin\theta\right]}{\frac{a}{c}(\omega+\omega_o)\sin\theta} e^{i\omega(t-\frac{\beta}{c})} d\omega \tag{40}$$

Except for extremely high bandwidths a good approximation for (40) is

$$I = 2a\, e^{i\omega_o(t-\frac{\beta}{c})} \frac{\sin\left(\frac{a\omega_o}{c}\sin\theta\right)}{\frac{a\omega_o}{c}\sin\theta} \int_{-\alpha}^{\alpha} e^{i\omega(t-\frac{\beta}{c})} d\omega$$

or

$$I = 4a\alpha\, e^{i\omega_o(t-\frac{\beta}{c})} \frac{\sin\left(\frac{a\omega_o}{c}\sin\theta\right)}{\frac{a\omega_o}{c}\sin\theta} \frac{\sin\left[\alpha(t-\frac{\beta}{c})\right]}{\alpha(t-\frac{\beta}{c})} \tag{41}$$

Figure 13 illustrates the graph of this expression.

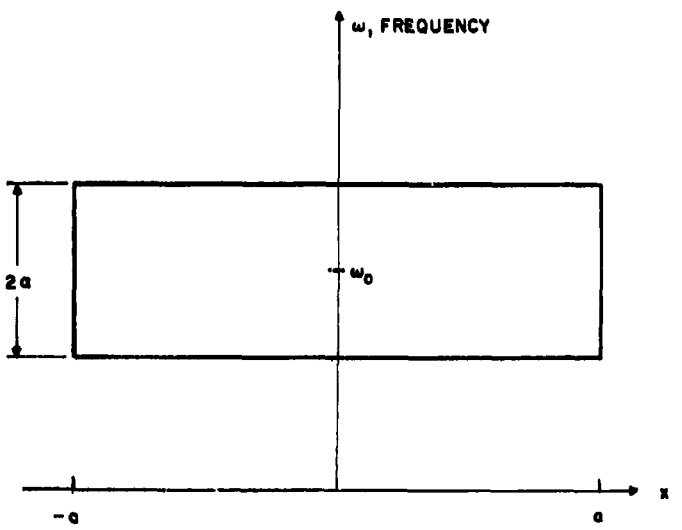

Figure 12 Rectangular Representation - Conventional Array

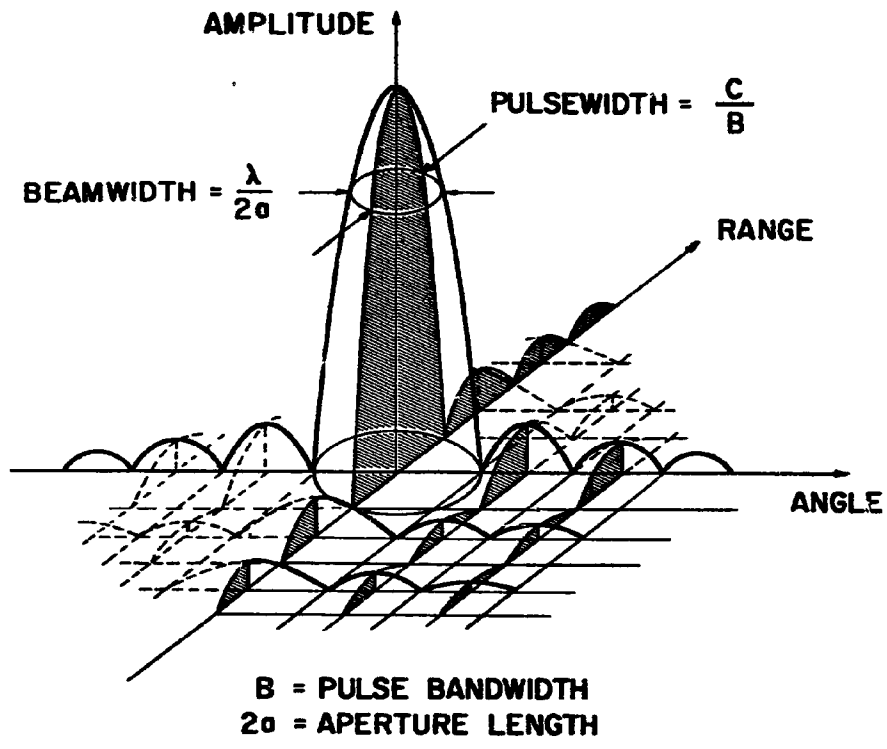

Figure 13 Field Intensity Pattern - Pulse Transmitting Array

Normally, there are a finite number of radiators, each of which emits a periodic signal. Periodicity implies a certain finite frequency spacing between the spectral components; hence, owing to the finite bandwidth assumption, these radiators emit only a finite number of frequency components. Such arrays are most conveniently represented as matrices. When the available spectral components and the radiators are evenly spaced, the matrix concept arises from the mesh-like structure imposed on the previous rectangle. As shown in Figure 14, the nodes of the mesh correspond to the matrix positions. Later, the concept of the array matrix will be useful in describing gain for the general array. It will be seen also that the matrix representation concisely describes the "time-integration process."

The patterns of two sample arrays will be considered first. Analogous to the continuous array above is the discrete array where all matrix elements have an amplitude of unity. Again, this is a conventional array since each radiator emits the same signal; the space pattern is the double summation

$$I = \sum_{K=-M}^{M} \sum_{m=-N}^{N} e^{i(\omega_0 + m\Delta\omega)(t - \frac{R}{c} + \frac{Kd}{c}\sin\theta)} \tag{42}$$

where d is the radiator spacing and $\Delta\omega$ is the spectral spacing. After making the small bandwidth assumption and then carrying out the summations, the space pattern becomes

$$I = e^{i\omega_0(t-\frac{R}{c})} \frac{\sin\left[(2N+1)\frac{\Delta\omega}{2}(t-\frac{R}{c})\right]}{\sin\left[\frac{\Delta\omega}{2}(t-\frac{R}{c})\right]} \frac{\sin\left[(2M+1)\frac{\omega_0 d}{2c}\sin\theta\right]}{\sin\left[\frac{\omega_0 d}{2c}\sin\theta\right]} \tag{43}$$

As in (41), the pattern will have a low amplitude when either t - R/c or the angle θ is large. The peakedness of the pattern is controlled in range by the bandwidth and in angle by the array length.

Another example which can be illustrated is the "random array." The matrix elements in this case are either 0 or 1, and the excited elements (1's) appear randomly in the matrix. The field strength for the point R = ct and θ = 0 will be equal to the sum of the matrix elements. Whereas the signal in other regions will have a low level noisy structure. In other words, the excitations coherently add for only one range-angle direction. This

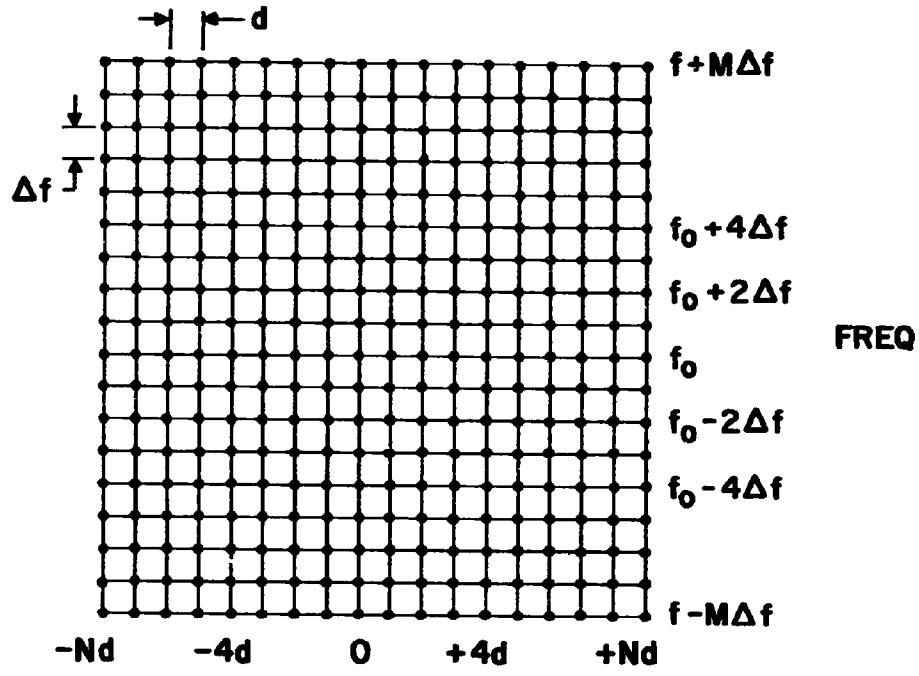

LENGTH OF ABSCISSA = (2N+1)d = ANTENNA LENGTH

LENGTH OF ORDINATE = (2M+1)Δf = PULSE BANDWIDTH

INTERVAL = d = RADIATOR SPACING

INTERVAL = Δf = PULSE REPETITION FREQUENCY

Figure 14 The Multiple Frequency Array Matrix

follows from the fact that randomly chosen Fourier components create noise-like signals. The plot of the pattern of this array appears in Figure 15.

B. Time Varying Distributions

A time-varying distribution is one which is represented by a series (in time) of static distributions. If each of the static distributions arises from a particular array (matrix), the excitation producing the time-varying distribution will be the time sequence of these arrays (matrices). Conversely, when a set of matrices are excited in sequence, a time-varying distribution of pattern ensues. Assuming the targets move little during the sequence period, the return will be a series of individual returns, corresponding to the various matrices. These returns consecutively follow one another. If it were possible to separate the individual returns and then coherently sum them, the resulting signal would be the same as if all the matrices where simultaneously excited. This is just an application of the superposition principle. Such a process can be carried out by storing the individual returns in a recirculating delay line. Each new return is automatically added to the signal present in the delay line. This operation is called the time-integration process. Through use of this process, the desired effect of any matrix can be achieved from a decomposition of that matrix. The set of matrices which are of interest here consists of 2N + 1 different multiple frequency arrays, where a typical frequency distribution appears in Figure 16. This figure shows that the parameter, r, serves to label the array excitations in the set. There are two important properties of this set of arrays. For any frequency distribution, a given frequency appears once and only once on the array. Secondly, the sum of all the matrices in the set is a matrix which represents a uniform weighted conventional array. Therefore, the set of multiple frequency arrays, as illustrated in Figure 16, combine by the time-integration process to give the effective pattern,

$$\sum_{K=-N}^{N}\sum_{m=-N}^{N} e^{i(\omega_0+m\Delta\omega)(t-\frac{\beta}{c}+\frac{kd}{c}\sin\theta)} \tag{44}$$

$$= e^{i\omega_0(t-\frac{\beta}{c})}\,\frac{\sin\left[(2N+1)\frac{\Delta\omega}{2}(t-\frac{\beta}{c})\right]}{\sin\left[\frac{\Delta\omega}{2}(t-\frac{\beta}{c})\right]}\;\frac{\sin\left[(2N+1)\frac{\omega_0 d}{2c}\sin\theta\right]}{\sin\left[\frac{\omega_0 d}{2c}\sin\theta\right]}$$

The expression (44) indicates two facts: (1) multiple frequency arrays can combine to give the range and angular resolution of a conventional array (2) the total power return from the time-integration process is the same as when a conventional array is used. The major sacrifice of the process is

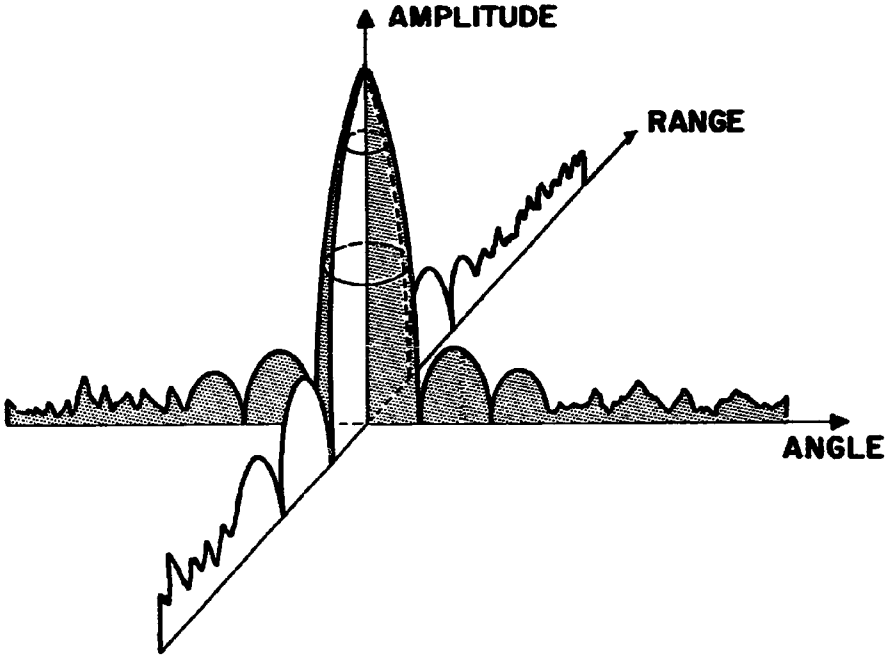

Figure 15 Field Pattern - Random Frequency Distribution

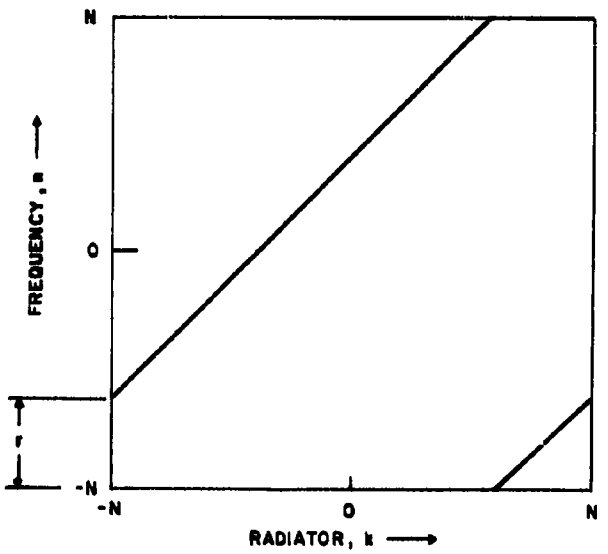

Figure 16 Typical Multiple Frequency Array In The Set

operational speed. Effectively 2N + 1 arrays are required to examine one angle, whereas normally one array is sufficient. The fact that the various arrays can be switched on and off in an electronic fashion will make the problem less severe. Also it will be shown next that the time-integration process is amenable to electronic scan techniques. In this way the operational speed can be maximized.

C. Transit-Time Compensation

Techniques for achieving electronic rotation of antenna patterns are limited by the transit-time problem. The problem arises in cases utilizing pulses which are shorter than the antenna length. Unless compensating time delay elements are used, the array signals (transmission or reception) will not coherently add for angles off the broadside of the antenna. The delay durations depend on the angle of interest; therefore, time varying time delays must be employed for scanning. These elements are to be avoided, for efficient variable time delays are beyond the state of the art.

The transit-time problem exists only when the radiating or receiving elements operate over a wide frequency band. Narrow band conventional arrays can use phase distributions in place of time delays. It will be shown here that multiple frequency arrays require a phase distribution, depending on the frequency distribution, to overcome the transit-time problem. This is reasonable because multiple frequency arrays have only one frequency per radiator, in which case a phase distribution is equivalent to a time delay distribution. The distinction between phase- and time-delay appears when more than one frequency is involved at an array position.

Consider the case described in the previous section in which 2N + 1 multiple frequency arrays combine to form the equivalent of a conventional array. Assume further that the receiver is a multiple frequency array superimposed on the transmitter, and that the receiver is matched to the transmitter. This means that for each array in the set a receiver element accepts only the frequency transmitted from the same point. In this case, the returned signal is the sum of the radiator signals with twice the delay as that experienced on transmission only. Hence, for a given array excitation the signal return may be written

$$\sum_{k=-N}^{N} e^{i\omega_0(k)\left[t - \frac{2R}{c} + \frac{2x(k)d}{c}\sin\theta\right]} \tag{45}$$

where x(k) is the position of the kth frequency. This consideration has the effect of doubling the range and sine of the angle in (44), and hence the processed signal will be

$$\sum_{k=-N}^{N}\sum_{m=-N}^{N} e^{i(\omega_0+m\Delta\omega)(t-\frac{2R}{c}+\frac{2kd}{c}\sin\theta)} \tag{46}$$

In order to rotate this pattern, $\sin\theta$ must change to $\gamma + \sin\theta$; the rotation will then be through an angular amount arc sin γ. It follows that by multiplying the pattern by the factor

$$e^{i(\omega_0+m\Delta\omega)\frac{2kd\gamma}{c}} \tag{47}$$

the term $\sin\theta$ is replaced by $\sin\theta + \gamma$, and the pattern will have been rotated by arc sin γ. This multiplication is the same as adding the phase distribution given by (47). The phase distribution is more conveniently written in terms of the parameter r. As stated before, this parameter identifies particular frequency distributions in the set. By Figure 16,

$$\omega_0(k) = m = k+r \quad , \quad \text{for } -N \le k \le N-r \tag{48}$$

$$\omega_1(k) = m = k+r-2N \, , \quad \text{for } N-r \le k \le N$$

is the frequency distribution corresponding to r. By substituting in (47) for m, the phase distribution which rotates the pattern becomes:

$$\begin{matrix} e^{i\frac{2\omega_0}{c}d\gamma k} & e^{i\frac{2\omega_0}{c}d\gamma k^2} & e^{i\frac{2\omega_0}{c}d\gamma rk} \\ e^{i\frac{2\omega_1}{c}d\gamma k} & e^{i\frac{2\omega_1}{c}d\gamma k^2} & e^{i\frac{2\omega_1}{c}d\gamma(r-2N)k} \end{matrix} \quad \begin{matrix} \text{for } -N \le k \le N-r \\ \text{for } N-r \le k \le N \end{matrix} \tag{49}$$

For a given array, r, in the set, the expression in (49) shows the required phase distribution to rotate the pattern by arc sin γ. In other words, this equation specifies the phase at a radiator, k, when the m-th frequency appears at that radiator. That frequency is given by (48). Hence the need for time delays has been eliminated and the time-integration process can operate with a wide frequency band, without the limitation of the transit-time problem.

V. Gain

Gain, like any other single measure of the antenna pattern, can supply only a limited amount of information concerning antenna properties. Evaluation of antenna patterns requires knowledge of the entire energy distribution rather than some characteristic of the distribution. Nevertheless, it is useful to know the peak power delivered to a target for a given input power. This is the purpose of the gain measure defined here; the purpose, as will be evident, is not to measure directive properties of the antenna.

The gain, G, is defined as the ratio of peak power to the input power. When the radiators emit only a finite number of frequency components, i.e., periodic signals, the input power is understood to mean the input power in one cycle. If the spectral content of the array as a function of radiator position is $A(x,\omega)$, the pattern will be

$$\iint A(x,\omega)\, e^{i\frac{\omega}{c}x\sin\theta}\, e^{i\omega(t-\frac{R}{c})}\, dx\, d\left(\frac{\omega}{2\pi}\right) \tag{50}$$

For uniform phasing the pattern assumes a maximum value when $\theta = 0$ and $t = R/c$ which is

$$\text{Max Power} = \left| \iint A(x,\omega)\, dx\, d\left(\frac{\omega}{2\pi}\right) \right|^2 \tag{51}$$

The input power is given by

$$\text{Input Power} = \iint |A(x,\omega)|^2\, dx\, d\left(\frac{\omega}{2\pi}\right) \tag{52}$$

Therefore, in general

$$G = \frac{\left| \iint A(x,\omega)\, dx\, d\left(\frac{\omega}{2\pi}\right) \right|^2}{\iint |A(x,\omega)|^2 dx\, d\left(\frac{\omega}{2\pi}\right)} \tag{53}$$

When $A(x, \omega)$ involves only a finite number of both frequency components, $(2N + 1)$, and radiators positions, $(2M + 1)$, the gain expression becomes

$$G = \frac{\left| \sum_{k=-M}^{M} \sum_{m=-N}^{N} A_{k,m} \right|^2}{\sum_{k=-M}^{M} \sum_{m=-N}^{N} |A_{k,m}|^2} \tag{54}$$

The symbol, $A_{k,m}$, denotes the magnitude and phase of the m-th frequency component at the k-th radiator. In the case where $A(x, \omega)$ or $A_{k,m}$ is either 1 or 0 (uniform weighting) the gain has a special geometrical interpretation. Referring to the rectangular representation for available frequencies and array positions, (53) may be identified as the area of the excited region within the rectangle. If the entire rectangle is excited, as for the conventional array, the gain is the area of that rectangle.

Referring to the matrix representation of arrays described earlier, (54) can be identified with the number of excited elements in the matrix. Thus the pulsed point source emitting N frequency components has the same gain as the array of N radiators operating at the same frequency. Notice in this latter case the gain definition coincides with the conventional one. The gain definition combines the concepts of angular directivity and range resolution; hence it is called the composite gain in range and angle.

VI. Ambiguity Function

In order to determine the inherent resolution characteristics of an antenna, the concept of an ambiguity function has been developed. Woodward [4] defined an ambiguity function to show the basic limitations in resolving the range and range-rate (doppier) of two targets. The concept

(4) P. M. Woodward, Probability and Information Theory with Applications to Radar, Pergamon Press, London, 1953.

was then extended by Urkowitz, Hauer, and Koval[5] to account for angular resolution. The basic objective of Urkowitz, et al, was to state quantitatively the difference in signals, processed by the antenna, originating from two sources separated in range, range-rate, and angle. Antennas whose signal differences were great for small separation of the sources were said to have fine resolution capability.

The first step, therefore, has been to define a quantitative measure of signal difference. The measure of difference defined here is designed to account for range and angular separation, and it differs from the previous measures of difference. It can be written:

$$\epsilon^2 = \iint |S_1 - S_2|^2 \, d\theta \, dR \tag{55}$$

where S_1 is the processed signal originating from a target at the point (R, θ) and S_2 is the processed signal originating from a target at $(R + \Delta R, \theta + \Delta\theta)$. The situation is shown in Figure 17. Note that this measure depends only on the separation of the two sources and not on the absolute coordinates.

When the squared term in (55) is expanded, there results

$$\epsilon^2 = \iint |S_1|^2 \, d\theta \, dR + \iint |S_2|^2 \, d\theta \, dR - 2 \mathrm{Re} \iint S_1 S_2^* \, d\theta \, dR \tag{56}$$

The first two terms represent the energy from the respective targets, and they are assumed to be equal. The third term contains the resolution information, and is defined as the ambiguity function, $\Phi(\Delta R, \Delta\theta)$:

$$\Phi(\Delta R, \Delta\theta) = \mathrm{Re} \iint S_1 S_2^* \, d\theta \, dR \tag{57}$$

When the signals S_1 and S_2 are such that the function $\Phi(\Delta R, \Delta\theta)$ is sharply peaked about the point $\Delta\theta = \Delta R = 0$, the range-angle resolution of the antenna will be good.

(5) H. Urkowitz, C. A. Hauer, J. F. Koval, "Generalized Resolution in Radar Systems," Proc. IRE, Vol. 50, Oct. 1962, pp. 2093-2105.

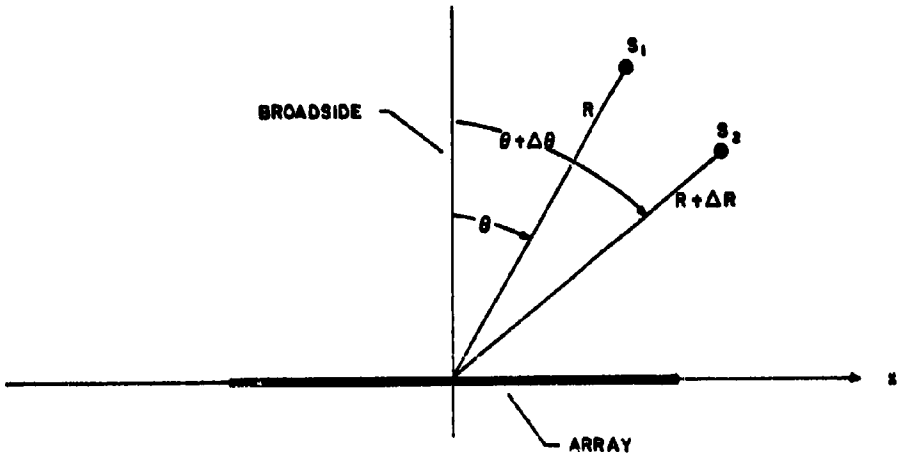

Figure 17 Target Separation Geometry

The processed signals, S_1 and S_2, merely represent the pattern of the antenna; for an illumination function, $a(x,t)$, these signals may be written

$$S_1 = \int a(x, t - \frac{R}{c} + \frac{x}{c}\sin\theta)\, dx$$

$$S_2 = \int a\left[x, t - \frac{R+\Delta R}{c} + \frac{x}{c}\sin(\theta+\Delta\theta)\right] dx \qquad (58)$$

The second signal is equivalent to the pattern shifted ΔR in range and $\Delta\theta$ in angle. Therefore, as a first formulation, the ambiguity function may be considered as the autocorrelation of the antenna pattern.

For purposes of resolution synthesis, the Fourier series formulation of the ambiguity function is useful. To obtain this series first substitute (58) into (57) to get:

$$\Phi = R_e \iiiint a(x_1, t - \frac{R}{c} + \frac{x_1}{c}\sin\theta)\, a^*\left[x_2, t - \frac{R+\Delta R}{c} + \frac{x_2}{c}\sin(\theta+\Delta\theta)\right] dx_1\, dx_2\, d\theta\, dR \qquad (59)$$

Assume the illumination function has a Fourier transform given by $A(x,\omega)$. By interchanging the integration order, and then applying Parseval's theorem, (59) becomes:

$$\Phi = \frac{1}{2\pi} R_e \iiiint A(x_1,\omega) A^*(x_2,\omega)\, e^{-i\frac{\omega}{c}\left[x_2\sin(\theta+\Delta\theta) - x_1\sin\theta\right]}\, e^{i\frac{\omega}{c}\Delta R}\, d\omega\, dx_1\, dx_2\, d\theta \qquad (60)$$

Integration over the variable θ involves the expression

$$\int_0^{2\pi} e^{-i\frac{\omega}{c}\left[x_2\sin(\theta+\Delta\theta) - x_1\sin\theta\right]} d\theta = 2\pi J_0\left[\frac{\omega}{c}\left(x_1^2 + x_2^2 - 2x_1x_2\cos(\Delta\theta)\right)^{1/2}\right] \qquad (61)$$

where J_0 is the Bessel function of the first kind of order zero. Application to (61) of the addition theorem[6] provides

(6) G. N. Watson, Theory of Bessel Functions, Second Edition, Macmillian Co., New York, 1944, p. 358, Equation (1).

$$J_0\left[\frac{\omega}{c}(x_1^2+x_2^2-2x_1x_2\cos\Delta\theta)^{1/2}\right] = \sum_{p=0}^{\infty}\epsilon_p J_p\left(\frac{\omega x_1}{c}\right)J_p\left(\frac{\omega x_2}{c}\right)\cos(p\Delta\theta) \tag{62}$$

where ϵ_p is the Neumann number ($\epsilon_p = 1$ for $p = 0$, $\epsilon_p = 2$ for $p \neq 0$). The ambiguity function can now be written

$$\Phi = R_e\sum_p \epsilon_p \cos(p\Delta\theta)\int_{-\infty}^{\infty} e^{i\frac{\omega}{c}\Delta R}\left|\int_{-a}^{a} A(x,\omega)J_p\left(\frac{\omega x}{c}\right)dx\right|^2 d\omega \tag{63}$$

Letting

$$A_p = \epsilon_p\int\cos\left(\frac{\omega}{c}\Delta R\right)\left|\int A(x,\omega)J_p\left(\frac{\omega x}{c}\right)dx\right|^2 d\omega \tag{64}$$

the ambiguity function can be written as a Fourier series with coefficients equal to A_p.

$$\Phi(\Delta\theta,\Delta R) = \sum_p A_p\cos(p\Delta\theta) \tag{65}$$

For multiple frequency arrays, described by the illumination function $a(x)\,e^{i\omega(x)t}$, a Fourier transform will not exist; the analysis must be altered for this situation. Referring to (59) one obtains

$$\Phi = R_e\iiiint a(x_1)a^*(x_2)e^{i(t-\frac{\Delta R}{c})[\omega(x_1)-\omega(x_2)]}e^{i\frac{\Delta R}{c}\omega(x_2)} \tag{66}$$
$$e^{\frac{i}{c}[\omega(x_1)x_1\sin\theta-\omega(x_2)x_2\sin(\theta+\Delta\theta)]}dx_1dx_2d\theta dR$$

Performing the range integration first and holding time constant there obtains:

$$\Phi = k_e \iiint a(x_1) a^*(x_2) \delta[\omega(x_1) - \omega(x_2)] e^{i\frac{\Delta R}{c}\omega(x_2)} e^{\frac{i}{c}[x_1\omega(x_1)\sin\theta - x_2\omega(x_2)\sin(\theta+\Delta\theta)]} dx_1 dx_2 d\theta \tag{67}$$

As usually defined, $\delta[\omega(x_1) - \omega(x_2)]$ is non-zero when $\omega(x_1) - \omega(x_2) = 0$. When no frequencies are repeated along the aperture $\omega(x_1) = \omega(x_2)$ only when $x_1 = x_2$, and (67) becomes:

$$\Phi = k_e \iint |a(x)|^2 e^{i\frac{x\omega(x)}{c}[\sin\theta - \sin(\theta+\Delta\theta)]} e^{i\frac{\Delta R}{c}\omega(x)} dx d\theta \tag{68}$$

Performing the integration with respect to θ, one obtains the final result:

$$\Phi(\Delta\theta, \Delta R) = \sum_{p=0}^{\infty} \epsilon_p \cos(p\Delta\theta) \int_{-a}^{a} |a(x)|^2 J_p^2\left[\frac{x\omega(x)}{c}\right] \cos\left[\frac{\Delta R}{c}\omega(x)\right] dx \tag{69}$$

Therefore, for this case the Fourier coefficient, A_p, is

$$A_p = \epsilon_p \int |a(x)|^2 J_p^2\left[\frac{x\omega(x)}{c}\right] \cos\left[\frac{\Delta R}{c}\omega(x)\right] dx \tag{70}$$

As asserted in previous sections, multiple frequency arrays where no frequency appears more than once on the aperture have large sidelobes. Equal power emanates in all directions from these arrays. By means of the ambiguity function and its Fourier series representation, however, it is seen that there exists latent directive or angular resolution characteristics for these arrays.

Let

$$\Psi(\Delta\theta) = \int_{-\infty}^{\infty} \Phi^2(\Delta\theta, \Delta R)\, d(\Delta R) \tag{71}$$

This quantity is the total power, as a function of angular separation $\Delta\theta$, in a radial pulse of the ambiguity function. Substitution of (65) into (71) yields

$$\Psi(\Delta\theta) = \int \sum_{p=0}^{\infty} \sum_{q=0}^{\infty} \cos(p\Delta\theta)\cos(q\Delta\theta) A_p A_q \, d(\Delta R) \tag{72}$$

Now substitute (70) for A_p and perform the integration over ΔR to obtain:

$$\Psi(\Delta\theta) = \sum_p \sum_q \epsilon_p \epsilon_q \cos(p\Delta\theta)\cos(q\Delta\theta) \iint \delta\left[\frac{w(x_1) - w(x_2)}{c}\right] \left|a(x_1)a(x_2)\right|^2 J_p^2\left[\tfrac{x_1}{2} w(x_1)\right] J_p^2\left[\tfrac{x_2}{2} w(x_2)\right] dx_1 dx_2 \tag{73}$$

For the frequency distributions of interest ($\omega(x_1) = \omega(x_2)$ only when $x_1 = x_2$) (73) becomes:

$$\Psi(\Delta\theta) = \sum_p \sum_q \epsilon_p \epsilon_q \cos(p\Delta\theta)\cos(q\Delta\theta) \int |a(x)|^4 J_p^2\left[\tfrac{x}{2} w(x)\right] J_q^2\left[\tfrac{x}{2} w(x)\right] dx \tag{74}$$

Unlike the radial power in the corresponding antenna pattern, the radial power in the ambiguity function is seen to depend on the angle $\Delta\theta$. The extent of sidelobe improvement can be determined by the use of the resolution constant, H. This is defined as the maximum value of ψ divided by the average value:

$$H = \frac{\Psi(0)}{\frac{1}{2\pi}\int_0^{2\pi} \Psi(\Delta\theta)\, d(\Delta\theta)} \tag{75}$$

Upon evaluating H in terms of the antenna illumination one obtains:

$$H = \frac{\sum_p \sum_q \epsilon_p \epsilon_q \int |a(x)|^4 J_p^2\left[\tfrac{x}{2} w(x)\right] J_q^2\left[\tfrac{x}{2} w(x)\right] dx}{\frac{1}{2}\sum_p \epsilon_p^2 \int |a(x)|^4 J_p^4\left[\tfrac{x}{2} w(x)\right] dx} \tag{76}$$

It is seen that the numerator of H contains all the terms in the denominator plus several others. Since all terms are positive, the resolution constant H could be substantial. In contrast, if in (71) the antenna pattern replaced the ambiguity function, the corresponding resolution constant would never be greater than unity. From this "gain" definition, therefore, note that $\Phi(\Delta R, \Delta\theta)$ is concentrated about $\Delta\theta = 0$.

SECTION VII

SUMMARY AND CONCLUSIONS

Theory of Resolution - Time Invariant Illumination Functions

One of the major conclusions of this section is that the resolution capability of an antenna is determined by the complex autocorrelation function of the field pattern. As a consequence, the point to be stressed is that angular resolution is not fundamentally dependent on the directivity of the pattern. In analogy to dispersion and compression of signals in the time domain, a "dispersed" pattern (one with no well-defined main beam) can be "compressed" into a high resolution pattern.

Considerable insight into the factors which determine resolution capability has come about through the concept of "spatial frequencies" in the field pattern (i.e., the Fourier decomposition of the field pattern). It has been shown that the Fourier coefficients of the ambiguity function are proportional to the squared magnitudes of the corresponding Fourier coefficients of the pattern. Hence, it follows that it is only the magnitudes of the spatial frequency content of the pattern, and not the phases, which are of importance in determining resolution capability. A number of field patterns of identical resolution capability can be obtained by assigning arbitrary sets of phases to the spatial frequency patterns.

An illumination function to independently control any spatial frequency component, thereby providing the capability of synthesizing any ambiguity function and pattern, has been derived. This "optimum" illumination function is shown to consist of the weighted sum of the delta function and its derivatives. Since these singular functions are not physically realizable, a particular approximation, the Gaussian-Hermite function, was examined and shown to provide independent control of the spatial frequency components with arbitrarily small error. Furthermore, as shown by Bouwkamp and de Bruijn,† patterns synthesized through the Hermite functions have the significant property of converging uniformly on a desired continuous pattern instead of converging only in the mean.

† op cit.

Theory of Resolution - Time Varying Illumination Functions

Generalizations of the previous analysis on time invariant illumination functions are considered in this section. In addition to considering the angular resolution obtainable with time varying illumination functions, the effects of the antenna on range resolution are also described. It is concluded that, for good resolution in angle and range, the signal must be "wideband" in spatial frequency as well as in temporal frequency. Furthermore, it has been shown that the combined range-angle ambiguity function, for periodic signals, is the time average of the angular autocorrelation function of the time varying pattern. This suggests the possibility of increasing the resolution capability of arrays through proper choice of the time varying function, since the resolution of arrays with the same time averaged pattern need not be the same.

A time varying illumination function can also be viewed as an aperture which transmits, or receives, different signal spectra from different portions of the aperture. An illustrative example utilizing this viewpoint has been suggested where, on reception, a filter is matched to the signal arriving from a particular angle in space and discriminates against all signals arriving from other angles. A set of such filters can be used to examine a particular sector in space.

Superdirectivity

The ambiguity function approach leads logically to a particular superdirective formulation. Using the Gaussian-Hermite functions, a number of illumination function-superdirective pattern pairs have been derived. The particularly attractive feature of synthesizing a continuous, but otherwise arbitrary, superdirective pattern with the Gaussian-Hermite functions is the assurance that the approximating pattern coverages uniformly to the desired superdirective pattern as higher order functions are instrumented.

The pattern characteristics with finite bandwidth signals have also been examined. An endfire pattern which is independent of frequency has been found indicating that there need not be any trade-off between range and angle resolution; the connection between range and angle resolution, in this specific case, appears to be one of limitations in practical implementation.

The superdirective formulation is strongly influenced by a factor, k. This factor modifies the free space wave number, which suggests that it be interpreted as the square root of the product of relative permittivity and

permeability. Viewed in this manner, superdirectivity requires a slow wave medium for its realization. It appears that the principle of similitude gives rise to the superdirective characteristics, i. e., that high resolution is achieved with a smaller structure because the characteristic wave velocity is smaller.

Two possible methods of implementing a superdirective array have been considered. One method is based on a similarity between the expressions for the fields in a confocal cavity and the illumination function required for superdirectivity. The other method, using synthetic aperture techniques, is devised to circumvent some of the severe problems normally associated with the implementation of superdirective arrays. The synthetic aperture technique is particularly attractive because mutual coupling problems simply do not exist. All of the processing to form the beam can be performed at video frequencies, and the superdirective output can be a supplemental, and not necessarily a primary, output.

Angular Dispersion and Compression

Some practical aspects of implementing angular dispersion - compression antenna systems are discussed in this section. Among the techniques considered is the novel concept of "spatial correlation." In this technique the pattern of a receiving antenna is used to collapse the dispersed pattern of a transmitting antenna. It has been shown that the integrated output of the receiving antenna is given by the ambiguity function, if the patterns are counter-rotated and are complex conjugates of each other. Dielectric disc antennas have been suggested as an economical method for implementation of pseudo-random counter-rotating antennas. An important feature of the technique is the relative simplicity of the receiver; the receiver requires an integrating device only, and need not contain complicated matched filters.

Optical correlation techniques have been found to have a number of properties suitable for angular dispersion - compression systems. Among these properties are the capability of performing simultaneous two-dimensional correlation, and the virtually unlimited storage and delay capability of the film which is employed in these devices.

It has been pointed out that, with the narrowband approximation, it may be possible to obtain dispersion and compression independently in each of the three basic dimensions of azimuth, elevation and range, and in addition extract resolution concerning the rates of changes of these coordinates. Although attention was centered on compression in one angle and range, an

important extension was suggested toward the instrumentation of a six-dimensional radar, i.e., one with resolving power in range, azimuth, elevation, and their respective rates of change.

Three main advantages of a dispersed antenna pattern were pointed out. These are low power density in space, lack of directivity, and the simplicity with which it can be instrumented. The first two are of particular importance to radars whose signals must be masked so as to prevent detection by the enemy. The third advantage is derived from the fact that resolution capability is totally independent of the phases of the spatial frequency components of the pattern. Hence, significant simplifications in phased array designs may be realized since random patterns do not require close phase tolerances at the radiating elements.

Multiple Frequency Array

The Multiple Frequency Array technique is a method to obtain wideband arrays with narrowband transmitters or radiating elements. The basic technique is a method to synthesize a wideband signal by means of a series of CW transmitters attached to separate radiators. Since the elements radiate at different frequencies, mutual coupling can be easily minimized by filtering. An additional advantage is that high peak power pulses can be synthesized using low power transmitters since the pulse is synthesized exterior to the array.

The fact that electronic beam steering can be accomplished with phase shifters, regardless of the bandwidth of the signal, is a significant property of the array. In contrast, a conventional array requires variable time delays at each element to steer the beam when the bandwidth of the signal approaches the inverse of the aperture transit time.

The unfortunate aspect of this basic array technique is that the power radiated per solid angle is independent of angle. However, this deficiency can be overcome by a generalization of the technique. It is shown that, by time varying the frequency distribution such that all frequency components are radiated, in time sequence, from all radiator positions, directivities equal to that of conventional arrays can be obtained when the received signals are integrated.